Modelling & Analysis of Hybrid Dynamic Systems Using a Bond Graph Approach

Margetts, Rebecca

Award date:
2013

Awarding institution:
University of Bath

MODELLING & ANALYSIS OF HYBRID DYNAMIC SYSTEMS USING A BOND GRAPH APPROACH

Rebecca Margetts
A thesis submitted for the degree of Doctor of Philosophy
University of Bath
Department of Mechanical Engineering
April 2013

Table of contents

Table of contents 1
Figures 4
Acknowledgments 6
Summary 7
Nomenclature 8
Chapter 1: Introduction 11
1.1 Background 11
1.2 Systems Modelling 12
1.2.1 Multi-Disciplinary Models 12
1.2.2 Hybrid Models 13
1.2.3 Hybrid Bond Graphs 14
1.3 Problem Formulation 15
1.4 Outline 15
1.5 Novelty & Contributions 16
1.6 Publications 17
Chapter 2: Literature Review 18
2.1 Preliminaries 18
2.2 The Bond Graph 18
2.3 Hybrid Models 19
2.3.1 Hybrid Systems 19
2.3.2 Boolean Algebra in Control 20
2.4 Hybrid Bond Graphs 21
2.4.1 Development of the Hybrid Bond Graph 21
2.4.2 Dynamic Causality in the Hybrid Bond Graph 24
2.4.3 Variable Topology and the Hybrid Bond Graph 24
2.4.4 Computation of the Hybrid Bond Graph 25
2.5 Control Properties 26
2.5.1 State and Implicit Models 26
2.5.2 Transfer Function & Canonical Forms 27
2.5.3 Solvability & Rank 28
2.5.4 Controllability 28
2.5.5 Observability 30
2.5.6 Asymptotic Stability: Eigenvalues & Zero Modes 30
2.5.7 Impulse Modes 31
2.6 Analysis of Model Structure 31
2.6.1 Terminology 32
2.6.2 Why Qualitative Analysis? 32
2.6.3 Exploiting Causality Assignment 33
2.6.4 Deriving the Transfer Function 34
2.6.5 Equation Generation from Bond Graphs 35
2.6.6 Use of Canonical Forms from Bond Graphs 36
2.6.7 Structural Analysis of Bond Graphs 37
2.6.8 Control Properties of Standard Bond Graphs 38
2.6.9 Control Properties of Hybrid Bond Graphs 42
2.7 Summary 45

Chapter 3: The Causally Dynamic Hybrid Bond Graph 46
3.1 Preliminaries 46
3.2 Constructing a Hybrid Bond Graph 46
3.2.1 Discontinuities and Hybrid Bond Graphs 46
3.2.2 Classification of Hybrid Behaviour 48
3.2.3 The Controlled Junction for Structural Discontinuities 49
3.2.4 Model Simplification with Controlled Junctions 51
3.2.5 A Dynamic Causality Assignment Procedure 54
3.2.6 The Controlled Element for Parametric Discontinuities 58
3.3 Implicit Formulation of the Hybrid Junction Structure Relation 62
3.3.1 Pseudo-States and Dynamic Causality 62
3.3.2 The General Hybrid Bond Graph 63
3.3.3 Notation 64
3.3.4 Comparison of Standard and Hybrid Model Equations 66
3.3.5 The Hybrid Junction Structure Matrix 68
3.3.6 The Reference Configuration and Other Configurations 70
3.4 The Unique Hybrid Implicit Equation 71
3.5 Properties of the Implicit Model 74
3.5.1 Properties of the Model in one Mode 74
3.5.2 Properties of the General Model 75
3.6 Comparison with Switching Sources and the Non-Ideal Approach 75
3.6.1 Implicit State Equations 75
3.6.2 Ideal and Non-Ideal Approaches 76
3.7 Summary 79
Chapter 4: Analysis of the Hybrid Bond Graph 80
4.1 Preliminaries 80
4.2 Observations on the Dynamic Causality Assignment 81
4.3 Further Equation Derivation 87
4.3.1 Transfer Function Using Shannon-Mason Loop Rule 87
4.3.2 The LTI Full Descriptor System 89
4.4 Impulse modes 94
4.5 Impulse Losses 98
4.6 Control Properties 99
4.6.1 Controllability 100
4.6.2 Observability 103
4.6.3 Asymptotic Stability 104
4.7 Summary 106
Chapter 5: Case Studies 107
5.1 Preliminaries 107
5.2 Power Converter 108
5.2.1 Overview 108
5.2.2 Hybrid Bond Graph 108
5.2.3 Deriving the Junction Structure and Implicit State Equations 109
5.2.4 Discontinuities on Variables at Commutation 114
5.2.5 Structural Analysis of the Power Converter 115
5.3 Landing Gear Drop Test 121
5.3.1 A High-Level Bond Graph of the Landing Gear 121
5.3.2 Structural Discontinuities: Contact with the Ground 122
5.3.3 Parametric Discontinuities: The Oleo Strut 123

5.3.4 Determination of the State Equations 125
5.3.5 Results & Discussion 127
5.4 Variable Topology Systems 131
5.4.1 Collision of Rigid Bodies: Newton's Cradle 131
5.4.2 Collision of Elastic Bodies 136
Chapter 6: Discussion & Conclusions 141
6.1 Discussion 141
6.2 Conclusions 143
6.3 Further Work 144
References 146

Figures

Figure 1: The Junction Structure of the General Bond Graph 36
Figure 2: Bond graph representation of switched junctions X1 and X0 50
Figure 3: An Example Subsystem with Neighbouring Regular and Controlled Junctions 52
Figure 4: An Example Subsystem with Neighbouring Controlled Junctions. 53
Figure 5: An Example System with a Ground. 54
Figure 6: An Example System with a Ground and a Controlled Junction. 54
Figure 7: An Example of Causality Assignments and their Effect around a Controlled Junction 56
Figure 8: Bond Graph 'Trees' for a Piecewise Linear Resistance Element, Assuming Three Modes of Operation. 59
Figure 9: The Piecewise Linear Resistance Element Subsystem, showing quantities used in Equation Generation. 60
Figure 10: The Junction Structure Matrix and Generalised Bond Graph. 64
Figure 11: Quantities used in Hybrid Junction Structure Matrix and Subsequent Development 66
Figure 12: An Example of causality assignment around a Non-Ideal [Flow] Switch 77
Figure 13: An Example of causality assignment around a Non-Ideal [Effort] Switch 78
Figure 14: An Example System with a Non-Ideal [Flow] Switch 79
Figure 15: Example of a Type 1 Structural Discontinuity 82
Figure 16: Example of a Type 2 Structural Discontinuity 84
Figure 17: Hard Contact with a Causal Path (indicated by arrow) affected by Causality Assignment 85
Figure 18: Notation used in Equation Derivation for the Hard Contact Example 85
Figure 19: A Causal Path crossing a Controlled Junction. 88
Figure 20: A Causal Path in Dynamic Causality. 88
Figure 21: The Detector Element shown taking a Signal from a Bond Graph Junction. 91
Figure 22: The General Hybrid Bond Graph with Signal Detectors giving Outputs. 92
Figure 23: Example System in Preferred Derivative Causality, with Ideal Clutch. 105
Figure 24: Schematic Diagram of a Boost Converter Supplying a D.C. Motor with Load 108
Figure 25: Hybrid Bond Graph Model of the Boost Converter. 109
Figure 26: Hybrid Bond Graph Model of the Boost Converter with Notation 111
Figure 27: Hybrid Bond Graph Model of the Boost Converter in Preferred Derivative Causality 116
Figure 28: Static Bond Graph of the Boost Converter showing a mode with least structural R-Controllability 117
Figure 29: Adding Detector Elements to the Model in Preferred Integral Causality, with Causal Paths marked 118

Figure 30: Hybrid Bond Graph in Preferred Integral Causality, Causal Paths representing Flat Loops Marked. 119
Figure 31: A Typical Aircraft Landing Gear 121
Figure 32: A High Level Bond Graph of a Landing Gear 122
Figure 33: The Tyre & Contact Model, with Dynamic Causality Notation 123
Figure 34: Detail of a Typical Two Stage Oleo-Pneumatic Strut 124
Figure 35: A 2-Stage Oleo represented by a 'Tree' of Bond Graph Elements. . 125
Figure 36: A 2-Stage Oleo represented by a Controlled Element 125
Figure 37: Complete Model of the Gear, Control Signals omitted for clarity ... 126
Figure 38: Simulation of the Drop Test, Pressure in Oleo Strut 128
Figure 39: Simulation of the Drop Test, Fuselage Vertical Displacement x_{AC} .. 129
Figure 40: Simulation of the Drop Test, Vertical Compression of Tyre 129
Figure 41: Simulation of the Drop Test, Contact 130
Figure 42: Examples of Rigid Contact, Snooker Balls [130] (left) and Newton's Cradle [131] (right) 132
Figure 43: Schematic of Rigid Balls acting in one-dimension 132
Figure 44: Hybrid Bond Graph of Rigid Balls acting in One Dimension 132
Figure 45: Motion of a Bouncing Ball 136
Figure 46: Hybrid Bond Graph of a Bouncing Ball 137

Acknowledgments

I would like to express my appreciation for the guidance and support of my supervisors Dr Roger Ngwompo and Prof Chris Budd, my colleagues at the Centre for Power Transmission and Motion Control (at the University of Bath) and my industrial supervisors Marcelin Fortes da Cruz, Christopher Dean and Sanjiv Sharma (at Airbus). I would also like to extend my thanks to Terence Frost and his staff in the Design Analysis - ELYD department at Airbus, for hosting me during my industrial placements.

This research was funded via a CASE Award from the Engineering and Physical Sciences Research Council (EPSRC) and Airbus UK.

Finally, I would like to acknowledge my family and friends for their unwavering support over the years and throughout this PhD. This thesis is written in memory of my Grandmother Florence 'Rona' Margetts and my Uncle Roland 'Jim' Marston, who both encouraged my interest in mathematics, science and technology.

Summary

Hybrid models are those containing continuous and discontinuous behaviour. In constructing dynamic systems models, it is frequently desirable to abstract rapidly changing, highly nonlinear behaviour to a discontinuity. Bond graphs lend themselves to systems modelling by being multi-disciplinary and reflecting the physics of the system. One advantage is that they can produce a mathematical model in a form that simulates quickly and efficiently. Hybrid bond graphs are a logical development which could further improve speed and efficiency. A range of hybrid bond graph forms have been proposed which are suitable for either simulation or further analysis, but not both. None have reached common usage.

A Hybrid bond graph method is proposed here which is suitable for simulation as well as providing engineering insight through analysis. This new method features a distinction between structural and parametric switching. The controlled junction is used for the former, and gives rise to dynamic causality. A controlled element is developed for the latter. Dynamic causality is unconstrained so as to aid insight, and a new notation is proposed.

The junction structure matrix for the hybrid bond graph features Boolean terms to reflect the controlled junctions in the graph structure. This hybrid JSM is used to generate a mixed-Boolean state equation. When storage elements are in dynamic causality, the resulting system equation is implicit.

The focus of this thesis is the exploitation of the model. The implicit form enables application of matrix-rank criteria from control theory, and control properties can be seen in the structure and causal assignment. An impulsive mode may occur when storage elements are in dynamic causality, but otherwise there are no energy losses associated with commutation because this method dictates the way discontinuities are abstracted.

The main contribution is therefore a Hybrid Bond Graph which reflects the physics of commutating systems and offers engineering insight through the choice of controlled elements and dynamic causality. It generates a unique, implicit, mixed-Boolean system equation, describing all modes of operation. This form is suitable for both simulation and analysis.

Nomenclature

A	The **A**-matrix in the standard Linear Time Invariant system equations
B	The **B**-matrix in the standard Linear Time Invariant system equations
BGD	Bond graph in preferred derivative causality
C	The **C**-matrix in the standard Linear Time Invariant system equations
D	The **D**-matrix in the standard Linear Time Invariant system equations
$\boldsymbol{D}$	The vector of all input/output variables to the resistance field
$\hat{\boldsymbol{D}}_{out}$	The input vector to the system from the resistance field in static causality (composed of e or f from the dissipative elements)
$\tilde{\boldsymbol{D}}_{e\_out}$	The effort input vector to the system from the resistance field in dynamic causality (composed of e from the dissipative elements)
$\tilde{\boldsymbol{D}}_{f\_out}$	The flow input vector to the system from the resistance field in dynamic causality (composed of f from the dissipative elements)
$\hat{\boldsymbol{D}}_{in}$	The output vector from the system to the resistance field in static causality (composed of e or f to the dissipative elements)
$\tilde{\boldsymbol{D}}_{e\_in}$	The effort output vector from the system to the resistance field in dynamic causality (composed of e to the dissipative elements)
$\tilde{\boldsymbol{D}}_{f\_in}$	The flow output vector from the system to the resistance field in dynamic causality (composed of f to the dissipative elements)
d	Subscript denoting derivative causality
E	The **E**-matrix in the standard Linear Time Invariant system equations
e	Generalised effort variable on a bond
f	Generalised flow variable on a bond
F	The matrix characterising the storage field. In the LTI case, this is a diagonal matrix of the linear coefficients for storage elements (relating the states to their complements)
G	Ground
G	Gain
i	Subscript denoting integral causality
in	Subscript denoting input
k	Number of zero (structurally null) modes
L	The matrix relating the outputs to inputs of the resistance field. In the LTI case, this is a diagonal matrix of the linear coefficients for resistance elements.
L	The linear coefficient for a single Inertia (I-element)
M	Mass
MTF	Modulated Transformer element

n	Model order
out	Subscript denoting output
p	Generalised Momentum
q	Generalised Displacement. Also used to denote bond-graph rank in structural analysis.
R	The linear coefficient for a single Resistance (R-element)
$\mathbf{S}$	The junction structure matrix
$\boldsymbol{T}$	The vector of input/output variables to switched sources
t	Time. Also used to denote the number of dynamical elements in the BGD
$\boldsymbol{U}$	The input vector to the system
$\boldsymbol{V}$	The vector of complementary variables to the inputs
V	Voltage
W	Weight
$\boldsymbol{X}$	The vector of all state variables
$\dot{\hat{\boldsymbol{X}}}_i$	The input vector to the system from storage elements in static integral causality (composed of $\dot{p}$ and $\dot{q}$)
$\dot{\tilde{\boldsymbol{X}}}_i$	The input vector to the system from storage elements in dynamic integral causality (composed of $\dot{p}$ and $\dot{q}$)
$\dot{\hat{\boldsymbol{X}}}_d$	The output vector from the system to storage elements in static derivative causality (composed of $\dot{p}$ and $\dot{q}$)
$\dot{\tilde{\boldsymbol{X}}}_d$	The output vector from the system to storage elements in dynamic derivative causality (composed of $\dot{p}$ and $\dot{q}$)
$\boldsymbol{Y}$	The output vector from the system
$\boldsymbol{Z}$	The vector of all complementary variables to the time-derivatives of the states
$\hat{\boldsymbol{Z}}_d$	The input vector to the system from storage elements in static derivative causality (composed of f and e)
$\tilde{\boldsymbol{Z}}_d$	The input vector to the system from storage elements in dynamic derivative causality (composed of f and e)
$\hat{\boldsymbol{Z}}_i$	The output vector from the system to storage elements in static integral causality (composed of f and e)
$\tilde{\boldsymbol{Z}}_i$	The output vector from the system to storage elements in dynamic integral causality (composed of f and e)
Δ	Graph Determinant
λ	Boolean parameter indicating the state of a single switch / controlled junction

$\boldsymbol{\lambda}$	The vector of eigenvalues for a system. Also a vector of Boolean parameters.
Φ	A nonlinear function: used to denote a nonlinear constitutive equation in a compliance, inertia or resistance element (with subscript *C*, *I* or *R* respectively)
$\boldsymbol{\Lambda}$	Switching law. In this thesis, it is the diagonal matrix of Boolean functions governing whether a mode of operation is active.
^	Denotes static causality
~	Denotes dynamic causality

Chapter 1: Introduction

1.1 Background

Modelling and simulation is a vital part of any engineering design process. Conceptual models and virtual prototypes aid in ensuring a design is fit for purpose before any physical models or prototypes are built, and this can significantly reduce time and costs. Models can also be used in assessing and understanding any behaviour observed later in the design phase or in operation of the physical product. Increasingly, computer models are used for hardware- and model-in-the-loop testing, online fault detection and isolation activities, and health and usage monitoring.

Historically, mathematical modelling relied on hand calculations. 'Models' were constructed using standard equations pertaining to a particular domain or discipline: Euler, Newton, Lagrange, Bernoulli or Kirchhoff equations (for example). As the use of computers became more commonplace, these divisions between engineering disciplines remained. Hence, the current state of the art with computer aided engineering software is that a package usually specialises in a particular domain, and often incorporates the same assumptions and simplifications that were once needed to make hand calculations possible. A classic example is the linearisation of systems and use of linear time-invariant model forms. This is unnecessary, since the analysis of nonlinear systems using the work of Routh or Lyapunov can easily be handled by a modern computer. Likewise, discontinuous behaviour such as switching or contact is typically poorly handled (resulting in stiff continuous models) despite the inherently discrete nature of computers and a wealth of work into the treatment of discontinuous behaviour.

As modelling and simulation plays an increasingly important role in the design process and maintenance of engineering systems, more accurate models are required. It is no longer sufficient to model subsystems in isolation, since they can interact and produce significant coupled dynamics. The use of novel and 'smart' materials and structures, and passive and active control devices, necessitates models which can describe the dynamic behaviour of a complex, possibly nonlinear system spanning several engineering domains. These system models are referred to as mechatronic, multi-disciplinary or multi-physics systems models.

Hence there are two important areas for improvement in modelling and simulation. The first is the construction of multi-disciplinary systems models. The second is the correct modelling of increasingly complex nonlinear and discontinuous systems: this can be achieved using *hybrid modelling*.

1.2 Systems Modelling

1.2.1 Multi-Disciplinary Models

In order to construct a multi-disciplinary model using current industry-standard tools, different software packages are either co-simulated (i.e. submodels are built in their respective ideal software packages and the packages are then virtually linked so as to simulate the submodels together) or are used to generate some code or an element which can be embedded in another software package. This approach is prone to difficulties, because models may need to be simplified further and/or simulated using non-ideal solvers in order to make these software packages compatible. Alternatively, separate systems models are constructed, which naturally involves some duplication of modelling effort and may lack the detail of the original subsystem models.

Systems modelling has its roots in electrical and control engineering, and the current industry standard approach is the use of block diagrams (in control engineering software packages such as SIMULINK) or signal-flow graphs, and linear time-invariant (LTI) models. A major limitation of this approach is the input/output thinking endemic in control engineering, i.e. the user must define the inputs and outputs to a model as it is being constructed, which necessitates knowing the mathematics beforehand. This makes sense in signal processing and feedback control tasks, but is not suited to physical system modelling where cause and effect may be unclear, and a modeller can unwittingly create physically meaningless or computationally inefficient models. Åström refers to this as the "control/physics barrier" [1].

Alternative tools and proposals for Idealised Physical Systems Modelling, Behavioural Modelling, and Object-Orientated modelling have been well-documented and available for some years, but have yet to become the standard approaches in the engineering community. These approaches revolve around using the physical system and/or its behaviour to develop a mathematical model. A common feature is acausality i.e. the model is constructed from reversible equations rather than statements, or submodels with energy- or power-conserving ports rather than inputs and outputs. Causality is then assigned *after* the model is built. This facilitates the reuse of models and parts, which can have a different

causality assigned in different situations. For example, the commercially available physical modelling package Dymola uses the acausal, object-orientated language Modelica.

For multi-disciplinary models in particular, port-based physical modelling is advantageous because energy and power exist across all disciplines, and can therefore be used to intuitively link submodels describing different engineering domains. This is facilitated by the use of generalised variables. The use of generalised momentum and generalised displacement can ensure that conservation of energy and conservation of momentum are respected. The standard equations used in classical mathematical modelling – Newton, Lagrange, Kirchoff – can all be derived in terms of generalised variables [2].

Bond graphs are a method which encompasses the above ideas. They describe the power in a system, in terms of effort and flow (the time derivatives of generalised momentum and displacement). As a lumped-parameter approach (routinely used in the modelling of dynamical systems) they relate effort and flow using generalised inertia, compliance and resistive elements, modulation elements, and ideal sources, which all have the same basic form irrespective of engineering domain. The model construction phase is acausal, and causality is then assigned using a visible notation of causal strokes: this allows causality to be exploited, providing insight to the model and the form of the underlying equations. The derivation of equations (state equations, transfer functions, Lagrange and Hamiltonian equations) is well documented. Although LTI state equations are frequently derived in the literature, bond graphs elements can easily take nonlinear constitutive equations and yield nonlinear mathematical models. For more information on Bond Graphs the reader is directed to Karnopp, Margolis and Rosenberg's standard text on the subject [3].

1.2.2 Hybrid Models

Hybrid mathematical models are models which incorporate both continuous and discontinuous equations. They include any behaviour that can be abstracted to a discontinuity, such as contact, or a nonlinear element with a piecewise continuous relationship. A discontinuity is a change in behaviour which occurs so rapidly as to be considered instantaneous. In a mathematical sense, a hybrid system is a set of continuous equations linked by discontinuous movements in state space.

All systems can be described by continuous equations. In software packages, these are usually in the form of differential algebraic equations (DAEs) which are

integrated by a *solver*. When rapidly-changing behaviour is described by a continuous differential equation, it must be integrated using very small time steps in order to achieve any level of accuracy. Replacing rapidly-changing behaviour with a discontinuous equation can therefore aid solvability and improve computer simulation times.

In addition, a user may find it intuitive to think of certain elements (like an electrical switch or hydraulic valve) or phenomena (such as contact, dry friction or breakage) as discontinuous.

1.2.3 Hybrid Bond Graphs

A hybrid bond graph has the potential to model complex multi-disciplinary nonlinear systems by encompassing the advantages of bond graph modelling (as a tool for intuitive, acausal, port-based, multi-disciplinary modelling) and hybrid modelling (as a method for treating highly nonlinear and discontinuous problems).

The standard bond graph notation has been extended by several authors to describe highly nonlinear systems (via field elements) and ideal switches. The latter is particularly interesting since it gives rise to the Switched or Hybrid Bond Graph.

The Switched or Hybrid Bond Graph is achieved using an ideal switch with some kind of Boolean modulation or control. A variety of methods for formalising this have been proposed in the literature, but no single method has reached common usage or inclusion as a standard element in a bond graph software tool. An issue which provokes discussion is that of dynamic causality, which occurs when the causality assignment differs according to the states of the switches. Another is the treatment of variable topology problems such as contact, where the size of the mathematical model literally changes. Some methods have been proposed for computer simulation, which sacrifice the insight gained from the idealised physical bond graph model by using parasitic elements or transferring the model to another environment. Other methods have been proposed which give a mathematical model for each mode of operation (defined by the states of the switches) but cannot yield a simulation, or require additional computation to link the models of each mode.

1.3 Problem Formulation

The goal of this research is to show how bond graphs could be used to analyse aircraft systems such as a landing gear, which are inherently highly nonlinear and would normally be abstracted to include discontinuous behaviour. In order to achieve this, the existing proposals for a Hybrid Bond Graph had to be reviewed to find a method which facilitated simulation as well as reflecting the physics of the system and providing some engineering insight.

The following objectives were therefore defined:

1. To propose a method for constructing a Hybrid Bond Graph which reflects the physics of the system, and is suitable for analysis and simulation purposes.

2. To validate this approach by deriving standard forms of mathematical model for the Hybrid Bond Graph, and comparing them to the existing literature on mathematical models.

3. To exploit the Hybrid Bond Graph and its causality assignment to derive information about the mathematical model.

4. To apply the method to a selection of illustrative case studies.

1.4 Outline

This thesis falls naturally into three parts: Background, Construction & Analysis of Hybrid Bond Graphs, and Case Studies.

The background to the project covers an extensive volume of existing literature, detailed in Chapter 2. An overview of hybrid modelling is given, followed by the development of switched and hybrid bond graphs. There are several variations on the latter, which are discussed with reference to the necessary considerations of dynamic / static causality assignment, impulses on commutation, and the graphical advantages of bond graphs. Aspects of classical and modern Control theory (which will be used in the analysis of bond graph models) are presented, along with their use on standard and hybrid bond graphs to date.

Chapter 3 presents a method for constructing a Hybrid Bond Graph, which includes two different kinds of discontinuity and a notation for dynamic causality. From this, the mixed-Boolean junction structure, and implicit state equations are derived. These are compared to the equations derived from other types of hybrid bond graph.

Chapter 4 presents some observations on the hybrid bond graph, derives further equations (output equation and transfer function) and exploits it for structural analysis (drawing parallels with matrix-rank criteria established in control theory).

Chapter 5 gives three case studies which show the range of applications for this method.

Chapter 6 discusses the method presented in this thesis and draws some conclusions about its validity and usefulness.

1.5 Novelty & Contributions

There are several novel aspects presented in this thesis:

- The classification of discontinuities into *structural* and *parametric*.
- The use of controlled junctions for the structural discontinuities and controlled elements for the parametric discontinuities. Although there are many proposed methods for constructing a Hybrid Bond Graph, including the use of controlled junctions, the method presented here is designed to be more intuitive and usable.
- The derivation of a new controlled element from a mode-switching 'tree' of controlled junctions and elements.
- The use of the controlled junction to place Boolean parameters in the Junction Structure Matrix, and hence generate mixed-Boolean equations.
- The dynamic causality notation, designed to aid construction and qualitative analysis. Dynamic causality is a hotly debated topic in the bond graph community (at the time of writing) and notation has been proposed before. This thesis argues the case for allowing dynamic causality in order to gain engineering insight.
- The adaptation of pseudo-state variables to describe storage elements in dynamic causality.
- The unique, implicit, mixed-Boolean system equation derived from the Hybrid Bond Graph and describing all modes of operation.

1.6 Publications

Margetts, R. and Ngwompo, R.F., Comparison of Modeling Techniques for a Landing Gear. *ASME IMECE 2010*, pp. 329-335 Vancouver, Canada, November 2010. (ASME Conference Proceedings, 2010).

Margetts, R., Ngwompo, R.F. and Fortes da Cruz, M., Construction and Analysis of Causally Dynamic Hybrid Bond Graphs. *Proceedings of the Institution of Mechanical Engineers Part I – Journal of Systems and Control Engineering*, March 2013, vol. 227 no. 3 pp. 329-346.

Margetts, R., Ngwompo, R.F. and Fortes da Cruz, M., Modelling a Drop Test of a Landing Gear using a Hybrid Bond Graph. *IASTED MIC 2013*, Innsbruck, Austria, February 2013. (Proceedings of the IASTED Multiconferences, 2013).

Chapter 2: Literature Review

2.1 Preliminaries

This research brings together several fields and ideas, and consequently a variety of topics were reviewed in the literature.

The bond graph is briefly reviewed as the chosen method for constructing a systems model. Hybrid modelling is then also introduced because it is fundamental to understanding the hybrid bond graph. The development of hybrid and switched bond graphs is reviewed in some detail, as there has been a substantial body of work conducted and several methods proposed.

The analysis of systems models is then addressed. Again, methods from classical control theory are overviewed, before demonstrating how control properties have been applied to both standard and hybrid bond graphs.

2.2 The Bond Graph

Bond Graph modelling was developed in the late 1950s by Paynter and formalised into a methodology by Karnopp, Margolis and Rosenberg. Their definitive textbook 'System Dynamics' was first published in 1971 and is still widely used today [3]. The concept of using generalised variables to model mechatronic systems is an important one in teaching dynamics, and is not limited to bond graphs. Parallels have been drawn with linear graph theory and combinatorics [4-7], and object-orientated computer programming [8]. A number of modelling and simulation software packages are either underpinned by, or explicitly support, bond graph modelling.

In essence, the bond graph consists of 'bonds' (drawn as half-arrows) which represent the power between standard elements. These standard elements are the point masses, compliances and resistances familiar to users who practise lumped-parameter modelling in mechanical engineering. The power across these elements is given as generalised effort and flow, and the method can therefore be extended to any engineering domain. The set of standard elements is completed by ideal sources (of effort and flow), junctions (about which either effort or flow is common), and transformer and gyrator elements (which modulate effort and flow to transform power between engineering domains). The method is acausal

(i.e. the inputs and outputs to each element are not defined, they are simply assigned a power-conserving port), and causality is assigned after the construction phase is complete, shown on the bond graph by causal strokes. Several causality assignment procedures have been proposed but the most widely used is SCAP (Sequential Causality Assignment Procedure). SCAP assigns computational causality so that the maximum possible number of elements is in integral causality, i.e. inertia and compliance elements are assigned an output so as to put the underlying equations in terms of the integral of the input. This is known as *integral causality* and the reverse situation (where there is a derivative term in the constitutive equation) is known as *derivative causality*. Placing a model in integral causality allows a computer to solve the model quickly and accurately using standard integrator routines. Solutions to any derivative terms are typically estimated using an iterative process, which can be inaccurate and slow down a simulation significantly.

Despite being assigned so as to aid computation, causality can be used to derive information about the model and the form of its underlying equations: this will be discussed further under the topic of bond graph structural analysis.

2.3 Hybrid Models

2.3.1 Hybrid Systems

A hybrid system is a system containing both continuous and discontinuous behaviour. This can be visualised as continuous modes on areas of state space linked by a discontinuous state mapping [9].

Definition 1: Hybrid Model
A Hybrid Model is any model which describes both continuous and discontinuous behaviour.

A system model can be described as a *hybrid automaton* i.e. one that contains both finite and continuous state spaces [10]. The dynamics consist of discrete transitions plus an evolution of the continuous part in each location.

The terms *hybrid* and *switched* system are used almost interchangeably in the bond graph literature, but there is a subtle difference. Switching systems *"comprise a family of dynamical subsystems together with a switching signal determining the active system at a current time"* [11]. They are a subset of hybrid systems, where there is some discontinuous behaviour modelled by an

on/off switch or other binary signal. Switched models can be used to describe multimodal systems and variable-structure systems, and it will be shown in this thesis that the Hybrid Bond Graph always gives a switched system.

Definition 2: Switched Model
A Switched Model is a subset of Hybrid Model, which contains continuous equations and binary switching devices. The 'switches' select the active continuous equation(s) or behaviours at a given time.

Branicky et al [12] categorise hybrid models into Switching and Impulse models, which can be Controlled or Autonomous. Switching models are defined as those where the vector field changes discontinuously when the state hits a boundary. Impulse models are those where the continuous state changes impulsively on hitting prescribed regions of state space. The classic example is Newton's Collision law, where the state of a body changes from positive to negative velocity on impact, and any dissipative effects are accounted for by a coefficient of restitution. These types of models have been created by some hybrid bond graph practitioners [13, 14] and are discussed here for completeness.

Definition 3: Impulse Model
An Impulse Model is a subset of Hybrid Model where the state changes impulsively, i.e. there is an impulse loss on commutation.

2.3.2 Boolean Algebra in Control

The technique developed in this thesis uses Boolean algebra and yields mixed-Boolean mathematical models. This is a new concept in bond graph analysis. However, there has been some work on Boolean control in general.

It is well established that a discontinuous control action – typically in the form of a switching input – causes the system's structure to vary, and these models are therefore referred to as *Variable-Structure Systems*. A subspace or hyperplane called the *switching surface* divides the state space of the model into two regions, each with a different control law (or form of). When the system operates on the switching surface, it is said to be in *sliding mode* and sliding control utilises this idea to give robust control in discontinuous and nonlinear systems. This method can be extended to variable-structure systems where the parameters – and not just the control inputs – are discontinuous [15].

Holderbaum [16] develops a Boolean control law for a power converter, directly from the Boolean input vector to the system, and assesses the system's stability. This work is in contrast to earlier work on control of switching electronic systems which uses mean values of inputs, such as Pulse Width Modulation (PWM). Boolean input systems – controlled by thyristors or transformers – are widely used in electrical industrial applications [17].

There is a significant body of work on hybrid models as *Boolean Control Networks*, particularly with bioscience applications. Boolean control networks are essentially linear graphs and are therefore closely related to bond graphs in principle. They have been analysed for control properties such as stability and observability [18-21]. The nodes in a Boolean network each represent a state variable which takes a value of 0 or 1 depending on whether it is 'active.' A regulation rule for each node is given as a Boolean function [20].

Other than a superficial similarity, this work does not directly influence the development of the hybrid bond graph.

2.4 Hybrid Bond Graphs

2.4.1 Development of the Hybrid Bond Graph

A number of methods have been proposed to model discontinuities in the bond graph framework. From early on in the development of bond graphs, there was a need to model discontinuities in the form of elements like switches and valves. This motivated Thoma's time-dependant junction (tdj) [22], and the use of modulated resistance elements to represent hydraulic valves [22, 23].

There was a significant interest in hybrid modelling using bond graphs in the 1990s, no doubt aided by the increased availability of computing power. At this point, the terms 'mode-switching,' 'switched bond graph' and 'hybrid bond graph' were all coined. The switching transformer element [24] which evolved into the Boolean-modulated transformer and resistor combination [25], switching bond [26] and switched source (sometimes known as a switched element) [27-30] were introduced. Shortly afterwards Mosterman and Biswas proposed the controlled junction (similar in principle to Thoma's earlier time dependent junction) [31] and Gawthrop presented the switched storage element [32]. Borutzky suggested the use of Petri-nets to link a collection of continuous models (one for each mode of operation) [33]. Later work on hybrid bond graphs has seen variations on these methods such as Samantaray's use of switched elements (which includes a switched resistance) [34], Umarikar and Umanand's

Switched Power Junction [35] and Low et al's version of the controlled junction [36]. Table 1 compares the main bond graph switching mechanisms.

These bond graph switching mechanisms generally work by imposing null flow or effort on the adjacent structure. This would be consistent with an ideal electrical switch (across which there is zero current when it is off), or ideal clutch (across which there is zero torque when it is disconnected), for example. In addition, Soderman [29] formalises the modelling of *mode-switching systems* (e.g. parts with piecewise continuous behaviour, where the system switches between modes of operation as opposed to on/off behaviour) using 'trees' of ideal switches and elements.

Throughout the latter half of the 1990s a body of work on the simulation of hybrid bond graph models was produced in which the key figures were Edström (working with switched sources) and Mosterman (working with controlled junctions). This work included ontologies, semantics, and methods for reinitialising state variables after a discontinuity occurs [9, 37-44]. Mosterman in particular establishes types of mode change, and investigates impulses occurring on commutation using implicit models of collisions [45].

Two later variations on the hybrid bond graph are interesting to note despite not reaching common use. The first is the Quantized Bond Graph [46] which, by being inherently discrete, neatly avoids variable causality and can be solved by Discrete Event Simulation (DEVS) [47, 48]. Kofman correctly asserts that, since computers inherently discretize models anyway, there is little advantage in placing too much importance on the continuous parts of a hybrid model. The second is the Impulse Bond Graph [14] which explicitly considers Dirac pulses by introducing the impulse bond and impulse switch (ISw – not to be confused with Gawthrop's switched inertia) element.

Switched sources and controlled junctions have fallen into more common usage than the other methods. This appears to be because they can model ideal switching, whereas the use of switched or modulating resistance and transformer components wrongly implies that switching is dissipative [41]. These methods also avoid some of the problems associated with others, such as 'hanging junctions' and computational difficulties. However, most recently, non-ideal switching using Boolean modulated transformers and resistance elements [25] has been revisited by Borutzky (who adapts it to a causally static form) for the purposes of FDI [49].

Table 1: Overview of Bond Graph Switching Mechanisms

Method	Bond Graph Representation			Description
	Element	Equivalent ON	Equivalent OFF	
Switched source (Switched element)	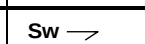	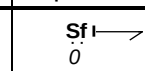	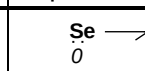	Commutates between a source of null flow and null effort, imposing zero flow/effort at the connecting junction when OFF.
		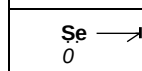	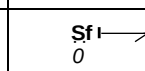	
Boolean-modulated transformer and resistor combination		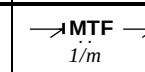	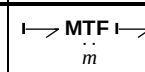	*m* is Boolean (1 when ON and 0 when OFF), Resistor commutates between conductance and resistance causality.
Controlled junction	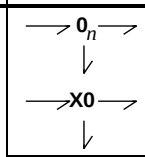	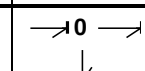	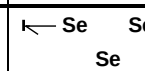	Is a regular 0- or 1-junction when ON and a null source on each bond when OFF
	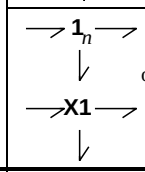	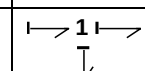	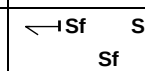	
Controlled storage element	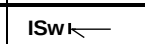	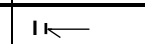	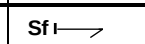	This is a compound element, acting as a regular storage element when ON and a Switched Source (i.e. null source) when OFF.
	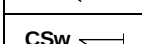	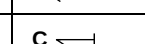	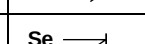	
Switched Power Junction	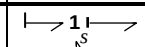	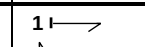	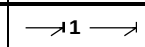	There are two mutually exclusive causal inputs to the junction, *s* denotes the active input bond.
	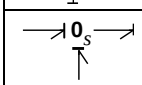	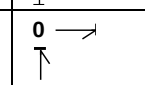	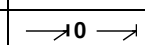	
Boolean-modulated transformer and resistor combination (modified)	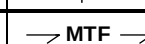	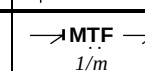	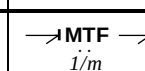	*m* is Boolean (1 when ON and 0 when OFF), the Resistor is in fixed conductance causality
Controlled Junction (modified)	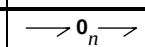	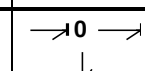	[deleted]	Is a regular 0- or 1-junction when ON and deleted (along with adjacent bonds) when OFF. This usually - but not always – gives the same effect as the original controlled junction.
	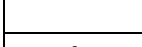	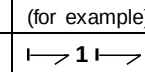	[deleted]	

2.4.2 Dynamic Causality in the Hybrid Bond Graph

It is immediately clear from Table 1 that the ideal causal assignment of the bond graph can change with commutation of the switching parts. The phenomena of variable topology and dynamic (or variable) causality were addressed separately by Asher [27], Cellier et al. [50], Stromberg et al. [30] and Bidard et al. [51], the latter proposing a notation for dynamic causality which is infrequently used. Dynamic causality is a feature of ideal switching, while variable topology is the case where the model changes significantly with commutation (e.g. a contact problem where the state equations change size). Cellier et al. [50] note that there can be impulse losses on commutation which must be considered.

Dynamic causality can be minimised and controlled using '*Causality Resistance*' as originally proposed by Asher [27]. This is significant because it facilitates the modelling of hybrid systems in a commercial software package. Breedvelt and others have produced a body of work modelling contact in the commercial bond graph package 20Sim. They use controlled junctions with causality resistance to model friction [52], a Newton's Cradle [53] and a copier machine [54]. While this work is of tremendous practical relevance to the engineer and 20Sim user, causality resistance can cause problems by creating an overly complex model [28], and is open to abuse in that there is a danger resistances may be added purely to aid computation with no consideration of the physical system.

Dynamic causality can also be minimised by revising the causality assignment procedure. For example, Low et al [36] propose Hybrid-SCAP for use with their version of the controlled junction which gives causally static hybrid bond graphs.

The debate regarding static versus dynamic causality is ongoing at the time of writing. The body of work using switched sources and controlled junctions generally accepts dynamic causality, but many practitioners use methods that give static or near-static causality for ease of representation and computation in a bond graph environment.

2.4.3 Variable Topology and the Hybrid Bond Graph

Variable topology systems are those where the size of the state equation matrices changes, such as contact. They are frequently represented by impulse models [12] such as Newton's Collision Law with restitution. This type of model exhibits an impulsive 'jump' in state space on commutation, which violates the conservation of energy fundamental to the bond graph. The Impulse Bond Graph [14] was developed to explicitly show the impulse of energy (or Dirac pulse) released on commutation. Mosterman asserts that it is conservation of

momentum, not energy, that is important and this is maintained in the hybrid bond graph. The state variables are unknown after commutation, hence the use of pseudo-Kroenecker form for state reinitialisation [13, 45] and state estimation techniques [55].

The hybrid bond graph produced in this thesis does not yield an impulsive model (although one can be subsequently derived). They are included here for background and comparison.

2.4.4 Computation of the Hybrid Bond Graph

The bulk of research on structural analysis and control of hybrid models uses switched sources. This is possibly because of the resemblance to a physical switch, the widespread use of binary / Boolean input devices in the electric industry, and for consistency with advances in control theory which assume discontinuous control inputs. However, the use of switched sources has been criticised because it implies the switch is an energy-processing element (like the other bond-graph elements) when it is, in fact, a control element [31, 56]. Hence Controlled junctions are used extensively by computer scientists and those interested in simulation.

There has been a move towards simulating hybrid systems using other techniques such as the acausal modelling language Modelica [57], its commercial GUI Dymola [58], and formalising the transformation of bond graph models into block diagrams for simulation in SIMULINK [59-62]. The potential for cosimulation of bond graphs and block diagrams has been explored [63], as has deriving input/output port-Hamiltonian models which allow the bond graph model to be embedded in or cosimulated with other environments [64-66]. This move makes sense from a computational point of view (and much of the research here was conducted by computer scientists) but loses the graphical advantages and relation to the physical system which are important to the user.

This work in other software packages – typically using controlled junctions – also yielded results in the field of FDI [67, 68] but the focus was on efficient simulation rather than exploiting the bond graph [55, 69, 70].

Hybrid bond graphs are tied to the developments in hybrid modelling in general, notably Hybrid Process Algebra (HyPA) which sought to bridge the gap between discrete modelling (as used by computer scientists) and continuous modelling (as used by control scientists and engineers), and formalise the initialisation of variables after a discontinuous event (which is necessary in causally dynamic

models) [71]. HyPA was developed with the principles of behavioural modelling in mind and does not rely on a rigorous input-state-ouput definition (for example, states can be outputs): this makes it a natural choice for application to hybrid bond graphs as proposed by Cuijpers, Broenink and Mosterman [72].

2.5 Control Properties

Before the qualitative analysis of bond graphs is investigated in more detail, it is imperative to outline the analysis of systems in general using tools from control theory. In this thesis, the term 'control properties' refers to those properties obtained from the model which can benefit the control engineer. These are typically stability, controllability/observability, solvability and related properties, which can aid the engineer in assessing a design and defining instrumentation and stabilising controllers.

2.5.1 State and Implicit Models

In the field of control theory, control properties are found from the state space representation of the model with causality assigned (i.e. the input/output model). This method originates from Kalman's General Theory of Control Systems [73] and a subsequent body of work carried out in response to problems generated by developments in communications and computers in the 1960s [74]. An overview is given by most standard textbooks such as Sontag [75]. Although there have been significant developments in control theory since that time, these basic parameters are still widely taught and used today, often in the context of the explicit linear time-invariant (LTI) state space equation (1):

$$\dot{\boldsymbol{X}} = \mathbf{A}\boldsymbol{X} + \mathbf{B}\boldsymbol{U} \qquad \textbf{(1)}$$

Where $\boldsymbol{X}$ is a vector of system state variables, $\boldsymbol{U}$ is a vector of inputs, and $\mathbf{A}$ and $\mathbf{B}$ are standard matrices of linear coefficients. The method developed in this thesis yields an implicit system model (2).

$$\mathbf{E}\dot{\boldsymbol{X}} = \mathbf{A}\boldsymbol{X} + \mathbf{B}\boldsymbol{U} \qquad \textbf{(2)}$$

Where $\mathbf{E}$ is an additional standard matrix of linear coefficients.

Authors typically strive to obtain the explicit regular state space system for ease of both computation and analysis. However, Implicit systems in various forms appear to arise naturally when looking at interconnected systems, and Lewis [76] argues that they are more suitable for signal processing and modelling tasks than explicit state space models.

Specific implicit forms which have been investigated in detail are *singular systems*, *semistate systems* and *descriptor systems*. Although they were originally coined for specific cases, the terms are used interchangeably in the literature.

Yip and Sincovec [77] establish properties of the descriptor system, and Verghese, Levy and Kailath [78] develop a generalised theory for singular systems: both essentially present control properties for implicit systems which mirror those established for explicit ones. Lewis [76, 79, 80] gives a useful review of implicit systems and techniques for analysing them, and Dai [81] looks specifically at matrix-rank criteria for singular systems. Their results will be extended to the equations generated by the hybrid bond graph in this thesis.

The main considerations for a singular system are the presence and treatment of impulsive modes, and of causality. Causality in this sense refers to whether a value can be calculated from past values (causal) or depends on both past and forward values (noncausal): implicit systems are by nature noncausal. This allows them to be manipulated into a state space form and – perhaps more significantly – they can be considered as behavioural models. Behavioural modelling [82], using port-based rather than input/output models, has become an established branch of control engineering despite the prevalence of input/output thinking in industry and commercially available software packages. Willems [1, 83] demonstrates that control can be studied from a behavioural point of view without introducing inputs and outputs. Lewis and Ozcaldiran [84] therefore investigate the geometric properties of implicit models referencing Willems, arguing that they give increased engineering insight.

2.5.2 Transfer Function & Canonical Forms

The transfer function was used extensively prior to state equations, and is still used as a way of understanding SISO (single-output-single-input) systems. The numerator and denominator give the poles and zeros of the system, and can be used to identify system dynamics, estimate stability margins and plot Bode or Nyquist diagrams by hand.

Various canonical forms of the state equations can be found which reveal more of the model's dynamics. For example, the Jordan Canonical form can be used in finding eigenvalues and establishing the matrices for the Popov-Belevich-Hautus test (for controllability). Popular forms include Control Canonical Form, Kroenecker Form and Smith Form. The latter two have been used to investigate bond graph dynamics.

2.5.3 Solvability & Rank

Rank refers to the number of linearly independent columns (or rows; column and row ranks are equal) in a matrix. It is an indication of whether the model is under- or over-defined, and hence whether it is solvable. Many of the standard control properties for descriptor systems are defined using matrix-rank criteria [81].

2.5.4 Controllability

Two of the most important results in the analysis of linear systems are controllability and observability matrices, usually given as functions of the **A**, **B** and **C** matrices of the standard LTI form, where **C** is obtained from the standard output equation:

$$\boldsymbol{Y} = \mathbf{C}\boldsymbol{X} + \mathbf{D}\boldsymbol{U} \text{ or } \boldsymbol{Y} = \mathbf{C}\boldsymbol{X} \quad \textbf{(3)}$$

Where $\boldsymbol{Y}$ is the vector of output variables and **C** and **D** are standard matrices of linear coefficients. Controllability is a widely used concept with numerous definitions, broadly referring to whether the system can be manipulated from its initial trajectory to a desired one. The definitions used in classical control theory – usually referred to as *state controllability* - originate from Kalman's observations.

Definition 4: State Controllability [74]
"A real, continuous-time, n-dimensional, constant, linear dynamical system Σ has the property 'every set of n eigenvalues may be produced by suitable state feedback' if and only if Σ is completely controllable."

Willems argues that state controllability is a property of the state representation rather than the system. He defines *behavioural controllability*, of which state controllability is a special case:

Definition 5: Behavioural Controllability [1]
"A behaviour is defined to be controllable if it is possible to transfer from any past trajectory to any future trajectory, while obeying the dynamical laws of the system ... This definition is applicable to nonlinear, discrete event and delay-differential systems without having to introduce a state representation."

Controllability is closely related to the concepts of *reachability* (the property that any state be reachable from the initial conditions i.e. zero) and *stabilizability* (the property that any state can be controlled to bring it to a trajectory that tends to zero with time) [75].

A number of tests for behavioural controllability [1] offer the opportunity to develop a general test for nonlinear hybrid bond graphs. However, linear time-invariant models are the initial focus of this research. Considering the LTI assumption, and reverting to state controllability, the Popov-Belevich-Hautus test may be used to assess controllability:

$$rank\left[\mathbf{A}-\mathbf{I}\lambda \quad \mathbf{B}\right]=dim\left(\boldsymbol{X}_i\right) \text{ for all } \lambda\in\mathbb{C} \qquad \textbf{(4)}$$

Where **A** and **B** are the matrices from the LTI state-space form (equation 1), λ is the vector of system eigenvalues, and $\boldsymbol{X}_i$ is the vector of state variables relating to dynamical elements in integral causality. This test is known to be equal to the well-known test for state controllability, using the controllability (or reachability) matrix:

$$rank\left[\mathbf{B} \quad \mathbf{AB} \quad \mathbf{A}^2\mathbf{B} \quad \ldots \quad \mathbf{A}^{n-1}\mathbf{B}\right]=n \qquad \textbf{(5)}$$

Where n is the order of the model. Since controllability is closely related to stabilizablity, the controllability matrix can be used for pole assignment. It is also possible to assess infinite structure and input/output paths for disturbance rejection [85]

2.5.5 Observability

Observability is the dual property of Controllability, and criteria for observability are usually linked to those for controllability.

This is embodied in the *Duality Principle*:

Definition 6: Duality Principle [74]
"Every problem of controllability in a real, (continuous-time, or discrete-time), finite dimensional, constant, linear dynamical system is equivalent to a controllability problem in a dual system."

Just as controllability is established by solving the state equation for the input (control function), observability is established by solving for the output *y(t)*. In classical control theory, the **A** and **C** matrices are inspected in much the same way as the **A** and **B** matrices are inspected for controllability. Hence the observability matrix:

$$rank\begin{bmatrix} \mathbf{C} \\ \mathbf{CA} \\ \mathbf{CA}^2 \\ \vdots \\ \mathbf{CA}^{n-1} \end{bmatrix} = n \qquad \textbf{(6)}$$

2.5.6 Asymptotic Stability: Eigenvalues & Zero Modes

Asymptotic stability is the property by which a system's behaviour will reach a steady state condition with time, for example the classic 'ring down' response seen in a damped system after an impulsive input.

Asymptotic stability can be established for each mode of operation by finding the roots of the system, which are the solutions of the characteristic equation. This is typically the characteristic polynomial set equal to zero (i.e. assuming an unforced system). Hence, for the descriptor system, the inputs are neglected and the characteristic polynomial of **A** is given by (7) [86]:

$$P(s) = |s\mathbf{E} - \mathbf{A}| \text{ or } P(s) = |\mathbf{A} - s\mathbf{E}| \qquad \textbf{(7)}$$

Which, for an explicit state space system, reduces to [87]:

$$P(s) = |s\mathbf{I}_n - \mathbf{A}| \qquad \textbf{(8)}$$

The solutions are found by taking eigenvalues $\boldsymbol{\lambda}$, which are the solutions to (9):

$$0 = |\boldsymbol{\lambda}\mathbf{E} - \mathbf{A}| \qquad \textbf{(9)}$$

The eigenvalues are usually complex and can be plotted: positive real parts indicate unstable behaviour. This is not strictly a structural analysis since the values of the roots will depend on the values of the system's parameters. However, structurally null modes (i.e. zero eigenvalues) can be identified, and the effects of structural changes (such as commutation) on roots and poles can be assessed.

2.5.7 Impulse Modes

Impulse modes (also referred to as *infinite frequency* modes) are a feature of hybrid systems. They occur where a storage element switches from integral to derivative causality, giving a step change in the value of the state. When all elements are in integral causality, **E** is an identity matrix and the model is in the explicit state-space form. When an element changes to derivative causality with commutation, an algebraic constraint is typically set up and a non-diagonal term manifests in **E**. This term, which changes instantaneously from zero to a finite factor of a state variable on commutation, is what gives the impulse mode [78].

2.6 Analysis of Model Structure

In the previous section, several developments in the analysis of systems were outlined. This section investigates the exploitation and analysis techniques used specifically on bond graphs. This includes both standard bond graphs and hybrid bond graphs incorporating switched sources, and their relationship to classical systems control theory.

2.6.1 Terminology

There are several forms of qualitative analysis which can be conducted on a bond graph prior to simulation. The term '*Exploiting Causality'* was used early on by Margolis and Rosenberg, and refers specifically to information obtained from the causal assignment in the bond graph [88, 89]. '*Structural Analysis'* refers to information that can be obtained from the bond graph structure, either by investigating the graph or the junction structure matrix. This information includes the form of the state equations, solvability, etc. and is analogous to the structural analysis of state matrices in control engineering. '*Equation Generation*' typically refers to obtaining the implicit or explicit state space equation(s) from the bond graph, which can then be manipulated into various forms and used to obtain information about the system. Although this is not strictly an analysis of the bond graph, it is imperative that the bond graph can yield equations suitable for this kind of analysis.

2.6.2 Why Qualitative Analysis?

There are a number of advantages to conducting a qualitative analysis of a model. The model can be manipulated to solve more accurately and efficiently. There is the potential to troubleshoot or improve a model prior to a lengthy simulation (which could be days, or even months, on large complex models), or to create simulations running in real time for online fault diagnosis and hardware/model-in-the-loop testing. In-depth understanding of the system – such as identifying structural parameters and interactions between subsystems - can also facilitate conceptual design, designing controllers, identifying interactions between subsystems and defining test strategies.

Initially the analysis must distinguish between system properties that are determined by the system structure (i.e. *structural properties*), and those determined by the parameter numerical values. Structural analysis yields structural properties.

The most basic structural analyses arise from looking at the causality assignment. An element in derivative causality is easily spotted, and there may be some computational problems associated with solving the model. Computer software typically uses integration methods (such as Euler or Runge-Kutta), and any derivative terms must be estimated by an iterative process which can be both slow and inaccurate. Furthermore, if an inertia element is in derivative causality and there is a causal path between it and another inertia element, a kinematic

constraint exists. The two inertias form a single rigid body, and the analyst may choose to include some compliance or lump the masses together if appropriate. Causal paths can also be traced between other elements to identify algebraic dependencies or loops in the underlying equations, which may also slow a simulation. Frequently the causality is investigated to determine the correctness of a model: an analyst can easily see derivative causality and algebraic loops where they were not intended.

Rosenberg [89] further exploits causality to give the engineer insight into the model or design. Causality can guide the engineer in assembling submodels and suggesting suitable test conditions. There is also the potential to look at interaction between nonlinear constitutive equations and uniqueness of system response.

Since state equations are easily derived from the bond graph, it follows that control properties normally found from the state equations are reflected in the bond graph's structure and causal assignment. A body of work by Sueur, Dauphin-Tanguy and others brings the notions of structural analysis and exploiting causality closer together. These properties (controllability, stability, (in)finite structure, etc.) aid with instrumentation for experimentation and fault diagnosis and identification (FDI).

During equation generation, a range of canonical forms of the state equations can be reached which can be used to look at further dynamic properties. These are generally a manipulation of the state equation, and outside the scope of bond graph analysis.

Finally, there is the opportunity to analyse the structural properties of a bond graph model in order to assess the feasibility of control strategies. It should be remembered that the analysis of systems with respect to control is still an active topic of research itself, and only a subset of established analysis techniques are discussed here.

2.6.3 Exploiting Causality Assignment

From the method's first publication in the 1970s there was immediately an interest in exploiting the bond graph's structure. The junction structure matrix (describing the bond graph's structure as a matrix of 1's and 0's relating system inputs to outputs) was defined and its properties (such as duality between effort and flow) discussed [90-93]. The state space equations [94], transfer function

[95] and Lagrangian Equations [96] were found from the bond graph, allowing comparison with classical control and dynamics theory. This work inherently involved looking at the way causality is assigned in the bond graph, and prompted the development of various causality assignment procedures, the best known of which is SCAP (Sequential Causality Assignment Procedure) [3].

Margolis and Rosenberg in particular showed how the bond graph's causal assignment (using SCAP) can be exploited to aid its computation, systematically derive state equations and gain insight into the system [88, 89].

In exploiting causality it is important to note that *computational causality* is used, which is applied according to a procedure such as SCAP (Sequential Causality Assignment Procedure). These procedures apply causality in a way that is beneficial to computation or analysis. Usually a model will be simulated at some point in a computer language or environment which uses an integrator, and this is why causality is typically assigned to put storage elements in *integral causality*. It is crucial to understand that causality is not a physical property of the system: it is something that the user applies, and could easily choose to apply differently. It is fundamentally a study of how to fit the underlying mathematical equations together to form a solvable set [88].

However, the causal assignment can tell the user something of the properties of the model. The classic example is that of the causal path existing between two lumped masses, rigidly coupled. Using SCAP, one lumped mass will be in integral causality and the other in differential causality. This is because there is a real kinematic constraint between the two bodies, and the causal path between them reflects an algebraic loop in the underlying equations. If the state equations are obtained, they will be in the implicit form. The user may decide to lump the masses together, or add some compliance if appropriate (as in the classic example of two railway carriages connected by a compliant link), to aid computation. This type of preliminary design assessment is an established advantage of bond graphs, and there are abundant examples of how an instance of derivative causality might provoke the engineer to revise their design assumptions (e.g. the Denny Theoretical Drive example provided by Rosenberg [89]).

2.6.4 Deriving the Transfer Function

A transfer function for a system can be found directly from the Bond Graph using Shannon-Mason Loop Rule [95]. The causal paths between elements in the bond graph are indicative of loops in a signal flow graph, and have gains related to the elements on those paths. In a bond graph, 'flat' loops are associated with

causal paths between passive 1-port elements and open loops associated with causal loops.

The general form of the transfer function between the *j*th input and *i*th output (the *k*th *path transmittance*) is:

$$h_{ij} = \frac{1}{\Delta}\sum_k G_k \Delta_k \qquad \textbf{(10)}$$

Where:
$$\Delta = 1 - \sum_i G_i + \sum_{i,j} G_i G_j - \sum_{i,j,l} G_i G_j G_l + \ldots \qquad \textbf{(11)}$$

$\sum_i G_i$ is the sum of all individual loops, while $\sum_{i,j} G_i G_j$ is the sum of the loop gains of sets of two loops that do not touch, $\sum_{i,j,l} G_i G_j G_l$ is the sum of the loop gains of sets of three loops that do not touch, etc. Loops are considered to be 'touching' if they share a node.

Δ_k is a reduced graph determinant, i.e. the determinant of the reduced graph, which results when the *k*th path is removed from the graph.

2.6.5 Equation Generation from Bond Graphs

In defining the control properties of the bond graph model, it is important to establish how equations are obtained from the bond graph. Karnopp et al [3] describe how to find the state space equations by hand from a bond graph (acknowledging that the integrals of the inputs to storage elements are the state variables). On larger models, this method can become impractical and the equations can be derived from the junction structure matrix instead.

The junction structure is the body of a model, relating the inputs from and outputs to the fields of elements: dissipative, storage, input and transformer fields. The junction structure matrix is a matrix representation of the bond graph's structure: 1's and 0's relate the inputs and outputs to the structure from each element. Some authors have a Transformer Field external to the structure, but it is common practise to bring any modulation terms $\boldsymbol{a}$ from transformer or gyrator elements inside the matrix to give terms other than 0 and 1. This is illustrated in Figure 1.

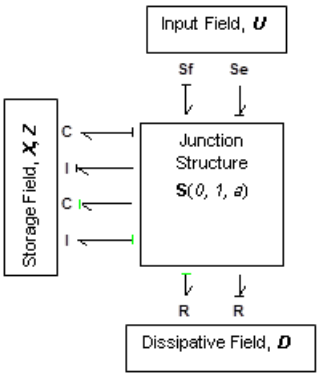

Figure 1: The Junction Structure of the General Bond Graph

$$\begin{bmatrix} \dot{\boldsymbol{X}}_i \\ \boldsymbol{Z}_d \\ \boldsymbol{D}_{out} \end{bmatrix} = \left[\mathbf{S}(0,1,a)\right] \begin{bmatrix} \boldsymbol{Z}_i \\ \dot{\boldsymbol{X}}_d \\ \boldsymbol{D}_{in} \\ \boldsymbol{U} \end{bmatrix} \qquad \textbf{(12)}$$

Where $\boldsymbol{X}$ is a vector of state variables, and the subscripts *i* and *d* denote integral and derivative causality. $\boldsymbol{Z}$ is the complement of the state variables, and $\boldsymbol{D}$ is the inputs and outputs (denoted *in* and *out*) from the resistance elements. $\boldsymbol{U}$ is the external inputs.

Once the bond graph is represented in a matrix format, model equations in more familiar forms can be derived from it, as demonstrated by Rosenberg [89] and Sueur and Dauphin-Tanguy [97]. The former gives general equations and the latter gives the familiar LTI form.

In establishing control properties for bond graphs, the submatrices of **S** will be referred to. These submatrices establish whether relationships exist between the storage, resistance and source elements.

2.6.6 Use of Canonical Forms from Bond Graphs

A popular analysis in the Bond Graph literature is the use of Kroenecker Canonical Form, which can split the system into known and unknown dynamics, for which there is an analytical answer [56]. Mosterman uses a pseudo-Kroenecker form in HyBrSim to reinitialise state variables after commutation [45]. It is a useful form because the Dirac pulses manifest. Buisson et al [98] use

the Smith Form of their implicit state equation to give an ODE and algebraic constraint, which can be used in defining hybrid automata.

The canonical forms are not found directly from the bond graph: they are found by manipulating the implicit state equation. In this thesis the canonical forms are not used, as the reinitialisation of variables or development of hybrid automata are not necessary. This is considered to be an advantage over other varieties of hybrid bond graph.

2.6.7 Structural Analysis of Bond Graphs

Sueur and Dauphin-Tanguy [97, 99-101] revisited the junction structure matrix and established the structural analysis of bond graphs using concepts from control theory. Since many well-known results from control theory typically use the LTI state space representation, and this representation can be obtained from the junction structure matrix of a bond graph, it follows that control properties are reflected in the bond graph itself. There has been further fundamental work on structural analysis of the bond graph with regard to decoupling and stability [102, 103], infinite structure [104], controller design [87] and extracting input/output equations for a generalized junction structure [105].

Once hybrid and switching bond graphs were defined, their control needed to be addressed. As has been noted already, the bulk of work on structural analysis of hybrid bond graphs assumes the use of a switched source element. Abadie et al [106] extended structural analysis of the standard bond graph to the 'switching system.' Buisson [28] looked at equation generation from a switched bond graph and computed the amplitudes of impulse losses on commutation as early as 1993, which led to a body of work on descriptor systems from hybrid bond graphs [107, 108]. In this work the junction structure matrix includes additional rows describing a switching law in terms of each switched source's input and output variables. A state equation for the reference mode of operation can be obtained from this, and other modes of operation derived in turn.

From this version of the hybrid bond graph, the use of bond graphs for control has been simplified [109] and extended to more complex, hierarchical systems [110]. A body of work applying structural analysis techniques to the hybrid bond graph was produced [98, 111-115] which had a focus on FDI and control.

The structural analysis of hybrid bond graphs containing controlled junctions was neglected until recently. Low et al [36, 116, 117] produced a series of papers looking at hybrid bond graphs for FDI, and defining a causality assignment

procedure for hybrid bond graphs. Although they initially used switched sources, they adopted controlled junctions and developed Hybrid-SCAP for them to give static causality assignments. While their research signifies a logical move towards analysis of bond graphs with controlled junctions, it is narrowly focussed on FDI and treats the controlled junction in an oversimplified manner.

2.6.8 Control Properties of Standard Bond Graphs

2.6.8.1 Order & Rank

The order of the model will be referred to throughout this thesis.

Definition 7: Bond Graph Order (*n*) [113]
The number of storage elements in integral causality when a preferred integral causality is assigned to the bond graph model.

The order *n* of a mathematical model is given by the number of state variables, and in a bond graph this is given by the inertia and compliance elements in integral causality. Hence the above definition is logical.

Rank is an important concept in establishing matrix rank criteria for a mathematical model, and it is reflected in the bond graph. Rank of the **A** matrix is an indication of solvability. Dauphin-Tanguy et al [87] define a 'bond graph rank' which corresponds to numerical rank because it takes parameter dependency (through the causal assignment) into account.

Definition 8: Bond Graph Rank (bg_rank) of the A-Matrix [113]
The number of storage elements in derivative causality when the bond graph is placed in preferred derivative causality.

The definition for rank is a little less obvious, but essentially shows those elements that are not independent, and therefore indicates linear dependency in the underlying matrix equations.

The preferred derivative causality bond graph - referred to as the BGD – essentially inverts the system matrices. It generates the system's mathematical model in the following alternative form [118]:

$$\boldsymbol{X} = \mathbf{A}^{-1}\dot{\boldsymbol{X}} + \mathbf{A}^{-1}\mathbf{B}\boldsymbol{U} \qquad \textbf{(13)}$$

When storage elements take integral causality in the BGD, **A** is not invertible i.e. it is singular and its determinant is therefore zero. If the system matrix **A** is singular then, by Cramer's Rule, the system of linear equations does not have a unique solution [119]. Hence, in order for **A** to be full rank and solvable, there must be no storage elements in integral causality in the BGD.

2.6.8.2 Controllability

In the field of bond graphs, the concept of *structural controllability* has been used as a more physically meaningful parameter than classical state controllability. Sueur and Dauphin-Tanguy [97, 99] have made the following observations for standard bond graphs.

Definition 9: Structural Controllability of a Bond Graph [99]
"The model is structurally state controllable iff:

1. *There is a causal path between each dynamical element [in integral causality] and a source, i.e. all states (nodes) are input-reachable.*
2. *Struct_Rank [**A B**] = n … Where the structural rank of [**A B**] is equal to*
    a. *the rank of (**S**$_{11}$ **S**$_{13}$ **S**$_{14}$) or*
    b. *n- t_s*

Where t_s is *"the number of the number of dynamical elements remaining in integral causality when :*

(a) a derivative causality assignment is performed,

(b) a dualization of the maximal number of input sources is performed in order to eliminate these integral causalities" [99]."

Point 1 is intuitive. Point 2 ensures that there are sufficient inputs for each independent state.

Alternatively, structural controllability can be deduced from the junction structure matrix:

Definition 10: Structural Controllability of a Bond Graph (JSM) [97]
"A linear system is structurally controllable iff both the following conditions are satisfied:

1. *There is at least one non-zero term in $\boldsymbol{S}_{14}$ or $\boldsymbol{S}_{24}$, for any independent decoupled subsystem constituting the global system;*
2. *There is no linear combination between the rows of ($\boldsymbol{S}_{11}$ $\boldsymbol{S}_{13}$ $\boldsymbol{S}_{14}$)"*

These observations amount to an alternative method for establishing paths between the dynamical and source elements, and ensuring the dynamical elements in integral causality are independent.

2.6.8.3 Observability

Typically, detector elements are added to the bond graph to give an output field (adding a fourth row to the Junction Structure Matrix), and these are used to observe the system. Observability is the dual property of controllability, and the criteria for structural observability of the bond graph are therefore similar to those for structural controllability.

Definition 11: Structural Observability of a Bond Graph [99]
The model is structurally state observable iff:

1. *There is a causal path between each dynamical element [in integral causality] and a detector.*
2. *Struct_Rank [**A, C**] = n. Where the structural rank of [**A, C**] is equal to*
   a. *the rank of ($\boldsymbol{S}^T_{11}$ $\boldsymbol{S}^T_{21}$ $\boldsymbol{S}^T_{31}$)^T or*
   b. *n- t_d*

Where t_d is *"the number of the number of dynamical elements remaining in derivative causality when :*

(a) a derivative causality assignment is performed,
(b) a dualization of the maximal number of output detectors is performed in order to eliminate these integral causalities" [99].

Definition 12: Structural Observability of a Bond Graph (JSM) [97]
"A linear system is structurally observable iff both the following conditions are satisfied:

1. *There is at least one non-zero term in ($\boldsymbol{S}_{31}$ $\boldsymbol{S}_{32}$ $\boldsymbol{S}_{33}$) for any independent decoupled subsystem constituting the global system;*
2. *There is no linear combination between the columns of ($\boldsymbol{S}^T_{11}$ $\boldsymbol{S}^T_{13}$ $\boldsymbol{S}^T_{14}$)^T"*

Alternatively, the *dual bond graph* could be constructed and assessed for controllability to give observability [120].

2.6.8.4 Asymptotic Stability

Where asymptotic stability does not exist, it indicates the presence of 'zero modes' (eigenvectors with vanishing eigenvalues). Dauphin-Tanguy and Sueur give the number of 'structurally null modes' (i.e. eigenvalues which are zero, or the poles at the origin) as:

Definition 13: Number of Structurally Null Modes in a Bond Graph [111]
"the number of I and C elements which have to stay in integral causality when a preferred derivative causality is assigned to the bond graph model."

Recall that the characteristic polynomial, and hence eigenvalues, of **A** are found from the determinant of $(s\mathbf{I}-\mathbf{A})$. Furthermore, recall that the BGD effectively inverts **A** and can be used to assess the rank. When storage elements remain in integral causality, **A** loses rank: it is singular and its determinant is known to be zero.

Specifically, the characteristic polynomial can be expanded to identify k structurally null modes which correspond to those elements remaining in integral causality [87]:

$$P(s)=|s\mathbf{I}-\mathbf{A}|=s^{k}\left(s^{q}+a_{q-1}s^{q-1}+\ldots+a_{1}s+a_{0}\right) \qquad \textbf{(14)}$$

Where q is the bond graph rank. The k structurally null modes have no steady state [118] and are therefore not asymptotically stable.

2.6.8.5 Lyapunov Stability

Lyapunov stability – which is typically derived from the physical model rather than numeric computation – is frequently used to inspect bond graph stability and there have been several papers on deriving the Lyapunov function from bond graphs or port-Hamiltonian systems (which can be found from bond graphs) [64,

121, 122]. It is particularly useful for nonlinear systems, where asymptotic stability using laws with an LTI assumption cannot be established.

Since LTI systems are the focus of this thesis, Lyapunov stability will not be used. However, it is important to note that it is an option for further work using nonlinear systems.

2.6.9 Control Properties of Hybrid Bond Graphs

2.6.9.1 Impulse Modes

Sueur and Dauphin-Tanguy [100] suggest the use of a 'pseudo-state variable' when analysing models with elements in derivative causality. This is not a conventional state variable, but the input to the junction structure from an element in derivative causality. When it is included in the state space matrices, it generates an algebraic constraint in the lower portion of the implicit form, which relates to the other state equations. The general form is shown in (15):

$$\begin{bmatrix} \mathbf{I} & \mathbf{E}_{12} \\ 0 & 0 \end{bmatrix} \begin{bmatrix} \dot{\boldsymbol{X}}_i \\ \dot{\boldsymbol{X}}_d \end{bmatrix} = \begin{bmatrix} \mathbf{A}_{11} & \mathbf{A}_{12} \\ \mathbf{A}_{21} & \mathbf{A}_{22} \end{bmatrix} \begin{bmatrix} \boldsymbol{X}_i \\ \boldsymbol{X}_d \end{bmatrix} + \begin{bmatrix} \mathbf{B}_1 \\ \mathbf{B}_2 \end{bmatrix} \boldsymbol{U} \qquad \textbf{(15)}$$

An impulse mode occurs where dynamic behaviour changes instantaneously. They can be clearly seen in the implicit state equations as rows where the time derivative term is zero i.e. the rows relating to elements in derivative causality. Where there is a cross coupling term in **E** (i.e. $\mathbf{E}_{12}$ is nonzero) these equations are differentiated, and since there is a step change between a zero initial value and a finite value at that time step, this differentiation yields an impulse [78]. It follows that the number of impulse modes is equal to the number of elements which are sent into derivative causality by commutation.

Impulse modes can therefore be assessed by inspecting **E** and **A,** as demonstrated by Buisson et al [108] and Rahmani et al [113]. The maximum number of finite modes (and hence minimum impulse modes) occurs in the *reference mode*, taken as the mode of operation where most elements are in integral causalities.

Rahmani's definition of impulse modes [113] is that they exist after commutation. Buisson et al [28, 98] also describe impulse modes as occurring after commutation: they define the model for the reference mode at its origin by converting it into Smith form, and then calculate the maximum possible impulsive modes assuming all switches commutate. These observations make sense for the implicit equations obtained by these authors, which describe a

reference mode and switching law(s) obtained from the use of switched sources. For the unique hybrid model developed here, it shall be seen that the situation is a little more complex.

2.6.9.2 Controllability

For the purposes of switched systems, Rahmani and Dauphin-Tanguy decompose structural controllability into *complete controllability*, *R-controllability* and *impulse controllability* [113]. *Complete Controllability* refers to models which are both R- and Impulse Controllable.

R-controllability refers to controlling the finite dynamic modes, i.e. the system is controllable within the set of reachable states [77]. Rahmani proposes the condition:

Definition 14: Structural R-Controllability of a Hybrid Bond Graph [113]
A Hybrid Bond Graph is R-Controllable iff:

1. *All storage elements are causally connected to a source, and*
2. *Bond Graph Rank* $[s\mathbf{E}-\mathbf{A},\ \ \mathbf{B}]=n$*, i.e. number of finite modes is equal to the model order.*

Where *Bond Graph Rank* [$s\mathbf{E}-\mathbf{A}$, $\mathbf{B}$] is given by causal manipulations in the model.

Definition 15: Bond Graph Rank of [$s\mathbf{E}-\mathbf{A}$, $\mathbf{B}$] **[113]**
"Bg-rank [$s\boldsymbol{E}-\boldsymbol{A}$, $\boldsymbol{B}$*] = n-*t_c *where* t_c *is the number of dynamical elements remaining in integral causality when a dualisation of the maximal number of input sources is performed in the BGD in order to cancel these integral causalities."*

Where BGD denotes the bond graph in preferred derivative causality. Note, therefore, that Point 2 of Definition 14 does *not* necessarily resolve to t_c =0.

Impulse controllability refers to whether impulse modes can be controlled (or excited) by non-impulsive inputs [123].

Both Rahmani et al [113] and Buisson et al [121] propose that impulse modes occur after commutation, and hence define a mode of operation in which every switch has commutated from the reference. Rahmani's observations for impulse

controllability establishes causal paths between switched sources and dynamical elements:

Definition 16: Structural Impulse Controllability of a Hybrid Bond Graph [113]
"A switched system is impulse controllable if and only if the number of impulse modes is equal to the number of disjoint causal paths between input sources and switches passing through (I,C) elements in derivative causality in the BGI."

Where BGI denotes the bond graph in preferred integral causality.

2.6.9.3 Observability

As observability is the dual property of controllability it follows that a hybrid system exhibits R- and Impulse Observability, again relating to the finite and impulse modes respectively. Rahmani defines these as:

Definition 17: Structural R-Observability of a Hybrid Bond Graph [113]
A Hybrid Bond Graph is R-Observable iff:

1. *All storage elements are causally connected to a detector, and*
2. *Bond Graph Rank* $\begin{bmatrix} s\mathbf{E}-\mathbf{A} \\ \mathbf{C} \end{bmatrix} = n$

Where *Bond Graph Rank* $\begin{bmatrix} s\mathbf{E}-\mathbf{A} \\ \mathbf{C} \end{bmatrix}$ is given by causal manipulations in the model.

Definition 18: Bond Graph Rank of $\begin{bmatrix} s\mathbf{E}-\mathbf{A} \\ \mathbf{C} \end{bmatrix}$

"Bg-rank $\begin{bmatrix} s\mathbf{E}-\mathbf{A} \\ \mathbf{C} \end{bmatrix} = n - t_o$ *where* t_o *is the number of dynamical elements remaining in integral causality when a dualisation of the maximal number of output detectors is performed in the BGD in order to cancel these integral causalities."*

Where BGD denotes the bond graph in preferred derivative causality. Note, therefore, that Point 2 of Definition 17 does *not* necessarily resolve to t_o =0.

Definition 19: Structural Impulse Observability of a Hybrid Bond Graph [113]

"A switching system is structurally impulse observable if and only if, the number of impulse modes is equal to the number of disjoint causal paths between the switches and the output detectors passing through (I,C) elements in derivative causality in the BGI."

Where BGI denotes the bond graph in preferred integral causality.

2.7 Summary

What becomes clear from the developments in bond graph modelling – especially with regard to hybrid bond graphs – is that developments have been made in a fragmented manner, with different techniques developed for different uses and applications. In order to bring hybrid models into more common usage and implement them in a commercial software package, a single method must be developed which is suitable for efficient simulation *and* structural analysis, whilst retaining the original principles of offering engineering insight via physical, behavioural modelling. Such a method must allow dynamic causality in order to facilitate engineering insight and prevent artificially stiff models. It must complement the standard bond graph method by representing discontinuities in a graphically intuitive way, and it must generate a concise, usable mathematical model.

There has been a body of work on the analysis of systems. Exploitation of causality and application of Shannon-mason loop rule are well-documented for the standard bond graph, but have not yet been extended to the Hybrid Bond Graph. Structural analysis using matrix-rank criteria from classical control theory are directly reflected in the bond graph. This type of analysis has been established on both standard and – in part – hybrid bond graphs (using switched sources). Qualitative analysis using both causality assignment and structural analysis techniques need extension to be applied to the Hybrid Bond Graph developed in this thesis.

Chapter 3: The Causally Dynamic Hybrid Bond Graph

3.1 Preliminaries

This chapter proposes a new method for constructing a hybrid bond graph. In order to do this, discontinuities are classified as structural and parametric. The controlled junction is proposed to represent structural discontinuities. Guidelines for constructing the hybrid bond graph are given, along with a new causality assignment procedure.

Parametric discontinuities are then described using a new controlled element, derived from a 'tree' of controlled junctions and elements. It will become evident that structural discontinuities will significantly affect the structural analysis of the model, whereas parametric discontinuities do not (and should not).

The general hybrid bond graph is then investigated. A mixed-Boolean junction structure matrix is obtained, and this is used to derive an implicit, mixed-Boolean system equation describing all possible modes of operation.

The method for constructing a causally dynamic hybrid bond graph with structural switching, and consequent derivation of the LTI implicit system equations, forms a separate paper available at http://online.sagepub.com [124].

3.2 Constructing a Hybrid Bond Graph

3.2.1 Discontinuities and Hybrid Bond Graphs

Recall that a hybrid model is a mathematical model which contains both continuous and discontinuous behaviour.

A discontinuity is an abstraction made in order to simplify a model: it is possible to model any system using continuous functions. They are artificial, and made at the discretion of the user. Their purpose is to simplify the equations used to describe a system's behaviour; where a system's behaviour changes rapidly with

time, describing that change as a discontinuity can improve simulation time, and aid engineering insight and analysis. They usually describe highly nonlinear behaviour which would be difficult to describe and time-consuming to compute using continuous functions. They can also describe variable topology problems, which are where the equations used for each mode of operation change significantly, with varying numbers of states and boundary conditions (for example, contact).

The variety of approaches to switching and hybrid bond graphs are a result of the variety of types of behaviour they can describe. Initially, a distinction must be made between the Hybrid Bond Graph and Switching Bond Graph.

Definition 20: Hybrid Bond Graph
A Hybrid Bond Graph is any bond graph that describes both continuous and discontinuous behaviour.

Recall that hybrid models can be categorised into *switching* and *impulse* models [12]. Likewise, Hybrid Bond Graphs can be categorised as Switching Bond Graphs and Impulse Bond Graphs. The term 'Hybrid Bond Graph' is widely applied to bond graphs featuring switching or Boolean-controlled elements, sources or junctions, which usually results in a switching bond graph.

Definition 21: Switching Bond Graph
A Switching Bond Graph is an extension of the standard bond graph method, in which some form of switching element is introduced to model instantaneous changes. They can be viewed as a collection of classical bond graphs, each one describing a mode of operation [44].

However, there are some varieties of hybrid bond graphs which describe impulsive rather than switching behaviour. The term 'impulse bond graph' refers to a specific method [14] but some other hybrid bond graphs can be developed which yield an impulse model.

The terms 'switching' and 'hybrid' bond graph have been used interchangeably in the literature. For consistency, the term Hybrid Bond Graph is used throughout this thesis because the general method should encompass all kinds of discontinuity.

3.2.2 Classification of Hybrid Behaviour

The term ‘discontinuity’ is fairly vague, and so a classification is made to aid application to engineering problems. Discontinuities are often classified as ideal (no losses) or non-ideal (associated with an energy loss) [113], switching or impulse [12] or according to whether they are autonomous or externally controlled. If they are assumed to be controlled by some form of automaton, they can be classified according to whether the controlling automata are *time-scale* dependant or *parameter* dependent [125]. For the purposes of this thesis, an additional distinction is made between *structural* and *parametric* discontinuities. This distinction is necessary to describe where in the model (and underlying equations) the discontinuity should occur: between elements or internal to an element.

Definition 22: Structural Discontinuities
Structural Discontinuities occur when parts of the model are connected or disconnected, interrupting power flow between components. These discontinuities often give rise to variable topology *models.*

Engineering examples of this type of discontinuity are the hydraulic valve, mechanical clutch, ideal electrical switch, or contact between bodies.

Definition 23: Parametric Discontinuities
Parametric Discontinuities occur when an element has a highly nonlinear constitutive equation, which has been abstracted to a piecewise continuous function. The structure of the model is unchanged, it is the equation describing the behaviour of an element which changes.

Common examples of parametric discontinuities are dry friction, tyre forces, a nonlinear damper ‘breaking out,’ or saturation of an electrical capacitor or hydraulic accumulator.

These two types of discontinuity can be represented differently in a hybrid bond graph: a controlled junction with dynamic causality for structural switching, and a controlled element for parametric switching.

In many cases – particularly the mechanical domain - the distinction between structural and parametric switching is clear. However, there are cases where it is less so. An electrical switch is physically an element which the user inserts into a circuit, and is often visualised in control theory as a discontinuous input, hence

the use of switching sources and elements in the literature. There is a strong case for treating it as parametric switching. Here the dynamic causal assignment is key: disconnecting a voltage or current source can force electrical storage elements to discharge, which is consistent with them switching to derivative causality. The controlled junction proposed for structural switching clearly shows where structure is disconnected and ideal causality assignment changes with commutation.

3.2.3 The Controlled Junction for Structural Discontinuities

Structural switching activates or deactivates part of a system, and a controlled junction can be used to (dis)connect or (de)activate part of the model accordingly. Controlled junctions, defined by Mosterman and Biswas [40], are recommended by other authors [36, 56] as an intuitive and physically correct representation for discontinuities. They were selected here to represent structural switching because they clearly show where structure connects and disconnects, and breaks the path of power flow. This is not only important from the point of view of engineering insight, but the controlled junction lends itself to being represented in the junction structure matrix and hence developing hybrid system equations.

A controlled junction behaves as a normal 1- or 0-junction when ON and a source of zero flow or effort (respectively) when OFF. A controlled 1-junction is therefore used to break or inhibit flow (for example, an electrical switch which breaks the flow of current) and a controlled 0-junction is used to inhibit effort (for example, a clutch or other physical non-contact in a mechanical system). This always gives rise to dynamic causality on one of the attached bonds. The commonly accepted notation for controlled junctions is X1 and X0, which will be used in this paper.

Based on the above description, controlled junctions X1 and X0 can be formally defined as 2-port elements with associated Boolean parameters λ. They are initially defined as 2-ports for clarity, and it can be seen that they bear a striking resemblance to the Boolean modulated transformer. However, the definition can easily be extended to more than 2 ports. The bond graph representations of controlled junctions X1 and X0 are as shown in Figure 1, and their defining relationships are given by Equations (16) and (17), respectively.

Figure 2: Bond graph representation of switched junctions X1 and X0

$$\begin{cases} \lambda\, f_1 = \lambda\, f_2 \\ \lambda\,(e_1 - e_2) = 0 \\ \bar{\lambda}\, f_1 = 0 \\ \bar{\lambda}\, f_2 = 0 \end{cases} \quad \textbf{(16)} \qquad \begin{cases} \lambda\, e_1 = \lambda\, e_2 \\ \lambda\,(f_1 - f_2) = 0 \\ \bar{\lambda}\, e_1 = 0 \\ \bar{\lambda}\, e_2 = 0 \end{cases} \quad \textbf{(17)}$$

The Boolean parameter λ selects the set of equations that are valid given the state of the switch: $\lambda = 1$ when the switch is ON and $\lambda = 0$ when the switch is OFF. For each controlled junction, the defining equations (16) and (17) lead to 3 possible causal configurations:

- 2 causal configurations when the switch is ON i.e. $\lambda = 1$ (first two equations equivalent to a normal 1 or 0 junction)
- a unique causal configuration when the switch is OFF i.e. $\lambda = 0$ (last two equations equivalent to null sources of flow or null sources of effort imposed by the element to both power ports with conjugate variables externally imposed to the element).

In switching between ON and OFF states, the causal assignment around a controlled junction must change. In the ON state, where it behaves as a regular junction, there must be a causal input (i.e. a bond with a causal stroke defining the common effort for a 0-junction or common flow for a 1-junction). In the OFF state, where the controlled junction becomes a null source on each incident bond, there is no causal input and the causal assignment on that one bond changes. This is known as *dynamic causality*, and – using this definition of a controlled junction – it is unavoidable.

Controlled junctions and their associated assignment statements are summarised in Table 2.

Dynamic causality will be discussed further in section 3.2.5, where it is clear that dynamic causality is necessary and representative of systems with structural discontinuities.

3.2.4 Model Simplification with Controlled Junctions

If a bond graph is constructed from the schematic diagram of a system, there is often potential to simplify the bond graph model. Since a controlled junction only behaves as a junction in one state, it cannot be eliminated and the rules for simplifying bond graphs must be augmented as follows.

Rule 1: 2-Port Controlled Junctions

A controlled junction with only two ports cannot be removed and replaced with a single bond (whereas a regular junction could).

A regular junction with 2-ports can be replaced by a single bond, since the efforts and flows on the two incident bonds are equal. A controlled junction with 2-ports connects and disconnects its incident bonds with commutation: in principle like a switching bond or Boolean-modulated transformer (with dynamic causality). Removing the controlled-junction would result in the surrounding structure being connected at all times.

Rule 2: Neighbouring Junctions – Controlled and Regular Junctions

When a regular junction and controlled junction of the same type are neighbouring, they can be merged into a single controlled junction.

I.e. When a 1-junction and X1-junction are next to each other, they can be merged into a single X1-junction .

Likewise, a 0-junction and X0-junction next to each other can be merged into a single X0-junction.

When two like regular junctions are next to each other, they can be merged into a single junction. When one of those junctions is controlled, the commutating behaviour must be retained. This simplification results in elements being disconnected with commutation, whereas they would have remained connected to some substructure without the simplification (shown in Figure 3).

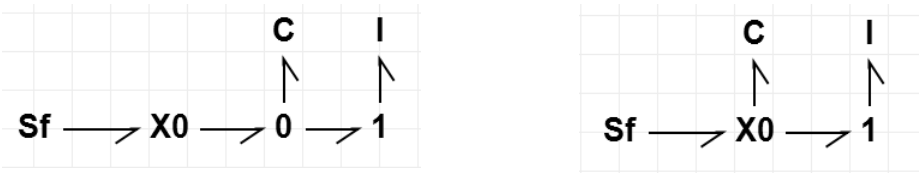

a) Unsimplified Model **b) Simplified Model**

Figure 3: An Example Subsystem with Neighbouring Regular and Controlled Junctions

---

Rule 3: Neighbouring Junctions – Multiple Controlled Junctions

When neighbouring controlled junctions have two ports only, they can be combined into a single controlled junction. This controlled junction is ON only when the states of both the constituent controlled junctions are ON.

When neighbouring controlled junctions have more than two ports, they cannot be combined. This is because the power to the incident elements or subsystems depends on the state of the individual controlled junction.

Figure 4 demonstrates how two neighbouring 2-port controlled junctions can be combined: the power source is only connected to the resistor when controlled junction 1 AND controlled junction 2 are ON. The causal conflict arising between the junctions when both are OFF may be ignored.

However, when the controlled junctions have additional elements attached, it is no longer appropriate to combine them. There is power flow across each junction when it is ON and the other is OFF. The two controlled junctions cannot be combined in any manner which would reflect this behaviour.

Structure which adds nothing to the model can frequently be removed. This often happens in the case of electrical and hydraulics circuits where there is a return line to a zero ground or open tank. Ground parts are source elements which also act as a sink. For example, a mechanical ground is represented by a Sf-element (which has zero velocity and is a sink for force), and grounds in other domains are represented by Se-elements (e.g. an electrical ground, which is a source of 0V and a sink for current). They are usually null sources, but can have nonzero values (such as a pressurised hydraulic tank or undulating mechanical ground).

Rule 4: Removal of Ground Parts

When a controlled junction is positioned between a dissimilar ground and the main structure, it is not appropriate to remove the ground. I.e. a null source of flow connected via a X0-junction cannot be removed. Likewise, a null source of effort connected via a X1-junction cannot be removed.

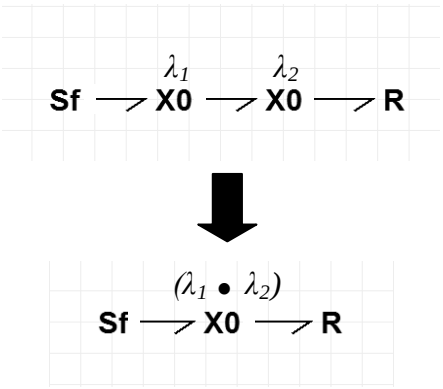

a) 2-Port Junctions, simplified to a single junction which is ON when λ_1 AND λ_2 are true

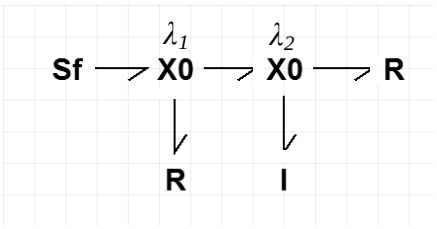

b) Additional Elements giving 3-Port Junctions

Figure 4: An Example Subsystem with Neighbouring Controlled Junctions.

When the ground or tank is a null source, and it is not a causal input to the structure of interest, it can be deleted. An example is given in Figure 5: the ground is a source of zero effort, and it adds nothing to the 1-junctions it is attached to (about which efforts are summed).

When a controlled junction exists between the ground and the main structure, it may not be appropriate to remove the ground. For example, in the system in Figure 6, an electrical switch (represented by a X1-junction) could be inserted so that the resistance is now a non-ideal switch, shown in Figure 6. In real terms, this breaks the circuit and changes its behaviour. In bond graph terms, this means that incident structure has a zero flow imposed on it when the X1-junction is OFF, rather than a zero effort (from the ground) which will have implications for the causal assignment. In simplifying the bond graph, the controlled junction and null source group must therefore be kept, because they can have a significant effect on the system.

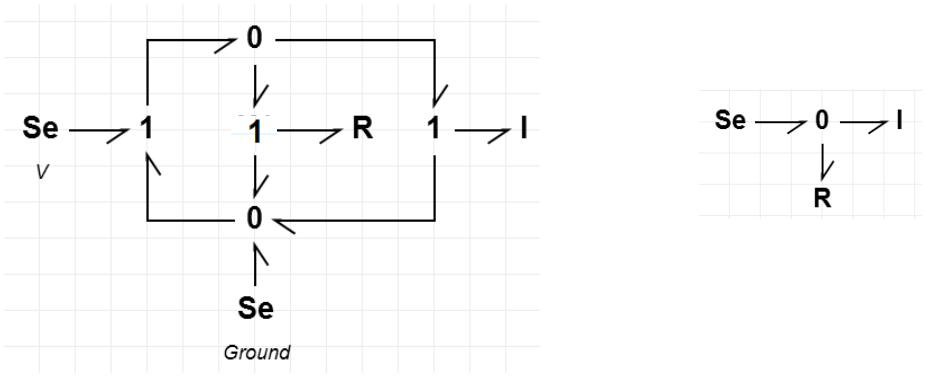

a) Full model **b) Simplified**

Figure 5: An Example System with a Ground.

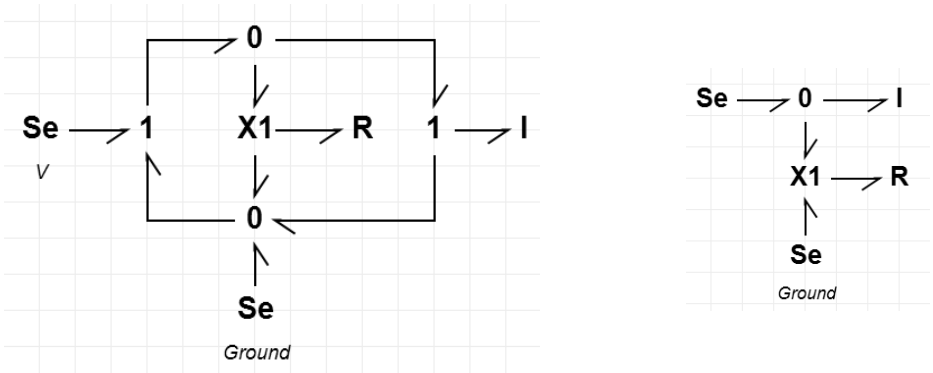

a) Full model **b) Simplified**

Figure 6: An Example System with a Ground and a Controlled Junction.

3.2.5 A Dynamic Causality Assignment Procedure

Causality in a bond graph is typically assigned using the *Sequential Causality Assignment Procedure (SCAP)* [3]. Using controlled junctions, dynamic causality is unavoidable. However, dynamic causality can be minimised (without artificially constraining it) in order to generate the smallest possible set of equations. Low et al [36] observe that dynamic causality can be minimised when a 1-port element is on the junction and propose SCAPH for hybrid bond graphs. However, their assertion that static causality can be maintained only applies to their method of deleting the controlled junction when it is OFF, potentially

giving rise to hanging junctions/elements and a different causality assignment (see Figure 7).

Table 2: Definition, causal configuration and equations of controlled junctions.

Controlled junction representation and defining equations	State of the switch	Possible causal configurations	Associated assignment statements
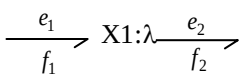 $\begin{cases}\lambda f_1 = \lambda f_2 \\ \lambda(e_1 - e_2) = 0 \\ \bar{\lambda} f_1 = 0 \\ \bar{\lambda} f_2 = 0\end{cases}$	ON ($\lambda = 1$)	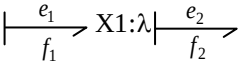 or 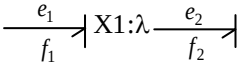	$e_1 := e_2$ $f_2 := f_1$ or $e_2 := e_1$ $f_1 := f_2$
	OFF ($\lambda = 0$)	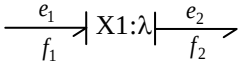	$f_1 := 0$ $f_2 := 0$ e_1 and e_2 arbitrary
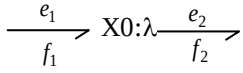 $\begin{cases}\lambda e_1 = \lambda e_2 \\ \lambda(f_1 - f_2) = 0 \\ \bar{\lambda} e_1 = 0 \\ \bar{\lambda} e_2 = 0\end{cases}$	ON ($\lambda = 1$)	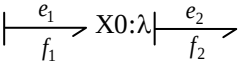 or 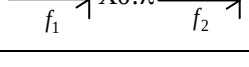	$e_2 := e_1$ $f_1 := f_2$ or $e_1 := e_2$ $f_2 := f_1$
	OFF ($\lambda = 0$)	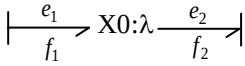	$e_1 := 0$ $e_2 := 0$ f_1 and f_2 arbitrary

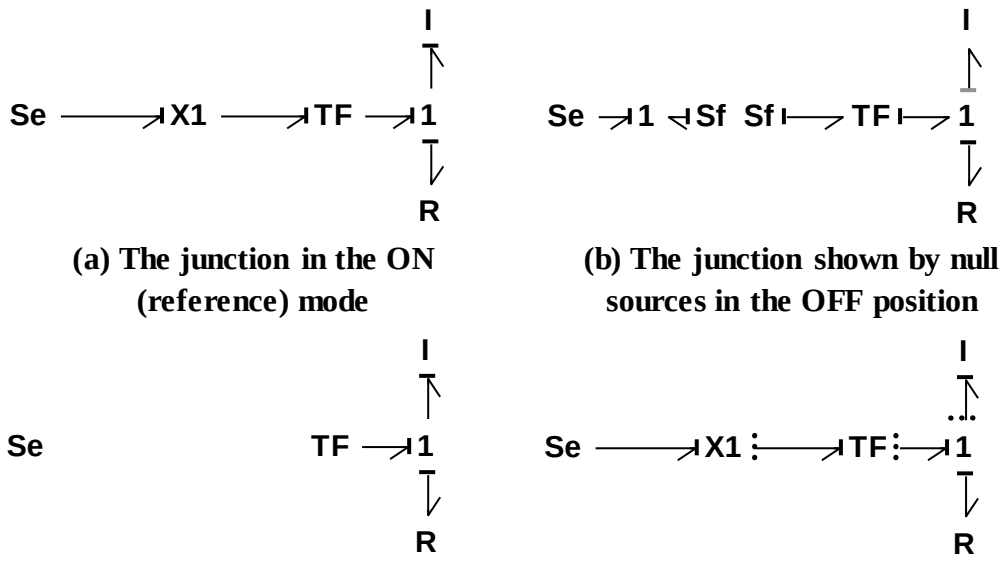

(a) The junction in the ON (reference) mode

(b) The junction shown by null sources in the OFF position

(c) The causality assignment gained when the switch is deleted in the OFF position (I remains in integral causality)

(d) The proposed method for showing dynamic causality

Figure 7: An Example of Causality Assignments and their Effect around a Controlled Junction

The causality assignment procedure for the hybrid bond graph proposed in this paper starts with a reference mode of operation. This is defined with a maximum number of elements in integral causality, and controlled junctions preferably ON. This is the mode which should be easiest to simulate. Deviations from this reference due to dynamic causality are marked as dashed causal strokes. This enables the user to see the effects of commutation on causality, and aids in equation generation. The Dynamic Sequential Causality Assignment Procedure (DSCAP) to represent all modes of a hybrid bond graph model can be summarised in the following procedure.

Procedure 1: Dynamic Sequential Causality Assignment Procedure (DSCAP) for hybrid bond graph

Step 1) Assign causality according to SCAP with preferred integral causality, stopping when a controlled junction is reached. i.e. start by assigning causality to a source element, and propagate causality throughout the bond graph as far as any controlled junctions. Repeat for other source elements, and then for any storage elements which have not yet been assigned causality. If causal conflict occurs in this stage, the model should be changed.

The causal assignment from step 1 may dictate whether some switches are ON or OFF.

Step 2) Choose a controlled junction which does not have its causality fully assigned. Assign causality around the controlled junctions assuming the switch to be ON (as indicated in Table 1) and propagate as far as possible. Repeat this stage until all controlled junctions have their causality fully assigned.

Step 3) Finish propagating causality throughout the bond graph to any resistance elements or remaining bonds and propagate as far as possible.

Step 4) Taking each controlled junction in turn, consider the causality assignment when it is in the other state to the reference configuration. Mark this causality assignment with a dashed causal stroke, and propagate throughout the bond graph (Figure 7d). If causal conflict occurs in this stage, then the other state of the controlled junction is not allowed.

Remark: Causal propagations in step 2 and step 4 of the algorithm above may dictate the state (ON or OFF) of some controlled junctions as a result of the assigned state of others. This reveals some constraints in the state of switches indicating the allowed configurations or physically feasible modes of operation.

Figure 7 shows a simple example of the effect of the causality assignment around a controlled junction when ON and OFF. The representation is compared in this example with the method of deleting the switch when OFF as proposed by Low et al [36].

3.2.6 The Controlled Element for Parametric Discontinuities

This section proposes a new *controlled element* for the modelling of parametric switching. They should not be confused with the existing switched element, which has an on/off behaviour [32].

Parametric switching has been defined as the case where an element has a piecewise continuous constitutive equation. These may be hard nonlinearities, where the behaviour of an element changes so quickly that it can be considered instantaneous. Alternatively, they can occur where some relationship (gained via empirical data or a high-order function) is best described using a piecewise continuous function. Classic examples are [coulomb and static] friction, and tyre lateral stiffness, shown in Table 3.

Table 3: Examples of Piecewise-Continuous Equations

'Hard' Friction	Generic Tyre Static Load / Deflection Curves
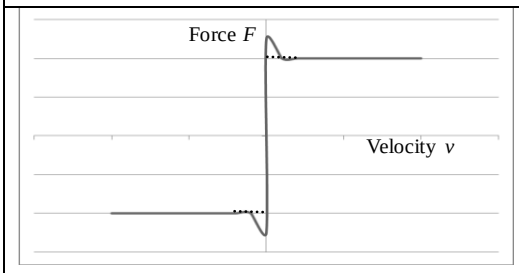	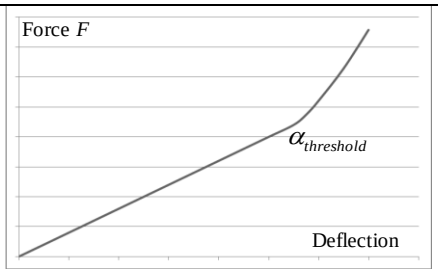
$F = \mu\lvert F_N\rvert \mathrm{sgn}(v)$ Where F_N is normal force and μ is friction coefficient	$F = f_1(\alpha) \quad \alpha \le \alpha_{threshold}$ $F = f_2(\alpha) \quad \alpha > \alpha_{threshold}$ Where α is slip angle, related to linear deflection

Parametric switching can be considered as mode switching, i.e. a collection of continuous modes of operation. These are controlled by an automaton, petri-net or similar, which allows the system to switch between modes of operation. Mode switching is historically modelled by a 'tree' of ideal switches and elements. Each element gives the constitutive equation for a specific mode of operation, and the ideal switches (de)activate it as required. Naturally, only one ideal switch can be ON at any time during a simulation. Strömberg [126] formulates mode switching trees of switched sources, and Mosterman and Biswas [40] present a multi-bond controlled junction selecting a continuous bond graph element from a number of possibilities.

Mode switching has a conceptual advantage in that it aids the development of finite state automata for simulation. However, the 'tree' notation means a model can rapidly grow to a vast size with multiple inputs and outputs for all possible modes of operation. This makes it less ideal for structural analysis and equation generation purposes. The multi-bond notation suggested by Mosterman and Biswas goes some way to controlling this, but is a little confusing because multibond notation is typically used for multiple degrees of freedom in a model. Their idea is used as a basis for the controlled element defined here.

Consider an element with a piecewise-continuous constitutive function. A mode-switching tree can be constructed using the controlled junctions with associated Boolean terms (as used for structural switching), as shown in Figure 8. Note that a resistance element is shown, but the principle holds true for inertia and compliance elements.

In this tree, controlled junctions (de)activate the modes of operation, which are given by resistance elements on each branch. These 'branches' are then connected by a regular junction which sums the output values.

a) A 'Tree' of X0-Junctions **b) A 'Tree' of X1-Junctions**

Figure 8: Bond Graph 'Trees' for a Piecewise Linear Resistance Element, Assuming Three Modes of Operation.

- In Figure 8a) efforts are summed about a 1-junction: these efforts are the effort exerted by the resistance when a junction is ON plus the zero efforts exerted by the XO-junctions when they are OFF.
- In Figure 8b), it is flows which are summed around a zero junction: these flows are the flow exerted by the resistance when a junction is ON plus the zero flows exerted by the X1-junctions when they are OFF.

In a bond graph tree it is important to note that the controlled junctions are constrained so that only one may be ON at any time.

In order to condense the 'tree' into a single controlled element, consider the underlying equations. Quantities are shown in Figure 9, which also includes some source elements in order to obtain the equations. A reference configuration of $\lambda_1 = 1$, $\lambda_2 = 0$, $\lambda_3 = 0$ is arbitrarily assumed. Note that dynamic causality is internal to the tree: there is static causality on the resistance elements and the input bond.

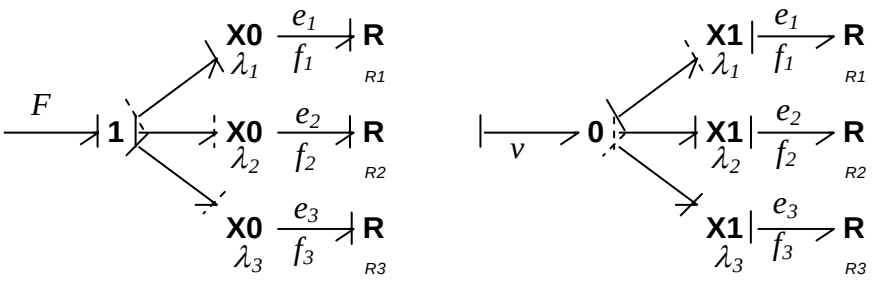

Figure 9: The Piecewise Linear Resistance Element Subsystem, showing quantities used in Equation Generation.

The Junction Structure Matrices are:

$$\begin{bmatrix} \lambda_1 & 0 & 0 \\ 0 & \lambda_2 & 0 \\ 0 & 0 & \lambda_3 \end{bmatrix} \begin{bmatrix} e_1 \\ e_2 \\ e_3 \end{bmatrix} = \begin{bmatrix} 0 & 0 & 0 & \lambda_1 \\ 0 & 0 & 0 & \lambda_2 \\ 0 & 0 & 0 & \lambda_3 \end{bmatrix} \begin{bmatrix} f_1 \\ f_2 \\ f_3 \\ F \end{bmatrix} \qquad \begin{bmatrix} \lambda_1 & 0 & 0 \\ 0 & \lambda_2 & 0 \\ 0 & 0 & \lambda_3 \end{bmatrix} \begin{bmatrix} f_1 \\ f_2 \\ f_3 \end{bmatrix} = \begin{bmatrix} 0 & 0 & 0 & \lambda_1 \\ 0 & 0 & 0 & \lambda_2 \\ 0 & 0 & 0 & \lambda_3 \end{bmatrix} \begin{bmatrix} e_1 \\ e_2 \\ e_3 \\ v \end{bmatrix}$$

And the Field Laws $D_{in} = LD_{out}$ are:

$$\begin{bmatrix} e_1 & 0 & 0 \\ 0 & e_2 & 0 \\ 0 & 0 & e_3 \end{bmatrix} = \begin{bmatrix} \lambda_1 R_1 & 0 & 0 \\ 0 & \lambda_2 R_2 & 0 \\ 0 & 0 & \lambda_3 R_3 \end{bmatrix} \begin{bmatrix} f_1 \\ f_2 \\ f_3 \end{bmatrix} \qquad \begin{bmatrix} f_1 & 0 & 0 \\ 0 & f_2 & 0 \\ 0 & 0 & f_3 \end{bmatrix} = \begin{bmatrix} \lambda_1 R_1^{-1} & 0 & 0 \\ 0 & \lambda_2 R_2^{-1} & 0 \\ 0 & 0 & \lambda_3 R_3^{-1} \end{bmatrix} \begin{bmatrix} e_1 \\ e_2 \\ e_3 \end{bmatrix}$$

Looking at the summation, we can write:

$$f = f_1 + f_2 + f_3$$
$$f = \lambda_1 R_1^{-1} e_1 + \lambda_2 R_2^{-1} e_2 + \lambda_3 R_3^{-1} e_3$$

And, since flow is constant,

$$e = e_1 + e_2 + e_3$$
$$e = \lambda_1 R_1 f_1 + \lambda_2 R_2 f_2 + \lambda_3 R_3 f_3$$

And, since effort is constant,

$$f = \left(\lambda_1 R_1^{-1} + \lambda_2 R_2^{-1} + \lambda_3 R_3^{-1}\right) F \qquad e = \left(\lambda_1 R_1 + \lambda_2 R_2 + \lambda_3 R_3\right) v$$

This principle will hold true for 'trees' of compliance and inertia elements. A general definition for the controlled element can therefore be defined as shown in Table 4.

Proposition 1: A Controlled Element for Parametric Switching

A mode-switching tree of controlled junctions and elements can be condensed into a single controlled element. This controlled element has the general constitutive function:

$$output = \sum_{n=1}^{i} \lambda_n \Phi_n (input) \qquad \textbf{(18)}$$

Where n is the number of branches to the tree, λ_n is the Boolean term associated with nth controlled junction and Φ_n is the constitutive function of the nth element.

Table 4: Controlled Elements and their Constitutive Equations (Causally Static, Linear Case)

⟶ XR or ⊢⟶ XR	$f = \left(\sum \lambda R^{-1}\right) e$ or $e = \left(\sum \lambda R\right) f$
⊢⟶ XC	$e = \left(\sum \lambda C^{-1}\right) \int f \cdot dt$
⟶ XI	$f = \left(\sum \lambda I^{-1}\right) \int e \cdot dt$

The controlled element may be in dynamic causality (i.e. the output is effort in some modes and flow in others) it can be treated in the same way as a standard element in dynamic causality i.e. having two input/output pairs for the two causal assignments. This would occur where a storage element saturates. For example, a hydraulic accumulator is a compliance element with an effort output in normal operation, but when it saturates it becomes a source of zero flow.

Table 5 overviews the possible controlled elements, defining them as elements with a Heaviside function as their constituent equations (which can be controlled either internally or by an external modulation signal).

Table 5: Proposed Constituent Equations for Controlled Elements (General Case)

⊢→ XC	$e = \begin{vmatrix} \Phi_{C1}^{-1}\left(\int f \cdot dt\right) \\ \vdots \\ \Phi_{Cn}^{-1}\left(\int f \cdot dt\right) \end{vmatrix}$
→⊣ XI	$f = \begin{vmatrix} \Phi_{I1}^{-1}\left(\int e \cdot dt\right) \\ \vdots \\ \Phi_{In}^{-1}\left(\int e \cdot dt\right) \end{vmatrix}$
→⊣ XR or ⊢→ XR	$f = \begin{vmatrix} \Phi_{R1}^{-1}(e) \\ \vdots \\ \Phi_{Rn}^{-1}(e) \end{vmatrix}$ or $e = \begin{vmatrix} \Phi_{R1}(f) \\ \vdots \\ \Phi_{Rn}(f) \end{vmatrix}$
⊢⇢ XC	$e = \begin{vmatrix} \Phi_{C1}^{-1}\left(\int f \cdot dt\right) \\ \vdots \\ \Phi_{Cn}^{-1}\left(\int f \cdot dt\right) \end{vmatrix}$ $f = \begin{vmatrix} \Phi_{C1d}\dfrac{d}{dt}(e) \\ \vdots \\ \Phi_{Cm}\dfrac{d}{dt}(e) \end{vmatrix}$
⇢→⊣ XI	$f = \begin{vmatrix} \Phi_{I1}^{-1}\left(\int e \cdot dt\right) \\ \vdots \\ \Phi_{In}^{-1}\left(\int e \cdot dt\right) \end{vmatrix}$ $e = \begin{vmatrix} \Phi_{I1i}\dfrac{d}{dt}(f) \\ \vdots \\ \Phi_{\mathrm{Im}}\dfrac{d}{dt}(f) \end{vmatrix}$
⊢⇢ XR	$f = \begin{vmatrix} \Phi_{R1}^{-1}(e) \\ \vdots \\ \Phi_{Rn}^{-1}(e) \end{vmatrix}$ $e = \begin{vmatrix} \Phi_{\hat{R}1}(f) \\ \vdots \\ \Phi_{\hat{R}n}(f) \end{vmatrix}$

3.3 Implicit Formulation of the Hybrid Junction Structure Relation

3.3.1 Pseudo-States and Dynamic Causality

Recall that, for a regular (causally static) bond graph, the inputs and outputs to the system from the various elements are used in generating equations. Specifically, the inputs to the system from the storage fields (i.e. the outputs of the compliance and inertia elements in integral causality) are usually taken as the time-derivatives of the state variables. The state variables are consequently displacement (for compliance elements) and momentum (for inertia elements). When elements are in derivative causality, the state equations are no longer independent: there are *dependent states* associated with the elements in

derivative causality which yield algebraic equations. Sueur and Dauphin-Tanguy [97] associate a *pseudo-state* variable with each element in derivative causality to generate an implicit mathematical model containing the relevant algebraic constraints.

When causality is dynamic, the underlying equations change. Storage elements may switch from integral to derivative causality, and the inputs and outputs of the resistance elements may reverse. The resulting state space matrices may change size depending on the mode.

Storage elements in dynamic causality can be described using a variable for each of the two possible causal assignments: a state variable for the integral causality case, and a pseudo-state variable for derivative causality. Buisson et al [98] do this to recover the implicit state equations from a single mode of operation. The philosophy of using two variables, a state and a pseudo-state, to represent the two modes of storage element can be extended here. The model describes all possible modes of operation by including input and output variables for both possible states of an element in dynamic causality. These are (de)activated in the appropriate modes of operation. The LTI form remains valid because the switching behaviour is not necessarily a function of time: the equations capture the model at all time points.

3.3.2 The General Hybrid Bond Graph

A causal bond graph model can be represented in matrix format, as a Junction Structure Matrix (JSM) consisting of ones and zeros which relate the system inputs and outputs. The JSM based on the Paynter Junction Structure is used here, since it has reached common use in bond graph structural analysis. The coefficients in the transformer field (representing any transformer or gyrator elements, sometimes expressed outside the junction structure matrix) are brought inside the JSM to give terms other than one and zero.

The General Bond Graph structure is shown in Figure 10, with a modified 'hybrid' version to capture structural switching behaviour and the induced dynamic causality. There are two significant differences:

1. Using the Dynamic Sequential Causality Assignment Procedure (DSCAP) proposed in section 3.2, the causal hybrid bond graph would display some elements with static causality and some with dynamic causality (represented by dashed causal strokes, as shown in Figure 10b).

The Hybrid Junction Structure Matrix (relating all possible system inputs and outputs) and state equation can be derived from this representation.

2. The Hybrid Junction Structure Matrix **S** contains Boolean parameters λ indicating the state of controlled junctions (used to describe structural switching). These Boolean 'switching terms' in the submatrices of **S** will therefore be carried through into the state equations derived from it.

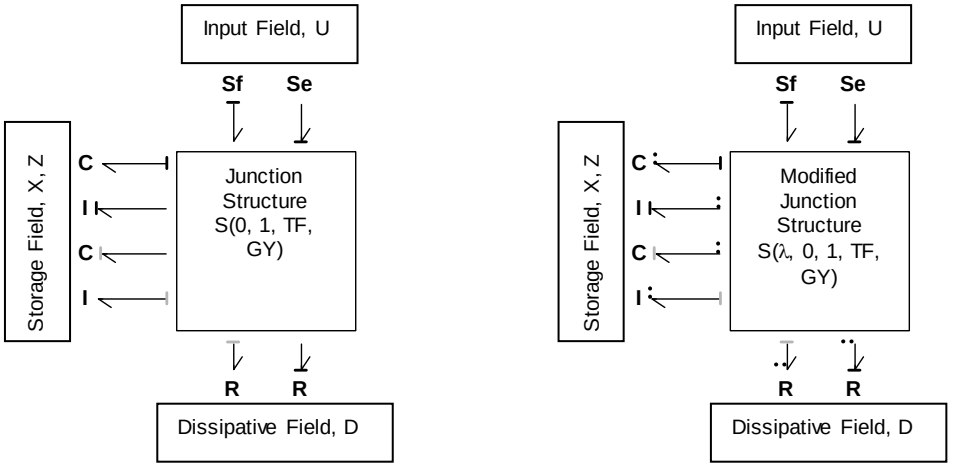

(a) General Junction Structure

(b) Hybrid Junction Structure incorporating switching (λ) coefficients and dynamic causality

Figure 10: The Junction Structure Matrix and Generalised Bond Graph.

Note that the Boolean terms λ appearing in the Junction Structure Matrix reflect controlled junctions between elements, and indicate where casual paths are severed or connected with commutation. There may be additional Boolean terms in the storage and resistance fields where parametric discontinuities exist within controlled elements.

3.3.3 Notation

Figure 11 represents the block diagram derived from the hybrid causal bond graph and the key variables used, which are defined as follows. Note that the inputs to the elements are the outputs from the junction structure, and vice versa.

i) Elements with static causality have the usually defined variables:
   - Input vectors denoted $\dot{\hat{\boldsymbol{X}}}_i$ composed of $\dot{p}$ and $\dot{q}$ on I and C elements in integral causality, $\hat{\boldsymbol{Z}}_d$ composed of f and e on I and C elements in derivative causality and $\hat{\boldsymbol{D}}_{out}$ composed of effort or flow variables into dissipative elements
   - Output vectors denoted $\hat{\boldsymbol{Z}}_i$ and $\dot{\hat{\boldsymbol{X}}}_d$ for storage elements and $\hat{\boldsymbol{D}}_{in}$ for dissipative elements

ii) However, dynamic causality is captured in the block diagram by specifying two sets of inputs and output variables:
   - Two input vectors. For storage elements in dynamic causality, these inputs are $\dot{\tilde{\boldsymbol{X}}}_i$ for the integral causality case and $\tilde{\boldsymbol{Z}}_d$ for the dynamic causality case, and are composed of $\dot{p}$, $\dot{q}$, f and e For dissipative elements in dynamic causality, there is an effort output $\tilde{\boldsymbol{D}}_{e\_out}$ and flow output $\tilde{\boldsymbol{D}}_{f\_out}$. In any single mode of operation, one input is active and the other is redundant.

   - Two output vectors which are the complements of the inputs above. For storage elements in dynamic causality, these are $\dot{\tilde{\boldsymbol{X}}}_d$ and $\tilde{\boldsymbol{Z}}_i$ composed of $\dot{p}$, $\dot{q}$, f and e. For dissipative elements in dynamic causality, there is an effort output $\tilde{\boldsymbol{D}}_{e\_in}$ and flow output $\tilde{\boldsymbol{D}}_{f\_in}$. Again, in any single mode of operation, one output is active and the other is redundant.

It is worth noting that an element can only have two modes of operation (flow input / effort output and effort input / flow output), although a model can have several modes of operation overall if it contains multiple controlled junctions.

Controlled junctions in the bond graph are assigned Boolean variables $\boldsymbol{\lambda}$ in the Junction Structure (which has a value of 1 when the junction is ON and 0 when OFF), signifying that there is a connection between two quantities when the junction is ON. A single bond graph therefore represents all possible modes of operation and causal assignments. Vectors $\dot{\boldsymbol{X}}_i = \left[\dot{\hat{\boldsymbol{X}}}_i \quad \dot{\tilde{\boldsymbol{X}}}_i\right]^{\mathrm{T}}$ and $\dot{\boldsymbol{X}}_d = \left[\dot{\hat{\boldsymbol{X}}}_d \quad \dot{\tilde{\boldsymbol{X}}}_d\right]^{\mathrm{T}}$ are the state and pseudo-state of the storage fields in integral and derivative causality respectively. $\boldsymbol{Z}_i = \left[\hat{\boldsymbol{Z}}_i \quad \tilde{\boldsymbol{Z}}_i\right]^{\mathrm{T}}$ and $\boldsymbol{Z}_d = \left[\hat{\boldsymbol{Z}}_d \quad \tilde{\boldsymbol{Z}}_d\right]^{\mathrm{T}}$ are the complementary vectors of these states (shown in Figure 10), related by $\boldsymbol{Z}_i = \mathbf{F}_i \boldsymbol{X}_i$ and

$\boldsymbol{Z}_d = \mathbf{F}_d \, \boldsymbol{X}_d$. Resistive field also have inputs and outputs $\boldsymbol{D}_{in} = \left[\hat{\boldsymbol{D}}_{in} \quad \tilde{\boldsymbol{D}}_{in}\right]^{\mathrm{T}}$ and $\boldsymbol{D}_{out} = \left[\hat{\boldsymbol{D}}_{out} \quad \tilde{\boldsymbol{D}}_{out}\right]^{\mathrm{T}}$ related by $\boldsymbol{D}_{in} = \mathbf{L}\, \boldsymbol{D}_{out}$.

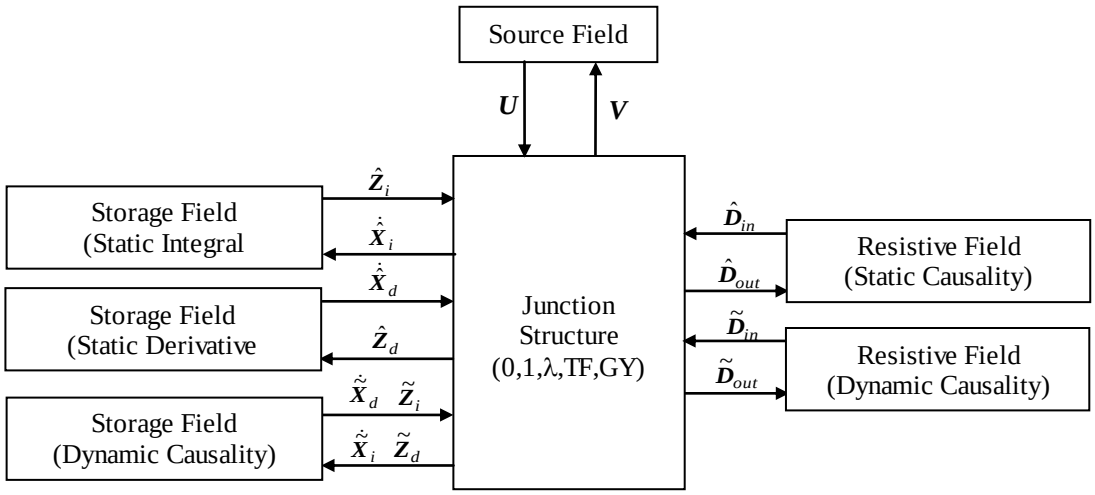

Figure 11: Quantities used in Hybrid Junction Structure Matrix and Subsequent Development

3.3.4 Comparison of Standard and Hybrid Model Equations

The process of deriving a Junction Structure Matrix, and then an implicit state equation, from a standard bond graph is well established [97], as is the process for equation generation from a bond graph using switched sources [97, 98, 113]. For the Hybrid bond graph (with controlled junctions) defined here, a similar procedure is followed with two important differences:

- The matrices obtained are functions of Boolean variables representing the controlled junctions parameters. The 1's and 0's in the junction structure matrix establish whether a causal path exists, and a Boolean term denotes that the path is dependent on the state of a switch(es).

- There is an additional matrix $\boldsymbol{\Lambda(\lambda)}$ which manages dynamic causality. Recall that an element in dynamic causality has two possible inputs and outputs. $\boldsymbol{\Lambda(\lambda)}$ multiplies the output vector by 0 or 1 (depending on the

state of the Boolean term) to (de)activate outputs depending on whether they occur in a given mode of operation (Table 6).

Hence, a single set of equations is generated which encompasses all possible modes of operation and caters for dynamic causality.

In the following development it will be assumed that the system elements are linear for ease of comparison with classical control theory. If the linear time-invariant (LTI) state space / implicit representation is derived from the junction structure matrix, Boolean factors λ naturally appear in the **A** and **B** matrices of the state equations, shown in Table 6. The LTI model is frequently used because no time is associated with the structural switching: it is simply acknowledged that there are different modes of operation. Note that this development assumes that each element has a linear, continuous constituent equation: a similar development could be followed for nonlinear elements.

Although the input and output vectors of the junction structure for both the standard bond graph and the hybrid bond graph in the concatenated form junction look similar, the difference in the dimensions should be noted. For the standard bond graph:

$$dim\left[\dot{\boldsymbol{X}}_i \quad \boldsymbol{Z}_d \quad \boldsymbol{D}_{out}\right]^{\mathrm{T}} = n_{\mathrm{IC}} + n_{\mathrm{R}} \qquad \textbf{(19)}$$

And for the hybrid bond graph:

$$dim\left[\dot{\boldsymbol{X}}_i \quad \boldsymbol{Z}_d \quad \boldsymbol{D}_{out}\right]^{\mathrm{T}} = n_{\mathrm{IC}} + n_{\mathrm{R}} + n_{dyn} \qquad \textbf{(20)}$$

Where n_{IC} is the total number of storage elements, n_{R} is the number of dissipative elements and n_{dyn} is the number of elements with dynamic causality (and hence the number of alternative outputs occurring in different modes of operation). Similar remarks can be made for the input vector.

Table 6: Junction structure and state space matrices forms for the standard and hybrid bond graphs

	Standard Bond Graph	Hybrid Bond Graph with Dynamic Causality
Junction Structure	$\begin{bmatrix} \dot{\boldsymbol{X}}_i \\ \boldsymbol{Z}_d \\ \boldsymbol{D}_{out} \end{bmatrix} = [\mathbf{S}(0,1,\mathrm{TF},\mathrm{GY})] \begin{bmatrix} \boldsymbol{Z}_i \\ \dot{\boldsymbol{X}}_d \\ \boldsymbol{D}_{in} \\ \boldsymbol{U} \end{bmatrix}$	$\boldsymbol{\Lambda}(\lambda) \begin{bmatrix} \begin{bmatrix} \dot{\hat{\boldsymbol{X}}}_i \\ \dot{\tilde{\boldsymbol{X}}}_i \end{bmatrix} \\ \begin{bmatrix} \hat{\boldsymbol{Z}}_d \\ \tilde{\boldsymbol{Z}}_d \end{bmatrix} \\ \begin{bmatrix} \hat{\boldsymbol{D}}_{out} \\ \tilde{\boldsymbol{D}}_{out} \end{bmatrix} \end{bmatrix} = [\mathbf{S}(0,1,\lambda,\mathrm{TF},\mathrm{GY})] \begin{bmatrix} \begin{bmatrix} \hat{\boldsymbol{Z}}_i \\ \tilde{\boldsymbol{Z}}_i \end{bmatrix} \\ \begin{bmatrix} \dot{\hat{\boldsymbol{X}}}_d \\ \dot{\tilde{\boldsymbol{X}}}_d \end{bmatrix} \\ \begin{bmatrix} \hat{\boldsymbol{D}}_{in} \\ \tilde{\boldsymbol{D}}_{in} \end{bmatrix} \\ \boldsymbol{U} \end{bmatrix}$ Which can be concatenated into: $\boldsymbol{\Lambda}(\lambda) \begin{bmatrix} \dot{\boldsymbol{X}}_i \\ \boldsymbol{Z}_d \\ \boldsymbol{D}_{out} \end{bmatrix} = [\mathbf{S}(0,1,\lambda,\mathrm{TF},\mathrm{GY})] \begin{bmatrix} \boldsymbol{Z}_i \\ \dot{\boldsymbol{X}}_d \\ \boldsymbol{D}_{in} \\ \boldsymbol{U} \end{bmatrix}$
Implicit State Space Equation	$\mathbf{E}\,\dot{\boldsymbol{X}} = \mathbf{A}\,\boldsymbol{X} + \mathbf{B}\boldsymbol{U}$	$\mathbf{E}(\boldsymbol{\Lambda})\dot{\boldsymbol{X}} = \mathbf{A}(\boldsymbol{\Lambda})\,\boldsymbol{X} + \mathbf{B}(\boldsymbol{\Lambda})\boldsymbol{U}$ with $\boldsymbol{\Lambda} = \mathbf{f}(\lambda_1, \lambda_2, \cdots \lambda_n)$ Hence, modes of operation are given by $\mathbf{E}(\boldsymbol{\Lambda}_1)\dot{\boldsymbol{X}} = \mathbf{A}(\boldsymbol{\Lambda}_1)\,\boldsymbol{X} + \mathbf{B}(\boldsymbol{\Lambda}_1)\boldsymbol{U}$ $\mathbf{E}(\boldsymbol{\Lambda}_2)\dot{\boldsymbol{X}} = \mathbf{A}(\boldsymbol{\Lambda}_2)\,\boldsymbol{X} + \mathbf{B}(\boldsymbol{\Lambda}_2)\boldsymbol{U}$ $\vdots$ $\mathbf{E}(\boldsymbol{\Lambda}_n)\dot{\boldsymbol{X}} = \mathbf{A}(\boldsymbol{\Lambda}_n)\,\boldsymbol{X} + \mathbf{B}(\boldsymbol{\Lambda}_n)\boldsymbol{U}$

3.3.5 The Hybrid Junction Structure Matrix

As shown in section 3.3.4, there is one input and one output variable for each 1-port element in static causality. There are two inputs and two outputs for each 1-port element in dynamic causality. The input/output sets are exclusive of each other, and the Boolean terms in the Hybrid Junction Structure Matrix (HJSM) will activate one of these for each mode of operation.

In order to establish which outputs of the junction structure are active, the vector of outputs must be multiplied by a diagonal matrix of Boolean expressions $\boldsymbol{\Lambda}(\lambda)$. In any one mode of operation, some rows of the matrices will be set to zeros and others will give the Junction Structure for that mode. Therefore, outputs which

are in static causality are assigned a '1' in the diagonal of the matrix $\mathbf{\Lambda}(\boldsymbol{\lambda})$ because they are fixed outputs, while variables associated with elements in dynamic causality are assigned a Boolean function $f(\lambda)$ determined by the combination of the switch parameters λ that dictates the output status of the variable. For each Boolean term $f(\lambda)$, there will always be a NOT term $\overline{f(\lambda)}$ present in the matrix $\mathbf{\Lambda}(\boldsymbol{\lambda})$ which activates another row to describe the dynamic element's behaviour in its other state.

Table 7: Example Truth table for two switches

Switch 1	Switch 2	Causality on 1-port Element	Output Variable	Associated term in $\mathbf{\Lambda}(\boldsymbol{\lambda})$
0	0	Derivative	Z_d	$\left(\overline{\lambda_1 \bullet \lambda_2}\right)$
0	1	Derivative		
1	0	Derivative		
1	1	Integral	$\dot{X}_i$	$\left(\lambda_1 \bullet \lambda_2\right)$

In order to construct the matrix $\mathbf{\Lambda}(\boldsymbol{\lambda})$, consider each 1-port element in dynamic causality in turn, determine any causal paths between this elements and the controlled junctions and report the state of the switch and the output variable in a truth table. The truth table can therefore be used to construct the combination of states, and hence function of Boolean variables, that result in each causal change. For example, if a storage element is in integral causality only when two switches are ON, this could be expressed by assigning the state variable a term in $\mathbf{\Lambda}(\boldsymbol{\lambda})$ of $\left(\lambda_1 \bullet \lambda_2\right)$ i.e. switch 1 AND switch 2 are true or ON (Table 7). The pseudo-state complementary variable Z_d would therefore be assigned $\left(\overline{\lambda_1 \bullet \lambda_2}\right)$ because the element is in derivative causality when switch 1 AND switch 2 is NOT true i.e. OFF.

Often a controlled junction simply creates a path of dynamic causality between it and a nearby element, and the term in $\mathbf{\Lambda}(\boldsymbol{\lambda})$ can be quickly and easily assessed. There is the potential to reduce the amount of work required to obtain the equations by modularising and reusing sub-models for larger systems.

The **S**-matrix is constructed in the same way as for a regular bond graph, by considering which inputs give each output (assigning a 1 to true relationship and a 0 otherwise). Where the path between input and output crosses a controlled

junction, a Boolean term λ expresses that the relationship holds true when that junction is ON. Where causal paths are created when the junction is OFF, or are affected by the commutation of a controlled junction(s), additional functions of λ will appear. The outputs of the hybrid dynamic junction structure can therefore be related to the inputs by Equation (21)

$$\boldsymbol{\Lambda}(\lambda)\begin{bmatrix} \dot{\boldsymbol{X}}_i \\ \boldsymbol{Z}_d \\ \boldsymbol{D}_{out} \end{bmatrix} = \begin{bmatrix} \mathbf{S}_{11}(\lambda) & \mathbf{S}_{12}(\lambda) & \mathbf{S}_{13}(\lambda) & \mathbf{S}_{14}(\lambda) \\ -\mathbf{S}_{12}^T(\lambda) & \mathbf{0} & \mathbf{0} & \mathbf{S}_{24}(\lambda) \\ -\mathbf{S}_{13}^T(\lambda) & \mathbf{0} & \mathbf{S}_{33}(\lambda) & \mathbf{S}_{34}(\lambda) \end{bmatrix}\begin{bmatrix} \boldsymbol{Z}_i \\ \dot{\boldsymbol{X}}_d \\ \boldsymbol{D}_{in} \\ \boldsymbol{U} \end{bmatrix} \qquad \textbf{(21)}$$

Where the matrices $\boldsymbol{\Lambda}(\lambda)$ and $\mathbf{S}_{ij}(\lambda)$ are functions of the controlled junctions' Boolean parameters $\boldsymbol{\lambda}$. To simplify the notation, these matrices will simply be denoted $\boldsymbol{\Lambda}$ and $\mathbf{S}_{ij}$ from this point forward.

The **S** matrix in Equation (21) is simplified since some properties always hold.

- The matrix is skew-symmetric, so $\mathbf{S}_{21}$ and $\mathbf{S}_{31}$ are equal to minus the transposes of $\mathbf{S}_{12}$ and $\mathbf{S}_{13}$. This is because of duality. Bonds represent power as the sum of flow and effort: if the flow input of one element is the flow output of another, then the efforts must also be connected.
- The complementary variable of the input (which would give row 4) can be ignored.
- When preferred integral causality is assigned, there can be no relation between the derivative causality and resistor fields, because this would imply a causal path that could be inverted to give integral causality [98]. There is also no relation between the derivative field and itself for the same reason. Hence $\mathbf{S}_{22}$, $\mathbf{S}_{23}$ and $\mathbf{S}_{32}$ are all $\mathbf{0}$.

Note that $\boldsymbol{\Lambda}$ only needs to be applied to the left side of the equation because the terms in the Junction Structure Matrix have been found by inspecting the causal paths in the model and therefore already contain Boolean values where needed.

3.3.6 The Reference Configuration and Other Configurations

A reference configuration has been used to aid the construction of the causally dynamic bond graph, and to act as a basis for the proposed dynamic causality notation. However, the Junction Structure matrix encapsulates all possible modes of operation and it is therefore of little consequence which mode is selected for the reference. This is in contrast to previous work on Bond Graphs with switched

sources, which gives a Junction Structure Matrix for a given reference mode, and other modes of operation are to be derived from it. As a consequence, other ideal approaches define the state of switches in each mode of operation relative to the reference mode (i.e. if λ is the parameter associated to a switch, $\lambda = 1$ if the switch has commutated with respect to the reference configuration and $\lambda = 0$ otherwise) whereas the present approach suggests that the parameter λ of a switch indicates the absolute state of the switch i.e. $\lambda = 1$ when the switch is ON and $\lambda = 0$ when the switch is OFF.

3.4 The Unique Hybrid Implicit Equation

The state equations express the time-derivatives of the states and (where there is derivative causality) the pseudo-states - $\dot{\boldsymbol{X}}_i$ and $\dot{\boldsymbol{X}}_d$ - in terms of their integrals, and the system inputs $\boldsymbol{U}$. An implicit form can be derived from the junction structure matrix using the following procedure.

Equation (21) can be written as:

$$\begin{bmatrix} \boldsymbol{\Lambda}_{11} & \mathbf{0} & \mathbf{0} \\ \mathbf{0} & \boldsymbol{\Lambda}_{22} & \mathbf{0} \\ \mathbf{0} & \mathbf{0} & \boldsymbol{\Lambda}_{33} \end{bmatrix} \begin{bmatrix} \dot{\boldsymbol{X}}_i \\ \boldsymbol{Z}_d \\ \boldsymbol{D}_{out} \end{bmatrix} = \begin{bmatrix} \mathbf{S}_{11} & \mathbf{S}_{12} & \mathbf{S}_{13} & \mathbf{S}_{14} \\ -\mathbf{S}_{12}^T & \mathbf{0} & \mathbf{0} & \mathbf{S}_{24} \\ -\mathbf{S}_{13}^T & \mathbf{0} & \mathbf{S}_{33} & \mathbf{S}_{34} \end{bmatrix} \begin{bmatrix} \boldsymbol{Z}_i \\ \dot{\boldsymbol{X}}_d \\ \boldsymbol{D}_{in} \\ \boldsymbol{U} \end{bmatrix} \qquad \textbf{(22)}$$

Looking at row 3 of equation (22), an expression for $\boldsymbol{D}_{in}$ in terms of the other elements in the system can be derived:

$$\boldsymbol{\Lambda}_{33}\boldsymbol{D}_{out} = -\mathbf{S}_{13}^{\mathrm{T}}\boldsymbol{Z}_i + \mathbf{S}_{33}\boldsymbol{D}_{in} + \mathbf{S}_{34}\boldsymbol{U} \qquad \textbf{(23)}$$

The constitutive equation for the dissipative field is:

$$\boldsymbol{D}_{in} = \mathbf{L}\,\boldsymbol{D}_{out} \qquad \textbf{(24)}$$

For linear elements, **L** is a diagonal matrix of linear coefficients R or R^{-1} pertaining to each element. If there were any piecewise linear resistance elements – represented by a controlled R-element – the terms would be $\sum \lambda R$ or $\sum \lambda R^{-1}$. For nonlinear models, **L** could contain any number of functions and off-diagonal terms; the following derivation would not be appropriate in this case because the LTI form would be invalid, but a similar derivation to obtain some nonlinear equations could be followed.

Substituting (24) into (23) and solving for $\boldsymbol{D}_{in}$ gives:

$$\boldsymbol{D}_{in} = \mathbf{L}(\boldsymbol{\Lambda}_{33} - \mathbf{S}_{33}\mathbf{L})^{-1}\left(-\mathbf{S}_{13}^{\mathrm{T}}\boldsymbol{Z}_i + \mathbf{S}_{34}\boldsymbol{U}\right) \qquad \textbf{(25)}$$

This allows the $\boldsymbol{D}_{in}$ terms can be eliminated from the system equations. Starting with row 1 of equation (22) for $\dot{\boldsymbol{X}}_i$:

$$\boldsymbol{\Lambda}_{11}\dot{\boldsymbol{X}}_i = \mathbf{S}_{11}\boldsymbol{Z}_i + \mathbf{S}_{12}\dot{\boldsymbol{X}}_d + \mathbf{S}_{13}\boldsymbol{D}_{in} + \mathbf{S}_{14}\boldsymbol{U} \qquad \textbf{(26)}$$

Substituting (25) into (26) gives:

$$\boldsymbol{\Lambda}_{11}\dot{\boldsymbol{X}}_i = \mathbf{S}_{11}\boldsymbol{Z}_i + \mathbf{S}_{12}\dot{\boldsymbol{X}}_d + \mathbf{S}_{13}\mathbf{L}(\boldsymbol{\Lambda}_{33} - \mathbf{S}_{33}\mathbf{L})^{-1}\left(-\mathbf{S}_{13}^{\mathrm{T}}\boldsymbol{Z}_i + \mathbf{S}_{34}\boldsymbol{U}\right) + \mathbf{S}_{14}\boldsymbol{U} \qquad \textbf{(27)}$$

Define $\mathbf{H} = \mathbf{L}(\boldsymbol{\Lambda}_{33} - \mathbf{S}_{33}\mathbf{L})^{-1}$ in order to simplify (27):

$$\boldsymbol{\Lambda}_{11}\dot{\boldsymbol{X}}_i = \left(\mathbf{S}_{11} - \mathbf{S}_{13}\mathbf{H}\mathbf{S}_{13}^{\mathrm{T}}\right)\boldsymbol{Z}_i + \mathbf{S}_{12}\dot{\boldsymbol{X}}_d + \left(\mathbf{S}_{13}\mathbf{H}\mathbf{S}_{34} + \mathbf{S}_{14}\right)\boldsymbol{U} \qquad \textbf{(28)}$$

Now consider row two of equation (22) and rearrange:

$$\begin{aligned}\boldsymbol{\Lambda}_{22}\boldsymbol{Z}_d &= -\mathbf{S}_{12}^{\mathrm{T}}\boldsymbol{Z}_i + \mathbf{S}_{24}\boldsymbol{U}\\ 0 &= -\mathbf{S}_{12}^{\mathrm{T}}\boldsymbol{Z}_i - \boldsymbol{\Lambda}_{22}\boldsymbol{Z}_d + \mathbf{S}_{24}\boldsymbol{U} \qquad \textbf{(29)}\end{aligned}$$

Writing equations (28) and (29) in a matrix form gives:

$$\begin{bmatrix}\boldsymbol{\Lambda}_{11} & -\mathbf{S}_{12}\\ \mathbf{0} & \mathbf{0}\end{bmatrix}\begin{bmatrix}\dot{\boldsymbol{X}}_i\\ \dot{\boldsymbol{X}}_d\end{bmatrix} = \begin{bmatrix}\mathbf{S}_{11} - \mathbf{S}_{13}\mathbf{H}\mathbf{S}_{13}^{\mathrm{T}} & \mathbf{0} & \mathbf{S}_{13}\mathbf{H}\mathbf{S}_{34} + \mathbf{S}_{14}\\ \mathbf{S}_{12}^{\mathrm{T}} & -\boldsymbol{\Lambda}_{22} & \mathbf{S}_{24}\end{bmatrix}\begin{bmatrix}\boldsymbol{Z}_i\\ \boldsymbol{Z}_d\\ \boldsymbol{U}\end{bmatrix} \qquad \textbf{(30)}$$

The complementary state variables are related to the states by the *constitutive law* for the storage elements. Just as **L** contained the constitutive law of the resistance elements, the constitutive law of the storage elements can be given in matrix format.

- For linear elements in integral causality, $\mathbf{F}_i$ is a diagonal matrix of linear coefficients C^{-1} or L^{-1} and any piecewise-linear storage elements (XC- or XI-elements) would yield the terms $\sum \lambda C^{-1}$ or $\sum \lambda L^{-1}$.
- For linear elements in derivative causality, $\mathbf{F}_d$ is a diagonal matrix of linear coefficients C or L and any piecewise-linear storage elements (XC- or XI-elements) would yield the terms $\sum \lambda C$ or $\sum \lambda L$.

- Cross-coupling matrix **F** is always a matrix of zeros in a linear model.

Again, linear coefficients are assumed in order to derive the LTI form. These matrices could contain any number of functions and off-diagonal terms (including terms in **F**) in a nonlinear model, and a similar derivation process can be followed to obtain nonlinear system equations.

$$\begin{bmatrix} \boldsymbol{Z}_i \\ \boldsymbol{Z}_d \end{bmatrix} = \begin{bmatrix} \mathbf{F}_i & \mathbf{F} \\ \mathbf{F}^{\mathrm{T}} & \mathbf{F}_d \end{bmatrix} \begin{bmatrix} \boldsymbol{X}_i \\ \boldsymbol{X}_d \end{bmatrix} \qquad \textbf{(31)}$$

Substituting (31) into (30) leads to the general implicit state equation:

$$\begin{bmatrix} \boldsymbol{\Lambda}_{11} & -\mathbf{S}_{12} \\ \mathbf{0} & \mathbf{0} \end{bmatrix} \begin{bmatrix} \dot{\boldsymbol{X}}_i \\ \dot{\boldsymbol{X}}_d \end{bmatrix} = \begin{bmatrix} \mathbf{K}\mathbf{F}_i & \mathbf{K}\mathbf{F} \\ -\mathbf{S}_{12}^{\mathrm{T}}\mathbf{F}_i - \boldsymbol{\Lambda}_{22}\mathbf{F}^{\mathrm{T}} & -\mathbf{S}_{12}^{\mathrm{T}}\mathbf{F} - \boldsymbol{\Lambda}_{22}\mathbf{F}_d \end{bmatrix} \begin{bmatrix} \boldsymbol{X}_i \\ \boldsymbol{X}_d \end{bmatrix} + \begin{bmatrix} \mathbf{S}_{14} + \mathbf{S}_{13}\mathbf{H}\mathbf{S}_{34} \\ \mathbf{S}_{24} \end{bmatrix} \boldsymbol{U} \qquad \textbf{(32)}$$

Where $\mathbf{H} = \mathbf{L}(\boldsymbol{\Lambda}_{33} - \mathbf{S}_{33}\mathbf{L})^{-1}$ and $\mathbf{K} = \mathbf{S}_{11} + \mathbf{S}_{13}\mathbf{H}\mathbf{S}_{31}$.

To obtain the implicit system equation (32), the following procedure is proposed.

Procedure 2: A Procedure for finding the implicit system equations of a hybrid bond graph

1. Construct the diagonal matrix $\boldsymbol{\Lambda}$
   a. Consider each 1-port element in dynamic causality in turn, and determine all paths of dynamic causality between these elements and the controlled junctions.
   b. Use a truth table to construct the combination of states, and hence function of Boolean variables, that result in each causal change.

2. Construct the Hybrid Junction Structure Matrix (HJSM) in form of equation (22).
   a. The HJSM relates system inputs to outputs. For elements in static causality, there will be one input and one output. For elements in dynamic causality, there are two inputs (effort and flow) and two outputs.
   b. For static causality, the HJSM is constructed by using 1's and 0's to denote whether quantities are related or not.
   c. Where a path between two elements crosses a TF or GY element, a variable or function other than one may appear in the Hybrid Junction Structure Matrix.
   d. Where a path between two elements crosses a controlled junction, a λ

(or function of λ) is used to show that the relationship only occurs when the junction is ON (or OFF).

d. Where an element is in dynamic causality (shown by a dotted causal stroke in addition to the solid one) each variable will only be an input to the system in certain modes of operation. Referring to the truth table constructed in step 1, assign a function of λ which denotes the modes in which the variable is an input.

e. Recall that the matrix should be skew-symmetric, and sub-matrices $\mathbf{S_{22}}$, $\mathbf{S_{23}}$ and $\mathbf{S_{32}}$ should be zeros.

3. Derive the LTI Implicit form.

a. Find matrices **L** and **F** from the (linear) relationships in the 1-port elements.

b. Take the sub-matrices of **S** and **Λ** from the Junction Structure Matrix equation, and insert them into the general implicit LTI form in equation (32).

c. Simplify this equation to give the state equations plus some additional equations relating to the pseudo-states.

3.5 Properties of the Implicit Model

3.5.1 Properties of the Model in one Mode

Recall equation (32), which gives the model for all potential modes of operation. To assess a single mode of operation, the Boolean terms in **Λ** and the Junction Structure Matrix **S** must be set to ones and zeros (denoting where each controlled junction is ON or OFF). There will be some redundancy in the equation, where some lines are zeros and can be deleted. This will give equation (33):

$$\begin{bmatrix} \mathbf{I} & -\mathbf{S}_{12} \\ \mathbf{0} & \mathbf{0} \end{bmatrix} \begin{bmatrix} \dot{\boldsymbol{X}}_i \\ \dot{\boldsymbol{X}}_d \end{bmatrix} = \begin{bmatrix} (\mathbf{S}_{11} + \mathbf{S}_{13}\mathbf{H}\mathbf{S}_{31})\mathbf{F}_i & (\mathbf{S}_{11} + \mathbf{S}_{13}\mathbf{H}\mathbf{S}_{31})\mathbf{F} \\ -\mathbf{S}_{12}^{\mathrm{T}}\mathbf{F}_i - \mathbf{F}^{\mathrm{T}} & -\mathbf{S}_{12}^{\mathrm{T}}\mathbf{F} - \mathbf{F}_d \end{bmatrix} \begin{bmatrix} \boldsymbol{X}_i \\ \boldsymbol{X}_d \end{bmatrix} + \begin{bmatrix} \mathbf{S}_{14} + \mathbf{S}_{13}\mathbf{H}\mathbf{S}_{34} \\ \mathbf{S}_{24} \end{bmatrix} \boldsymbol{U} \quad \textbf{(33)}$$

Where the matrices $\mathbf{S}_{ij}$ are evaluated for the parameters λ of the controlled junctions in the mode of operation and all null rows are removed.

For a reference mode where all storage elements are in integral causality, $\mathbf{\Lambda}_{11}$ is an identity matrix and $-\mathbf{S_{12}}$ is a matrix of zeros. The second rows of **Λ** and **S** also become zero, since this line would relate to elements in derivative causality. Equation (32) therefore becomes an ordinary state equation:

$$\dot{\boldsymbol{X}}_i = \left[(\mathbf{S}_{11} + \mathbf{S}_{13}\mathbf{H}\mathbf{S}_{31})\mathbf{F}_i\right]\boldsymbol{X}_i + \left[\mathbf{S}_{14} + \mathbf{S}_{13}\mathbf{H}\mathbf{S}_{34}\right]\boldsymbol{U} \qquad \textbf{(34)}$$

The resulting state equation for one mode can be manipulated and analysed for the properties of that mode as already described extensively in the literature. For example, it can be put into Smith or Kroenecker Canonical forms to allow inspection of the dynamics.

3.5.2 Properties of the General Model

Equation (32) is comparable to the upper rows of the implicit state equation derived by Buisson et al [98] using switched sources. In their model, the additional lower rows relate to the switch states whereas here the switching manifests in the submatrices of **S**.

It follows that structural properties (observability and controllability, asymptotic stability, and dynamic properties such as gain and the number of zeros and poles), can be functions of structural switching. This is investigated in more detail in chapter 4.

3.6 Comparison with Switching Sources and the Non-Ideal Approach

The Literature Review (Chapter 2) highlighted that the bulk of work to date on hybrid bond graph structural analysis has been conducted using switching sources. This section compares equation generation from a switched bond graph as developed by Buisson et al [98] with the one obtained in this paper and also investigates how the ideal controlled junction can be modified to account for dissipative effect on commutation.

3.6.1 Implicit State Equations

The methods differ significantly in that hybrid bond graphs constructed using switching sources are built for an initial (reference) mode, and subsequent modes of operation are derived from it. By contrast, the method presented here builds a model for all modes, and derives the equations for a single mode after.

For a model with switched sources, the junction structure matrix and standard implicit state equation contain extra states ($\boldsymbol{T}_i$ and $\boldsymbol{T}_o$) relating to the input and output to the switch(es). These rows contain the constitutive relation for the switches in terms of a commutation matrix $\boldsymbol{\Lambda}$. Note that the indices of $\mathbf{S}$ are slightly different, because the Junction Structure Matrix also has additional terms due to $\boldsymbol{T}_i$ and $\boldsymbol{T}_o$, and that $\boldsymbol{\Lambda}$ is a square diagonal matrix with terms that are 1 or 0 depending on whether a switch has commutated. Buisson et al [98] note that this form is not suitable for simulation.

$$\begin{bmatrix} \mathbf{I} & -\mathbf{S}_{12} & \mathbf{0} & \mathbf{0} \\ \mathbf{0} & \mathbf{0} & \mathbf{0} & \mathbf{0} \\ \mathbf{0} & \mathbf{S}_{24}^{\mathrm{T}} & \mathbf{0} & \mathbf{0} \\ \mathbf{0} & \mathbf{0} & \mathbf{0} & \mathbf{0} \end{bmatrix} \begin{bmatrix} \dot{\boldsymbol{X}}_i \\ \dot{\boldsymbol{X}}_d \\ \dot{\boldsymbol{T}}_i \\ \dot{\boldsymbol{T}}_o \end{bmatrix} = \begin{bmatrix} \mathbf{K}\mathbf{F}_i & \mathbf{K}\mathbf{F} & \mathbf{S}_{14}+\mathbf{S}_{13}\mathbf{H}\mathbf{S}_{24} & \mathbf{0} \\ -\mathbf{S}_{12}^{\mathrm{T}}\mathbf{F}_i-\mathbf{F}^{\mathrm{T}} & -\mathbf{S}_{12}^{\mathrm{T}}\mathbf{F}-\mathbf{F}_d & \mathbf{S}_{24} & \mathbf{0} \\ -\left(\mathbf{S}_{14}^{\mathrm{T}}-\mathbf{S}_{34}^{\mathrm{T}}\mathbf{H}\mathbf{S}_{13}^{\mathrm{T}}\right) & \mathbf{0} & \mathbf{S}_{14}-\mathbf{S}_{34}^{\mathrm{T}}\mathbf{H}\mathbf{S}_{34} & -\mathbf{I} \\ \mathbf{0} & \mathbf{0} & \mathbf{I}-\boldsymbol{\Lambda} & \boldsymbol{\Lambda} \end{bmatrix} \begin{bmatrix} \boldsymbol{X}_i \\ \boldsymbol{X}_d \\ \boldsymbol{T}_i \\ \boldsymbol{T}_o \end{bmatrix} + \begin{bmatrix} \mathbf{S}_{15}+\mathbf{S}_{13}\mathbf{H}\mathbf{S}_{35} \\ \mathbf{S}_{25} \\ \mathbf{S}_{45}-\mathbf{S}_{34}^{\mathrm{T}}\mathbf{H}\mathbf{S}_{35} \\ \mathbf{0} \end{bmatrix} U \quad \textbf{(35)}$$

$$\text{where } \mathbf{H}=\mathbf{L}(\mathbf{I}-\mathbf{S}_{33}\mathbf{L})^{-1} \text{ and } \mathbf{K}=\mathbf{S}_{11}+\mathbf{S}_{13}\mathbf{H}\mathbf{S}_{31}$$

This standard implicit form compares well to the model derived here to give equation (32). The different indices of the submatrices reflect the smaller Junction Structure Matrix, and Boolean variables occur throughout the equation in the $\mathbf{S}$ and $\boldsymbol{\Lambda}$ submatrices.

Whereas the implicit state equation (35) by Buisson et al [98] is obtained using straightforward standard bond graph techniques, the model is derived and valid for a reference configuration only. Recovering the implicit form for any other configuration requires complex matrix operations because of elements changing causality and the dimension and components of key vectors $\boldsymbol{X}_i$, $\boldsymbol{X}_d$,… changing accordingly. In the approach proposed in this paper, non-standard techniques are used to generate the unique implicit state equation (32) that encompasses all configurations. Once the model (32) is obtained, any configuration can easily be obtained by evaluating Boolean expressions for the associated combination of switches. Due to the fact that the method exploits the graphical properties of causal bond graphs combined with some symbolic operations, it is believed the method can be conveniently implemented in existing software packages.

3.6.2 Ideal and Non-Ideal Approaches

Both switching sources and controlled junctions are ideal approaches, i.e. no energy is dissipated on commutation. This is in contrast to earlier work using non-ideal approaches, i.e. switches modelled by modulated resistors, or resistors associated with modulated transformers (which gives a unique, causally static

bond graph). Buisson et al [98] discuss ideal and non-ideal modelling, and show that the ideal approach is a limit case of the non-ideal approach.

In some cases a system cannot be assumed to be ideal (for example, a hydraulic valve which acts as an orifice when open) and dissipation needs to be modelled. Buisson et al [98] propose a semi-ideal approach, where the switching source is modelled as a variable resistance, and the constitutive relationship for the switching variables includes a resistance term.

Controlled junctions can be easily made semi-ideal in a similar manner, by simply adding a resistance element so as to dissipate energy when the junction is ON. This coincidentally acts as a 'causality resistance,' limiting dynamic causality.

An interesting feature of the Hybrid Bond Graph presented in this paper is that the non-ideal case is remarkably similar to the Boolean MTF and Resistor representation proposed by Dauphin-Tanguy and Rombaut [25] and used most recently in a causally static form by Borutzky [49] A comparison of an example system is shown in Figure 12, which is typical of an electrical switch.

a) The Switch represented by a Boolean MTF and Resistor

b) The Switch represented by a Controlled Junction and additional Resistance

Figure 12: An Example of causality assignment around a Non-Ideal [Flow] Switch

In both cases, the R-element imposes flow on the junction when ON. When $\lambda = 1$ (i.e. the switch is ON) the flow is governed by the R-element as a function of effort. When $\lambda = 0$ (i.e. the switch is OFF), the flow is zero and the effort associated with the resistance is disconnected from the system. The dynamic causality associated with the controlled junction is limited to the R-element.

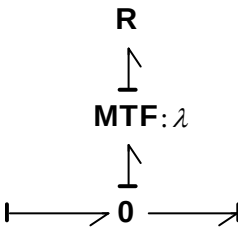

(a) A Switch represented by a Boolean MTF and Resistor

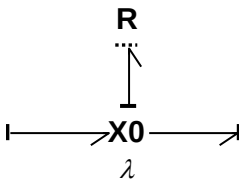

(b) A Switch represented by a Controlled Junction and additional Resistance

Figure 13: An Example of causality assignment around a Non-Ideal [Effort] Switch

The similarity holds for switching parts where effort commutates between zero and a finite quantity (shown in Figure 13), typical of mechanical and hydraulic switching devices.

However, the similarity between the two techniques does not always hold true: there are cases where the R-element does not govern the flow on a 1-junction (or effort on a 0-junction). In these cases, the MTF-R representation would not act as a switch (because it would not be imposing a null quantity on the system: it would simply disconnect the R-element): parasitic elements may need to be added to the model to manipulate the causal assignment, as shown in Figure 14. This would be the case for systems where the non-ideal switch is modelled using a modulated resistance too. The controlled junction, however, works regardless of the casual assignment on the incident bonds. Note that a kinematic constraint exists between the controlled junction and the I-element when the switch is 'off.' the analyst may now make an informed decision whether to revise the modelling assumptions, break this constraint using parasitic elements or allow it to remain.

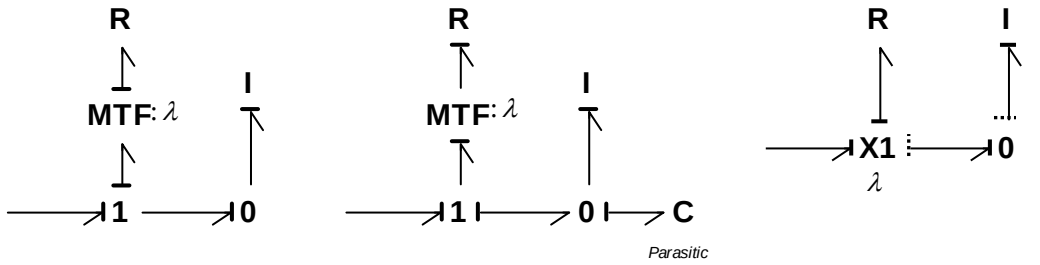

(a) The Switch represented by a Boolean MTF and Resistor

(b) A Parasitic Element added to control Causality and ensure the MTF-R acts as a switch

(c) The Switch represented by a Controlled Junction

Figure 14: An Example System with a Non-Ideal [Flow] Switch

3.7 Summary

A method has been proposed with classifies discontinuities as *structural* and *parametric* and represents them in the hybrid bond as controlled junctions and a new controlled element respectively. The controlled element is derived from a mode-switching 'tree' of controlled junctions.

A new dynamic causality notation and Dynamic Sequential Causality Assignment Procedure (DSCAP) are proposed. This is used to generate a mixed-Boolean Junction Structure Matrix and implicit system equation. The latter is compared to equations generated from existing variations on the hybrid bond graph, and they are shown to be similar. The hybrid bond graph proposed here essentially yields the same model in a more usable form.

Chapter 4: Analysis of the Hybrid Bond Graph

4.1 Preliminaries

This chapter identifies the structural properties of the hybrid bond graph with dynamic causality.

It is well-documented that system properties can be established from the structure of the mathematical model (e.g. matrix-rank criteria) and the structure of the bond graph and its causal assignment. However, this work has been conducted on regular bond graphs and, to a limited extent, on hybrid bond graphs featuring switched sources. It is therefore not directly applicable to the hybrid bond graph proposed here, and must be reviewed with special consideration given to the dynamic causal assignment.

A number of observations on the dynamic causal assignment and its implications with regard to exploitation are made. This leads naturally onto deriving the transfer function by inspecting causal paths, and other equation generation such as the output equation (to complement the unique implicit system equation and give a full LTI Descriptor System). The matrices from this equation will be used in the subsequent chapters.

Where storage elements are in dynamic causality, there will be an impulsive mode. This is shown to only have a value in one of two types of structural discontinuity. State variables do not need to be reinitialised in this model.

The control properties (normally found by matrix-rank criteria) are then reviewed, using the matrices of the full LTI Descriptor System to confirm the properties indicated by the bond graph.

Variable structure systems and their associated impulse losses are addressed. It is demonstrated that the controlled junction yields a switching system with no inherent impulsive loss.

Control engineering is a continuously evolving field, and this chapter covers only the basics of what may be observed on the bond graph. There is tremendous scope for future work on nonlinear models, stability, defining observers, and other aspects of dynamic analysis and control.

4.2 Observations on the Dynamic Causality Assignment

The dynamic causality notation was designed to give some insight into the model and be more usable than existing notation [51]. This section presents a series of observations on dynamic causality manifesting in the hybrid bond graph.

An immediate observation is that paths of dynamic causality between controlled junctions and elements can be identified, and these clearly show the elements affected by commutation of a controlled junction. This means that compiling a truth table for the model and constructing the Λ-matrix for any subsequent equation derivation is greatly simplified. Rather than constructing a truth table for the whole model with 2^i possible modes of operation (where i is the number of controlled junctions), a series of smaller truth tables can be constructed for each segment of the model in dynamic causality.

Additional observations on the paths of dynamic causality can be made in line with those already made for causally static bond graphs, such as Margolis and Rosenberg's work on exploiting causality [88, 89] and Rosenberg and Andry's work on solving causal loops [93].

The number of storage elements in dynamic causality is a measure of the variation in model size. Recall that elements in integral causality provide the state variables in deriving the state equations. Therefore, when all of storage elements are in integral causality, the maximum number of states is active. In a well-constructed model, there are no elements in static derivative causality and this mode (the reference mode) gives a fully explicit state space model. Likewise, the mode of operation where most storage elements are in derivative causality gives the minimum number of state variables (and the maximum number of pseudo-states which yield additional algebraic equations).

Dynamic causality on resistance elements does not affect the model size. The notation allows the user to see how 'causality resistance' elements can restrict the propagation of dynamic causality and control model size.

If dynamic causality is not controlled, it can be exploited in much the same way as static causality. Causal paths between elements (in the reference or other modes) can be traced, and signify various types of algebraic or kinematic constraint. In addition to identifying these paths in the case of dynamic causality, it is possible to further classify them.

The classic variable topology problem – ideal 'hard' contact resulting in coalescence – is visible via a controlled junction which is OFF in the reference

mode and results in a kinematic constraint between rigid bodies (i.e. a causal path between two I-elements, one of which will be in derivative causality) when it is ON. This usually manifests as a path of dynamic causality between a controlled junction and I-element, shown in Figure 15. It is also possible for compliance elements to become kinematically constrained.

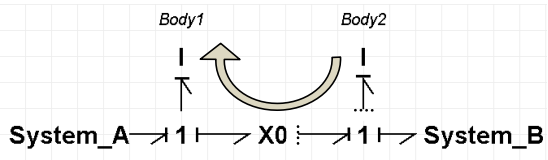

a) 'Hard' Contact resulting in a Kinematic Constraint (shown by the arrow) between Bodies 1 and 2.

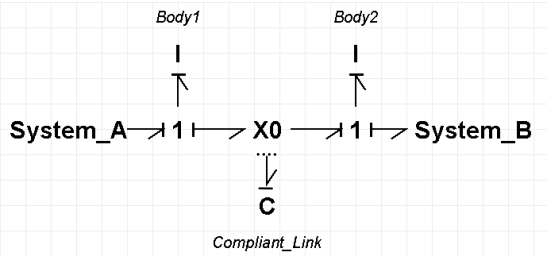

b) Compliant Contact

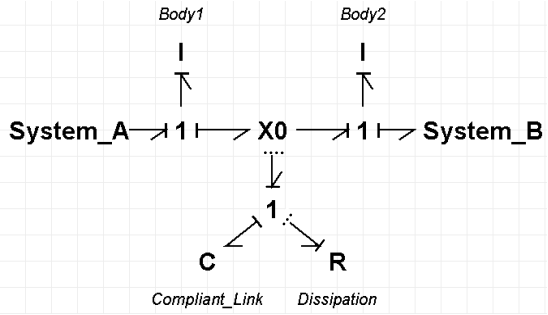

c) Compliant Contact with Resistance

Figure 15: Example of a Type 1 Structural Discontinuity

A user may choose to break the kinematic constraint by revising modelling assumptions: the classic approach is to redefine a hard contact problem as stiff contact, by adding a stiff compliance between the inertia elements. This may not always be appropriate, especially if a 'proper model' or model devoid of high frequency stiff dynamics is required. If the mode(s) of operation for which the constraint exists were to be considered in isolation, the constrained storage

elements could be lumped together: this may be laborious by hand, but a computer programme could feature an algorithm for lumping constrained elements or using relaxed causalities [3] in the appropriate modes of operation.

Where there is compliant contact, the inertia elements will remain in integral causality and there is no kinematic constraint. There will be a path of dynamic causality between the junction and a compliance element instead. There is typically some dissipation associated with this type of contact, and a resistance element may be added which will act as causality resistance: in this case the path of dynamic causality will be between the controlled junction and resistance element. The advantage of using causality resistance is that the number of state equations remains constant with commutation, which greatly facilitates computation. Indeed, bespoke subsystems describing controlled junction and causality resistance elements have already been used successfully in 20Sim (as outlined in Chapter 2), although coding bespoke subsystems can lose the graphical advantages of the bond graph notation and is open to abuse by novice users. It is important that causality resistance is only used where there is dissipation in real life, and a known or representative coefficient can be assigned to the element. The use of parasitic elements to aid simulation violates the principles and advantages of idealised physical modelling, and can result in overly complex and inaccurate models.

Definition 24: Type 1 Structural Discontinuity
A Type 1 *structural discontinuity is OFF in the reference configuration. When it is ON, two subsystems are joined and a kinematic constraint may result.*

The alternative situation is a controlled junction which is ON in the reference configuration, and divides the model into subsystems when it is OFF, as shown in Figure 16. Disconnecting a power source – for example, in an electrical or hydraulic circuit - can result in storage elements discharging, and this is reflected by them switching to derivative causality. As with the type 1 structural discontinuities, parasitic elements (additional compliance, causality resistance) can be used to control this dynamic causality but must be used with caution.

Definition 25: Type 2 Structural Discontinuity
A Type 2 *structural discontinuity is ON in the reference configuration. When it is OFF, the system is divided into subsystems, and storage elements may discharge to compensate for a lack of power source in a subsystem.*

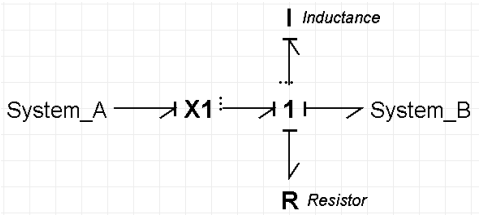

Figure 16: Example of a Type 2 Structural Discontinuity

As dynamic causality occurs, various other paths and loops may be created or broken with commutation. These are not a feature of the type of discontinuity.

Some observations may be made regarding the control properties of the system. Assume a system is [structurally] controllable and observable in the reference mode. If the system contains type 1 discontinuities, the system's finite dynamics remain controllable and observable after commutation. If it contains type 2 discontinuities, the model may be subdivided into uncontrollable and unobservable subsystems with commutation. Control properties will be discussed in more detail in section 4.6.

In assigning the causality around a controlled junction, the user may make an arbitrary decision regarding which element to place in dynamic causality. Consider Figure 15a: dynamic causality was assigned to Body 2 but could just as easily have been assigned to Body 1. The basic effects on the system are the same:

- When the controlled junction is OFF the I-elements
  - are both in integral causality and
  - both yield a state variable and equation.

- When the controlled junction is ON,
  - one of the I-elements switches to derivative causality,
  - the order of the model is reduced by one, and
  - the elements yield one state variable and equation, and an additional pseudo-state providing an algebraic constraint between the two bodies.

The only time that the choice of element to place in derivative causality may be significant is when there is an existing causal path between an element and some other structure. This will still be captured via the new causal paths, but may be less immediately obvious to the user and computationally inefficient. An example is shown in Figure 17.

The causality assignment in Figure 17a) results in a static causal path between Body 1 and the spring. The equally legitimate causality assignment in Figure 17b) does not have this static causal path. Instead, there is a causal path between the spring and Body 1 only when the controlled junction is OFF. When the controlled junction is ON, this path no longer exists but another causal path appears between the spring and Body 2. Inspecting the structure and causality of the systems (using the notation in Figure 18) yields the equations in Table 8. It can be seen that the first set of equations is more elegant and concise. The second set still relates the spring to Body 1, but when the controlled junction is ON this is done via the algebraic constraint between the bodies.

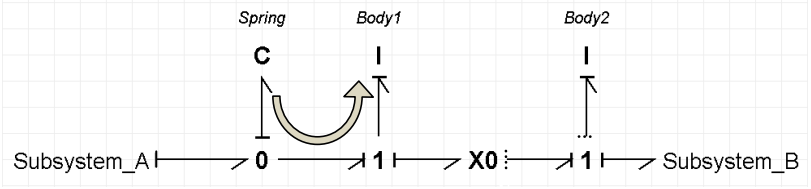

a) Body 2 in Dynamic Causality

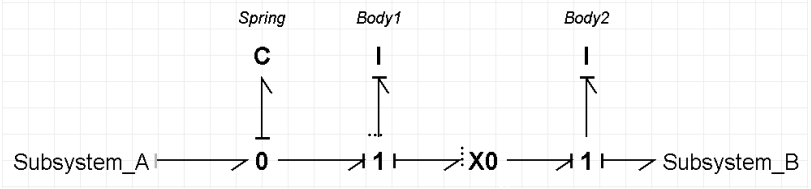

b) Body 1 in Dynamic Causality

Figure 17: Hard Contact with a Causal Path (indicated by arrow) affected by Causality Assignment

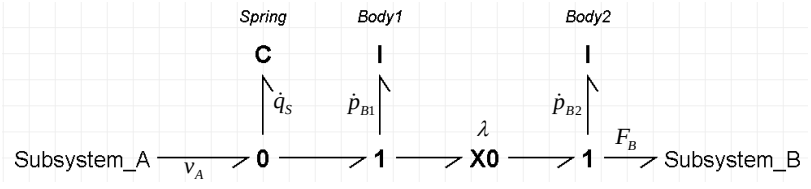

Figure 18: Notation used in Equation Derivation for the Hard Contact Example

Table 8: Junction Structure & Implicit State Equations for the Hybrid Bond Graph in Figure 17

Body 2 in Dynamic Causality	Body 1 in Dynamic Causality
$\boldsymbol{\Lambda}\begin{bmatrix}\hat{\dot{q}}_S\\ \hat{\dot{p}}_{B1}\\ \tilde{\dot{p}}_{B2i}\\ \tilde{f}_{B2d}\end{bmatrix}=\begin{bmatrix}0&-1&0&0&1&0\\ 1&0&0&-\lambda&0&\lambda\\ 0&0&0&0&0&-\bar{\lambda}\\ 0&\lambda&0&0&0&0\end{bmatrix}\begin{bmatrix}\hat{e}_S\\ \hat{f}_{B1}\\ \tilde{f}_{B2i}\\ \tilde{p}_{B2d}\\ v_A\\ F_B\end{bmatrix}$ $\boldsymbol{\Lambda}=diag\begin{bmatrix}1&1&\bar{\lambda}&\lambda\end{bmatrix}$	$\boldsymbol{\Lambda}\begin{bmatrix}\hat{\dot{q}}_S\\ \tilde{\dot{p}}_{B1i}\\ \hat{\dot{p}}_{B2}\\ \tilde{\dot{p}}_{B1d}\end{bmatrix}=\begin{bmatrix}0&-\bar{\lambda}&-\lambda&0&1&0\\ \bar{\lambda}&0&0&0&0&\lambda\\ \lambda&0&0&\lambda&0&-1\\ 0&0&\lambda&0&0&0\end{bmatrix}\begin{bmatrix}\hat{e}_S\\ \tilde{f}_{B1i}\\ \hat{f}_{B2}\\ \tilde{p}_{B1d}\\ v_A\\ F_B\end{bmatrix}$ $\boldsymbol{\Lambda}=diag\begin{bmatrix}1&\bar{\lambda}&1&\lambda\end{bmatrix}$
$\begin{bmatrix}1&0&0&0\\ 0&1&0&\lambda\\ 0&0&\bar{\lambda}&0\\ 0&0&0&0\end{bmatrix}\begin{bmatrix}\hat{\dot{q}}_S\\ \hat{\dot{p}}_{B1}\\ \tilde{\dot{p}}_{B2i}\\ \tilde{\dot{p}}_{B2d}\end{bmatrix}=\begin{bmatrix}0&-1/L_{B1}&0&0\\ -1/C_S&0&0&0\\ 0&0&0&0\\ 0&\lambda/L_{B1}&0&-\lambda/L_{B2}\end{bmatrix}\begin{bmatrix}\hat{q}_S\\ \hat{p}_{B1}\\ \tilde{p}_{B2i}\\ \tilde{p}_{B2d}\end{bmatrix}+\begin{bmatrix}1&0\\ 0&\lambda\\ 0&-\bar{\lambda}\\ 0&0\end{bmatrix}\begin{bmatrix}v_A\\ F_B\end{bmatrix}$	$\begin{bmatrix}1&0&0&0\\ 0&\bar{\lambda}&0&0\\ 0&0&1&-\lambda\\ 0&0&0&0\end{bmatrix}\begin{bmatrix}\hat{\dot{q}}_S\\ \tilde{\dot{p}}_{B1i}\\ \hat{\dot{p}}_{B2}\\ \tilde{\dot{p}}_{B1d}\end{bmatrix}=\begin{bmatrix}0&\bar{\lambda}/L_{B1}&-\lambda/L_{B2}&0\\ -\bar{\lambda}/C_S&0&0&0\\ \lambda/C_S&0&0&0\\ 0&0&-\lambda/L_{B2}&-\lambda/L_{B1}\end{bmatrix}\begin{bmatrix}\hat{q}_S\\ \tilde{p}_{B1i}\\ \hat{p}_{B2}\\ \tilde{p}_{B1d}\end{bmatrix}+\begin{bmatrix}1&0\\ 0&0\\ 0&-\lambda\\ 0&0\end{bmatrix}\begin{bmatrix}v_A\\ F_B\end{bmatrix}$

In Step 4 of the Dynamic Sequential Causality Assignment Procedure (Procedure 1) it was noted that a causal conflict may occur for some isolated modes of operation. These have the property of indicating a forbidden mode of operation. For example, in the Case Study of the power converter (section 5.2) a causal conflict occurs when both electrical switches are ON and the voltage source is short-circuited.

Property 1: Casusal Conflict in the Dynamic Causal Assignment

Where a causal conflict occurs in the dynamic causal assignment, this indicates a conflict in a specific mode of operation, and the mode is a 'forbidden mode.' Forbidden modes may be a consequence of the modelling assumptions, or reflect a real case such as a short-circuit.

A mode in which there is a causal conflict is 'forbidden' in the sense that causality cannot be assigned, and hence the mathematical model cannot be constructed for that mode, and the model cannot be simulated. An interesting property of the hybrid bond graph presented in this thesis is that causal conflicts reflect modes that would be undesirable or impossible in reality. This is because the method was developed to reflect the physics of the system.

4.3Further Equation Derivation

It has already been shown in Chapter 3 that an implicit state equation can be found from the Junction Structure Matrix. It was also shown in Section 4.2 that the causal assignment can be exploited to give insight to the system. In this section, some additional equation derivation activities are carried out to provide more information about Hybrid Bond Graph with dynamic causality.

4.3.1 Transfer Function Using Shannon-Mason Loop Rule

It is well-documented that causal paths in a bond graph are equivalent to signal loops, and a transfer function can therefore be found directly from the causal bond graph using Shannon-Mason loop rule [95]. In the hybrid bond graph proposed here, commutation clearly affects the causal paths in the model (where they cross a controlled junction), and commutation will therefore also clearly manifest in the transfer function. By looking at the causal paths present in the reference configuration, and then each path of dynamic causality, a transfer function for all possible modes of operation can be obtained. Where the paths cross a controlled junction, or are induced by a certain combination of operations, the relevant Boolean term can be inserted into the expression for gain in the transfer function as follows.

Property 2: Gain of a Causal Path crossing a Controlled Junction

Where a causal path crosses a controlled junction, the Boolean variable related to that controlled junction is a factor of the gain.

In constructing the transfer function, causal paths between elements and sources are used to generate gain terms in the determinant. Where that path crosses a controlled junction, it only exists in the ON state. Multiplying the gain term by the Boolean factor ensures it is sent to zero when OFF. An example of this situation is shown in Figure 19, where the causal path indicated by the arrow has a gain of $-\lambda/s^2IC$.

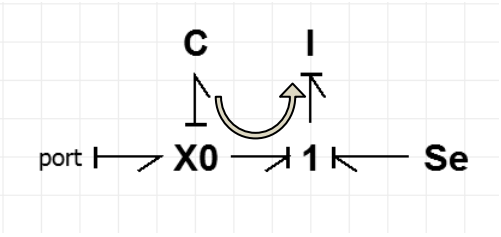

Figure 19: A Causal Path crossing a Controlled Junction.

Property 3: Gain of a Causal Path in Dynamic Causality

Where a causal path is dynamic or partially dynamic, the gain is factored by the Boolean function (term in **Λ**) which activates the path to give the signal loop under consideration.

Where a path between two elements is in dynamic causality, the complete path only exists in a certain mode of operation. For the example in Figure 20, the causal path between the I- and R-elements (shown by the arrow) is partially in dynamic causality. This means that there is a path between the two elements in some modes of operation only (those where the I-element is in integral causality). Hence, the Boolean function associated with activating integral causality of the I-element must be used as a factor in the gain, giving $-(\lambda_1 \oplus \lambda_2)R/sI$. When the I-element is in derivative causality, there is no causal path and the gain term is sent to zero.

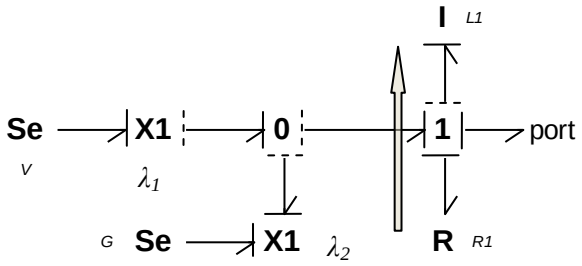

Figure 20: A Causal Path in Dynamic Causality.

The general form of the transfer function is therefore identical to that of the standard bond graph:

$$h_{ij} = \frac{1}{\Delta}\sum_{k} G_k \Delta_k \qquad \textbf{(36)}$$

Where k denotes the kth path between input and output, and the graph determinant is:

$$\Delta = 1 - \sum_{i} G_i + \sum_{i,j} G_i G_j - \sum_{i,j,k} G_i G_j G_k + \ldots \qquad \textbf{(37)}$$

However, for the Hybrid Bond Graph G is not only a function of any resistance, inertia or compliance coefficients relating to elements in the loop, but can also contain Boolean terms.

Where a controlled junction breaks/joins the causal paths in a model, the dynamic behaviour of the system is affected with commutation. The following points follow logically:

- If a controlled junction is in a path, then a Boolean term will be present in the graph determinant and hence the denominator of the transfer function. The roots of the denominator are the eigenvalues of the system, so it follows that the system will lose/gain one or more poles with commutation.

- If a controlled junction is in a path which does not 'touch' the input-output path (i.e. the paths do not share any nodes), then the 'reduced determinant' and hence the numerator of the transfer function will also contain a Boolean term. It follows that the system will lose/gain zeros with commutation.

- If a controlled junction is on the input-output path, the gain of the system will be affected. The numerator of the transfer function will again contain a Boolean and the system will lose/gain zeros with commutation.

- Where elements are in derivative causality, a path will only be present in some modes of operation and a Boolean function will denote this. Some paths will never touch because they are in exclusive modes of operation, and this must be taken into account when calculating the determinants.

4.3.2 The LTI Full Descriptor System

It was seen in chapter 3 that the states of the bond graph model can be used to generate an implicit system equation from the junction structure. For models where all storage elements are in integral causality, **E = I** (i.e. **E** is non-singular)

and the well-known explicit or regular *state space equation* is generated. For models where some storage elements are in derivative or dynamic causality, **E** is singular and the system is an *implicit*, *singular*, *semistate* or *descriptor* system [80]. Hybrid Bond Graphs with storage elements in dynamic causality will always generate implicit equations, because the derivative causality cases generate algebraic equations with no differential term (and hence a zero term in **E**) and the constraints they represent give off-diagonal coupling terms in **E**.

The LTI implicit equation gained in Chapter 3 forms one part of a descriptor system (equation 38), the other part being given by the *output equation* (equation 39).

$$\mathbf{E}\dot{\boldsymbol{X}} = \mathbf{A}\boldsymbol{X} + \mathbf{B}\boldsymbol{U} \qquad \textbf{(38)}$$

$$\boldsymbol{Y} = \mathbf{C}\boldsymbol{X} + \mathbf{D}\boldsymbol{U} \qquad \textbf{(39)}$$

The **A**, **B**, **C**, **D** and **E** matrices of these equations are used in defining control parameters such as controllability and observability, usually using matrix-rank criteria [81].

There is no standard output element in the bond graph framework. Some authors take an output as being the complementary variable of an input, which is logical in systems where source-elements are also used as sinks. A fairly common notation is that of Detector-elements (De- or Df-elements) which are essentially null sources added to junctions. These act in precisely the same manner as a source/sink, and simply have a different notation for clarity. However, output is not a property of a system, and the use of detector elements with a power flow suggests that sensors are energy-processing.

Consequently, Signal Detectors similar to those in the commercial package 20Sim are used here, shown in Figure 21. These are not power elements, but take a reading from the bond graph via a signal output (marked by a full-arrow), usually taken from a common-flow or common-effort junction. There is no power flow to or from the detector: it simply takes a flow or effort reading.

Detectors inherently yield outputs that are always efforts and flows, whereas a real system may have other output devices such as measured displacements, accelerometers or strain gauges, for example. The associated readings can be obtained by integrating or differentiating the output signal from a detector element. In principle, the output can be any quantity (such as a state) and should not be limited to effort or flow variables: the notation (and associated signal

integration/differentiation blocks to give other quantities) is proposed for use where a detector needs to be recorded on the bond graph.

a) The Effort Detector Element **b) The Flow Detector Element**

Figure 21: The Detector Element shown taking a Signal from a Bond Graph Junction.

Outputs can be added to the junction structure, shown graphically in Figure 22, and hence expressed in terms of the junction structure and system inputs, shown in Equation (40):

$$\begin{bmatrix} \boldsymbol{\Lambda}_{11} & 0 & 0 & 0 \\ 0 & \boldsymbol{\Lambda}_{22} & 0 & 0 \\ 0 & 0 & \boldsymbol{\Lambda}_{33} & 0 \\ 0 & 0 & 0 & \mathbf{I} \end{bmatrix} \begin{bmatrix} \dot{\boldsymbol{X}}_i \\ \boldsymbol{Z}_d \\ \boldsymbol{D}_{out} \\ \boldsymbol{Y} \end{bmatrix} = \begin{bmatrix} \mathbf{S}_{11} & \mathbf{S}_{12} & \mathbf{S}_{13} & \mathbf{S}_{14} \\ -\mathbf{S}_{12}^T & 0 & 0 & \mathbf{S}_{24} \\ -\mathbf{S}_{13}^T & 0 & \mathbf{S}_{33} & \mathbf{S}_{34} \\ \mathbf{S}_{41} & \mathbf{S}_{42} & \mathbf{S}_{43} & \mathbf{S}_{44} \end{bmatrix} \begin{bmatrix} \boldsymbol{Z}_i \\ \dot{\boldsymbol{X}}_d \\ \boldsymbol{D}_{in} \\ \boldsymbol{U} \end{bmatrix} \quad \textbf{(40)}$$

Note that signals are inherently causal (i.e. they have an input and output defined, indicated by the direction of the arrow) and an output is always an output. Hence detectors are never in dynamic causality and $\boldsymbol{\Lambda}_{44} = \mathbf{I}$. Following the same derivation as for the implicit state equation, an expression for $\boldsymbol{D}_{in}$ in terms of the other elements in the system can be derived:

$$\boldsymbol{D}_{in} = \mathbf{L}(\boldsymbol{\Lambda}_{33} - \mathbf{S}_{33}\mathbf{L})^{-1}\left(-\mathbf{S}_{13}^{\mathrm{T}}\boldsymbol{Z}_i + \mathbf{S}_{34}\boldsymbol{U}\right) \quad \textbf{(41)}$$

Hence the $\boldsymbol{D}_{in}$ terms can be eliminated from the system equations. From row 4 of (40):

$$\boldsymbol{Y} = \mathbf{S}_{41}\boldsymbol{Z}_i + \mathbf{S}_{42}\dot{\boldsymbol{X}}_d + \mathbf{S}_{43}\mathbf{L}(\boldsymbol{\Lambda}_{33} - \mathbf{S}_{33}\mathbf{L})^{-1}\left(-\mathbf{S}_{13}^{\mathrm{T}}\boldsymbol{Z}_i + \mathbf{S}_{34}\boldsymbol{U}\right) + \mathbf{S}_{44}\boldsymbol{U} \quad \textbf{(42)}$$

Since $\mathbf{H} = \mathbf{L}(\boldsymbol{\Lambda}_{33} - \mathbf{S}_{33}\mathbf{L})^{-1}$ this can be simplified to:

$$\boldsymbol{Y} = \left(\mathbf{S}_{41} - \mathbf{S}_{43}\mathbf{H}\mathbf{S}_{13}^{\mathrm{T}}\right)\boldsymbol{Z}_i + \mathbf{S}_{42}\dot{\boldsymbol{X}}_d + \left(\mathbf{S}_{43}\mathbf{H}\mathbf{S}_{34} + \mathbf{S}_{44}\right)\boldsymbol{U} \quad \textbf{(43)}$$

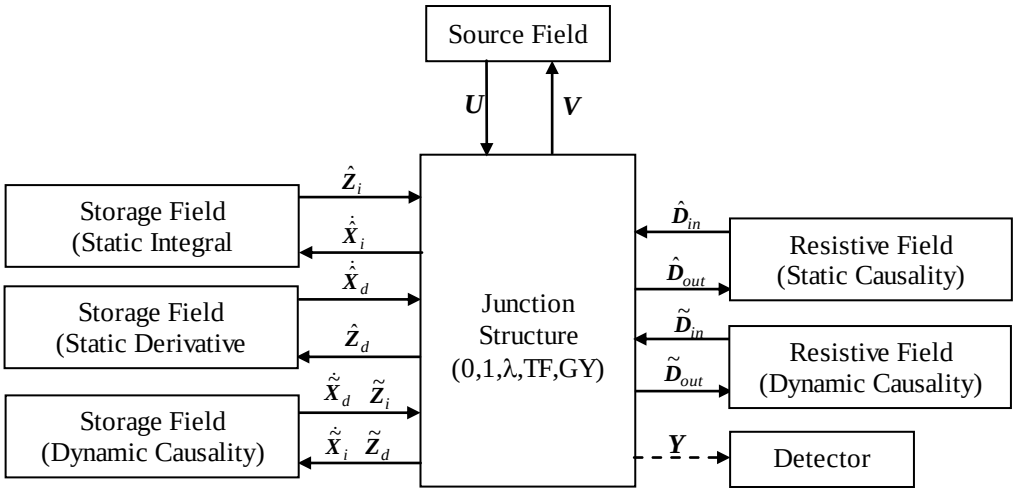

Figure 22: The General Hybrid Bond Graph with Signal Detectors giving Outputs.

Considering the constitutive law for the storage elements:

$$\begin{bmatrix} \boldsymbol{Z}_i \\ \boldsymbol{Z}_d \end{bmatrix} = \begin{bmatrix} \mathbf{F}_i & \mathbf{F} \\ \mathbf{F}^{\mathrm{T}} & \mathbf{F}_d \end{bmatrix} \begin{bmatrix} \boldsymbol{X}_i \\ \boldsymbol{X}_d \end{bmatrix} \qquad \textbf{(44)}$$

Substituting (44) into (43) leads to the general implicit state equation:

$$\boldsymbol{Y} = \left(\mathbf{S}_{41} - \mathbf{S}_{43}\mathbf{H}\mathbf{S}_{13}^{\mathrm{T}}\right)\left(\mathbf{F}_i\,\boldsymbol{X}_i + \mathbf{F}\,\boldsymbol{X}_d\right) + \mathbf{S}_{42}\,\dot{\boldsymbol{X}}_d + \left(\mathbf{S}_{43}\mathbf{H}\mathbf{S}_{34} + \mathbf{S}_{44}\right)\boldsymbol{U} \qquad \textbf{(45)}$$

Assume $\mathbf{J} = \mathbf{S}_{41} - \mathbf{S}_{43}\mathbf{H}\mathbf{S}_{13}^{\mathrm{T}}$ and reorganise to give:

$$\boldsymbol{Y} = \mathbf{J}\mathbf{F}_i\,\boldsymbol{X}_i + \mathbf{J}\mathbf{F}\,\boldsymbol{X}_d + \mathbf{S}_{42}\,\dot{\boldsymbol{X}}_d + \left(\mathbf{S}_{43}\mathbf{H}\mathbf{S}_{34} + \mathbf{S}_{44}\right)\boldsymbol{U} \qquad \textbf{(46)}$$

This is a rather unorthodox form of the output equation, since it is a function of $\dot{\boldsymbol{X}}_d$ rather than taking the expected $\boldsymbol{Y} = \mathbf{C}\,\boldsymbol{X} + \mathbf{D}\boldsymbol{U}$ form. When all storage elements are in static causality, this is of little consequence, since $\dot{\boldsymbol{X}}_d = 0$. The expected descriptor system can then be found, and standard matrix-rank criteria can be used to analyse the hybrid bond graph.

Property 4: Output Equation for a Hybrid Bond Graph with Causally Static Storage Elements

The output equation takes the usual LTI Descriptor System form iff there is static causality on the storage elements.

However, in a hybrid bond graph, storage elements can take dynamic causality and the $\dot{\boldsymbol{X}}_d$ term must be considered. Impulse modes (where there is a step change in state on commutation) occur, where $\dot{\boldsymbol{X}}_d$ has a value that tends to infinity. This concept is elaborated on in section 4.4. Storage elements only take dynamic causality in the case of ideal switching: i.e. there is no dissipation (otherwise a dissipative R-element would act as a 'causality resistance,' and there would be no dynamic causality and hence no impulse mode). Since ideal switching is instantaneous, the impulse loss has infinite frequency but no width, and hence there is no energy loss. So, although $\dot{\boldsymbol{X}}_d \to \infty$ in some cases, there is no energy loss. Ignoring the $\mathbf{S}_{42}\,\dot{\boldsymbol{X}}_d$ will have no effect on the control properties of the model.

Property 5: Output Equation for a Hybrid Bond Graph with Causally Dynamic Storage Elements

If there is dynamic causality on one or more storage elements, there is an $\dot{\boldsymbol{X}}_d$ term in the output equation which can tend to infinity. Since there is no real energy loss associated with this term, it does not affect the control properties and can be neglected.

The Hybrid Bond Graph can be used to generate the standard LTI Descriptor System form. This allows comparison with control properties using established techniques such as matrix-rank criteria.

Definition 26: LTI Descriptor System for a Hybrid Bond Graph

The LTI Descriptor System is:

$$\begin{aligned} \mathbf{E}\,\dot{\boldsymbol{X}} &= \mathbf{A}\,\boldsymbol{X} + \mathbf{B}\boldsymbol{U} \\ \boldsymbol{Y} &= \mathbf{C}\,\boldsymbol{X} + \mathbf{D}\boldsymbol{U} \end{aligned} \qquad \textbf{(47)}$$

Where:

$$\mathbf{E} = \begin{bmatrix} \boldsymbol{\Lambda}_{11} & -\mathbf{S}_{12} \\ \mathbf{0} & \mathbf{0} \end{bmatrix},\ \mathbf{A} = \begin{bmatrix} \mathbf{K}\mathbf{F}_i & \mathbf{K}\mathbf{F} \\ -\mathbf{S}_{12}^{\mathrm{T}}\mathbf{F}_i - \boldsymbol{\Lambda}_{22}\mathbf{F}^{\mathrm{T}} & -\mathbf{S}_{12}^{\mathrm{T}}\mathbf{F} - \boldsymbol{\Lambda}_{22}\mathbf{F}_d \end{bmatrix},\ \mathbf{B} = \begin{bmatrix} \mathbf{S}_{14} + \mathbf{S}_{13}\mathbf{H}\mathbf{S}_{34} \\ \mathbf{S}_{24} \end{bmatrix},$$

$$\mathbf{C} = \begin{bmatrix} \left(\mathbf{S}_{41} - \mathbf{S}_{43}\mathbf{H}\mathbf{S}_{13}^{\mathrm{T}}\right)\mathbf{F}_i & \left(\mathbf{S}_{41} - \mathbf{S}_{43}\mathbf{H}\mathbf{S}_{13}^{\mathrm{T}}\right)\mathbf{F} \end{bmatrix},\ \mathbf{D} = \left(\mathbf{S}_{43}\mathbf{H}\mathbf{S}_{34} + \mathbf{S}_{44}\right).$$

4.4 Impulse modes

Recall the implicit equation derived in chapter 3, and compare it to the standard implicit equation.

$$\begin{aligned} &\mathbf{E}\,\dot{\boldsymbol{X}} = \mathbf{A}\,\boldsymbol{X} + \mathbf{B}\boldsymbol{U} \\ &\begin{bmatrix} \boldsymbol{\Lambda}_{11} & -\mathbf{S}_{12} \\ \mathbf{0} & \mathbf{0} \end{bmatrix}\begin{bmatrix} \dot{\boldsymbol{X}}_i \\ \dot{\boldsymbol{X}}_d \end{bmatrix} = \begin{bmatrix} \mathbf{K}\mathbf{F}_i & \mathbf{K}\mathbf{F} \\ -\mathbf{S}_{12}^{\mathrm{T}}\mathbf{F}_i - \boldsymbol{\Lambda}_{22}\mathbf{F}^{\mathrm{T}} & -\mathbf{S}_{12}^{\mathrm{T}}\mathbf{F} - \boldsymbol{\Lambda}_{22}\mathbf{F}_d \end{bmatrix}\begin{bmatrix} \boldsymbol{X}_i \\ \boldsymbol{X}_d \end{bmatrix} + \begin{bmatrix} \mathbf{S}_{14} + \mathbf{S}_{13}\mathbf{H}\mathbf{S}_{34} \\ \mathbf{S}_{24} \end{bmatrix}\boldsymbol{U} \end{aligned} \qquad \textbf{(48)}$$

i.e. $\mathbf{E} = \begin{bmatrix} \boldsymbol{\Lambda}_{11} & -\mathbf{S}_{12} \\ \mathbf{0} & \mathbf{0} \end{bmatrix}$, $\mathbf{A} = \begin{bmatrix} \mathbf{K}\mathbf{F}_i & \mathbf{K}\mathbf{F} \\ -\mathbf{S}_{12}^{\mathrm{T}}\mathbf{F}_i - \boldsymbol{\Lambda}_{22}\mathbf{F}^{\mathrm{T}} & -\mathbf{S}_{12}^{\mathrm{T}}\mathbf{F} - \boldsymbol{\Lambda}_{22}\mathbf{F}_d \end{bmatrix}$ and $\mathbf{B} = \begin{bmatrix} \mathbf{S}_{14} + \mathbf{S}_{13}\mathbf{H}\mathbf{S}_{34} \\ \mathbf{S}_{24} \end{bmatrix}$

There is a time-varying term $\dot{\boldsymbol{X}}_d$ in the algebraic equations yielded by the pseudo-states of the storage elements in derivative causality. This is multiplied by zero (by the lower portion of **E**) to give an algebraic constraint. However, where storage elements in derivative causality are coupled to the states (i.e. $\mathbf{S_{12}}$, and therefore $\mathbf{E_{12}}$ in the implicit equation, are nonzero), a $\dot{\boldsymbol{X}}_d$ term is present and the pseudo state is differentiated across the commutation. The pseudo-state is nominally assumed to have a zero initial value, and take a non-zero value on commutation. This means that there is a step increase in the pseudo-state between the initial condition (incrementally before commutation) and the finite value it holds at time *t* (incrementally after commutation). The first row of (48) after commutation therefore gives:

$$\boldsymbol{\Lambda}_{11}\,\dot{\boldsymbol{X}}_i - \mathbf{S}_{12}\,\dot{\boldsymbol{X}}_d = \mathbf{K}\mathbf{F}_i\,\boldsymbol{X}_i + \mathbf{K}\mathbf{F}\,\boldsymbol{X}_d + \left(\mathbf{S}_{14} + \mathbf{S}_{13}\mathbf{H}\mathbf{S}_{34}\right)\boldsymbol{U} \qquad \textbf{(49)}$$

Where:

$$\dot{\boldsymbol{X}}_d = \frac{(\boldsymbol{X}_d)_t - (\boldsymbol{X}_d)_0}{dt} \text{ and } dt \to 0 \text{ therefore } \dot{\boldsymbol{X}}_d \to \infty \qquad \textbf{(50)}$$

Differentiating this step change over zero time yields a mode of infinite frequency: this is the impulse mode.

Commutation does not always result in a step change and subsequent impulse mode. Recall that the states and pseudo-states are intimately connected: each energy-storage element in dynamic causality has both a state variable (active when the element is in integral causality) and a pseudo-state (active when it is in derivative causality). By considering the type of discontinuity, some observations can be made on the relationship between states and pseudo-states.

Property 6: Impulses on Type 1 Structural Discontinuities

A type 1 structural discontinuity yields an impulse on initial commutation as two subsystems with different dynamic properties become joined and constrained (setting a storage element to derivative causality).

When the system returns to its original state on subsequent commutation, there is no impulsive mode.

For a type 1 structural discontinuity, where bodies are disconnected (OFF) in the reference mode and the commutation connects them, the initial value of the pseudo-state may indeed be zero if that body was at rest. Alternatively, it may have another value if it is controlled by another source or subsystem. There is typically an energy loss as the body changes its behaviour suddenly (for example, a falling rigid body hitting the ground, or a truck clutch being engaged: both of which give an audible loss). In real life - which is continuous - this is a measurable dissipation occurring over a finite time (albeit a small one). The abstraction to a discontinuity with no resistance is responsible for the impulse loss. The equations for an example system are shown in Table 9.

Table 9: Equations for Modes in Isolation, Type 1 Discontinuity

a) Reference Mode	b) After Commutation of the X1-Junction
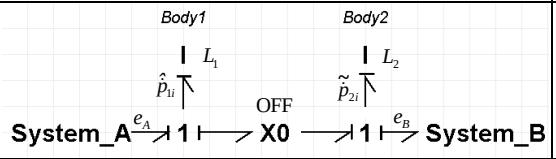	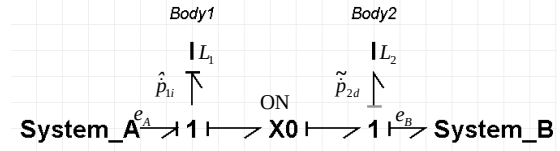
$\begin{bmatrix} 1 & 0 \\ 0 & 1 \end{bmatrix}\begin{bmatrix} \dot{\hat{p}}_{1i} \\ \dot{\tilde{p}}_{2i} \end{bmatrix} = \begin{bmatrix} 0 & 0 \\ 0 & 0 \end{bmatrix}\begin{bmatrix} \hat{p}_{1i} \\ \tilde{p}_{2i} \end{bmatrix} + \begin{bmatrix} 1 & 0 \\ 0 & 1 \end{bmatrix}\begin{bmatrix} e_A \\ e_B \end{bmatrix}$	$\begin{bmatrix} 1 & 1 \\ 0 & 0 \end{bmatrix}\begin{bmatrix} \dot{\hat{p}}_{1i} \\ \dot{\tilde{p}}_{2d} \end{bmatrix} = \begin{bmatrix} 0 & 0 \\ L_1 & L_2 \end{bmatrix}\begin{bmatrix} \hat{p}_{1i} \\ \tilde{p}_{2d} \end{bmatrix} + \begin{bmatrix} 1 & 1 \\ 0 & 0 \end{bmatrix}\begin{bmatrix} e_A \\ e_B \end{bmatrix}$

Assume that a commutation occurs at time *t* during a simulation. Prior to commutation (at time *t*-1) the system is in the reference mode and both storage elements are in integral causality. After commutation, Body 2 is in derivative causality. The second row of the implicit equation gives an algebraic term for $\tilde{p}_{2d}$, but there is also a differential $\dot{\tilde{p}}_{2d}$ term in the first row. Looking at the differentiation across the commutation:

$$\dot{\tilde{p}}_{2d} \approx \frac{\tilde{p}_{2d(t)} - \tilde{p}_{2i(t-1)}}{\Delta t} \qquad \textbf{(51)}$$

Where $\tilde{p}_{2i(t-1)}$ is known from the previous time-step's calculation, and $\tilde{p}_{2d(t)} = \hat{p}_{1i(t)}$ because the two inertia elements are now rigidly constrained. Note that all values are known, so there is no need to reinitialise the variables using canonical forms. The time step is also nonzero and known, and governed by the integrator parameters used for computation. A large step change (compared to the time step) may cause computational difficulties at this point as the left hand side of the state equation can become large. In this case it may be advantageous to set $\dot{\tilde{p}}_{2d(t)} = 0$, $\tilde{p}_{2d(t)} = \hat{p}_{1i(t)}$ and neglect the impulse. This naturally violates conservation of energy but would ease computation considerably.

If the reverse situation is true, i.e. there is a type 2 structural discontinuity where the bodies are connected in the reference mode and the commutation disconnects them, the initial value of the pseudo state is not zero.

Property 7: Impulses on Type 2 Structural Discontinuities

A type 2 structural discontinuity does not yield an impulse on initial commutation. In this case, the state of the storage element which switches to derivative causality is identical to its value immediately before commutation. Hence there is no step change in state variable and no energy loss.

When the system returns to its original state on subsequent commutation, there is a step change in state variable. However, this does not manifest as an impulsive off diagonal term in the E matrix: it is simply the newly activated $\dot{\boldsymbol{X}}_i$ term. This term is the output calculated from the state variables and inputs at the current time, and there has been no differentiation over a zero time step. Hence there is no impulse.

In this case, the initial value of the pseudo-state is equal to the [usually finite] value of the corresponding state variable immediately before commutation. Furthermore, after commutation the pseudo-state is not sent to zero. The behaviour of the element may be controlled by some other system, or may tend to zero over time (for example, a clutch disconnecting a load which freewheels until it finally reaches rest). In this case there is no step change in variable and no impulse. However, when commutation occurs again and the disconnected body is reconnected to the system (going from zero to a finite value), a step change in state variable may then occur. Consider a system with one element in dynamic causality, which has just commutated back to the mode in which it is in integral causality. Row 1 of the implicit equation (which is now explicit) gives:

$$\mathbf{I}\,\dot{\boldsymbol{X}}_i = \mathbf{KF}_i\,\boldsymbol{X}_i + \left(\mathbf{S}_{14} + \mathbf{S}_{13}\mathbf{H}\mathbf{S}_{34}\right)\boldsymbol{U} \qquad \textbf{(52)}$$

Here, $\dot{\boldsymbol{X}}_i$ is the output, stated in terms of the state variables and input at the current time step. Although a step change may have occurred, there is no impulsive term in the equation.

Hence each term in $\mathbf{E_{12}}$ potentially represents an impulse mode, but in reality there is only an impulse loss where there are type 1 discontinuities. Any algorithm for computing impulsive modes must take the variety of possible cases into account.

The use of pseudo-states means that the state variable never needs to be reinitialised using the algorithms developed by Mosterman [45] or Podgursky [55]. In type 1 systems, the pseudo-state variable arises because there is a kinematic constraint between two elements, and the pseudo-state of one is equal

to the state of the other. In type 2 systems, there is no step change on the initial commutation, but a subsequent commutation may result in a step change: this does not result in an impulsive term in the equations because the differential term is explicit.

A mathematical impulse has infinite magnitude and zero width, hence there is no actual energy loss. In reality, there can be dissipation in the form of an audible noise, spark or heat loss. This can be represented on the bond graph via a resistance element, or neglected in which case conservation of energy does not hold true. Mosterman [42] suggests that conservation of state is the important concept in system modelling, and the impulse energy dissipated during discontinuous events is 'free energy.'

Each mode change is a sliding mode change and the implicit equation can always be used because one side of it is always known. The use of impulse models like Newton's collision law (i.e. restitution) are a different case. In impulse models there is a jump in state space between modes of operation and an associated energy loss. This type of impulsive loss should not be confused with the impulse modes described above. Impulse models are discussed in section 4.5.

4.5 Impulse Losses

A key concept in variable topology systems is that of impulsive losses. The term 'impulse' is used in conjunction with two subtely different issues which must be distinguished here. The first is the impulse modes associated with the causally dynamic model and the initial value of the pseudo-state: i.e. the mathematical treatment of ideal switching. The second is the abstraction of the modes of operation themselves: much of the existing work on the subject investigates collisions using restitution, where the contact phase itself (and consequent dissipation) is so short as to be abstracted to a discontinuity.

Considerable work has been dedicated to the question of impulse losses on commutation, including Mosterman's work on implicit modelling [45] and Zimmer & Cellier's proposal for an Impulse Bond Graph [14]. Mosterman's work in particular gave rise to a body of work where state variables are reinitialised after each discontinuous event. These authors use the classical case study of Newton's Collision Law with restitution. Collision is an example of a subset of hybrid model called the Impulse model [12]. Here, the continuous state changes impulsively on hitting prescribed regions of state space. The 'jumps' in state space are not energy conserving: and hence an impulse loss must be accounted for. In the case of collision, the continuous state changes from positive

to negative velocity with any energy loss accounted for via the coefficient of restitution.

The use of a Boolean controlled junction in the hybrid bond graph dictates the way a discontinuity is abstracted: a switch must be ON or OFF, contact TRUE or FALSE, etc. In the case of a collision (see Section 5.4), this means that the short 'in contact' phase is modelled (whereas Newton's collision law neglects this). Any energy dissipation is modelled on the bond graph during this phase: there is no restitution. The hybrid bond graph with structural switching is always a 'Switching model' as defined by Branicky et al [12] i.e. the vector field changes discontinuously when the state hits a boundary, but these changes are not impulsive.

It was seen in Section 4.4 that where an impulse mode occurs there is a discontinuous change in the value of a state variable, but the state does not need to be reinitialised (it can be computed from the rest of the system) and there is no energy loss. The leads to the following property:

Property 8: Impulse Losses in a Hybrid Bond Graph

This Hybrid Bond graph does not undergo impulsive discontinuous state changes. There are no energy losses on commutation.

The case study in Section 5.4 investigates a collision in more detail and show that Newton's collision law and an associated coefficient of restitution can be derived from a Hybrid Bond Graph.

4.6 Control Properties

Analysis of the state and implicit equations using matrix rank criteria – with or without transforming the model to various canonical forms – is well established and perhaps the most common form of system analysis. Some background is given in the literature review, and results are therefore quoted in this chapter without proof.

The use of matrix rank criteria necessitates an input-output model, i.e. they must be applied after causality has been assigned. The validity of this approach has been called into question, as discussed in the literature review. A more promising approach, in keeping with the ideals of physical and behavioural modelling,

would be a geometric one as proposed by Lewis [80] and Willems [83]. This is recommended as a topic for further study.

4.6.1 Controllability

It is well established that a controllability matrix can be constructed for an LTI descriptor system, which has rank equal to model order when the system is controllable. This controllability matrix is a function of the **A** and **B** matrices, which are in turn comprised from the submatrices of **S**. Controllability can hence be seen on the bond graph by analysing the causal paths, or established from the junction structure matrix **S**.

Previous work on hybrid bond graphs (using switched sources) has investigated R-Controllability and Impulse-Controllability, relating to the finite and impulse modes respectively. The same distinction is made here.

Recall that the order of the model, and hence the number of finite modes of the system, are given by the number of storage elements in integral causality. It therefore follows that the maximum number of finite modes occurs when most storage elements are in integral causality, i.e. the reference mode.

Property 9: Finite Modes of a Hybrid Bond Graph

The maximum number of finite modes is given by the order of the model in the reference mode. This is the maximum number of storage elements in integral causality: $dim[\boldsymbol{X}_i]$.

R-controllability of these finite modes is an intuitive concept, fundamentally the same as the structural controllability defined for a continuous LTI system. The model is R-controllable when independent relationships in the equations – corresponding to causal paths on the bond graph which exist both when preferred integral and preferred derivative causality are applied – are present between each storage element and a source element.

When there is a controlled junction in a causal path, that path is severed or ceases to exist when the junction is OFF. It is intuitive that when a controlled junction occurs between the storage element in integral causality and a source element:

- a Boolean term occurs in the underlying equations which sets the relationship to zero when the junction is OFF, and
- the dynamic causality around the junction clearly shows that the causal path is broken when the junction is OFF.

There are two possible outcomes when this happens. The first is that the storage element remains in integral causality, in which case it may be controlled by another source, or it may be uncontrolled i.e. there is an uncontrolled finite mode. The other outcome is that the storage element changes its causal assignment and the finite mode ceases to exist: in this case the impulse controllability must be assessed.

There may also be instances where a nearby controlled junction(s) results in dynamic causality on a causal path between the storage element in integral causality and a source element. The controlled junction(s) does not physically sever the causal path, but still clearly affects controllability because the relationship between the source and storage elements is nonexistent in some modes of operation.

Property 10: Structural R-Controllability of a Hybrid Bond Graph

A Hybrid Bond Graph is structurally R-Controllable iff:

1. There is a causal path between each storage element in integral causality and a source element in all modes of operation i.e.:
    a. the causal path does not cross a controlled junction or,
    b. there is another path between it and a storage element crossing a controlled junction which operates in a mutually exclusive manner with the first, or,
    c. the causal path crosses a controlled junction which forces the storage element into derivative causality when it is OFF.
2. In the reference mode, the rank of the controllability matrix is equal to the model order: i.e. the number of storage elements in integral causality when preferred integral causality is applied is equal to the number of storage elements in derivative causality when preferred derivative causality is applied (allowing dualisation of source elements).

This is an extension of R-controllability for a static bond graph, acknowledging the observations made for structural switching and dynamic causality i.e. that relationships in the model can be dependent on commutation.

Impulse controllability has been established by hybrid bond graph practitioners such as Rahmani et al. [113] by inspecting the switching sources, which is clearly not applicable here as there are none. An equivalent criteria of establishing causal paths between controlled junctions and storage elements could be stated. However, the impulse modes in the underlying equations no longer relate to the switching laws present in the hybrid bond graph with switching sources. In this Hybrid Bond Graph, the impulse modes relate solely to storage elements in dynamic causality. Impulse controllability, in the classical sense, is whether these impulse modes can be controlled by a non-impulsive input, verified by the algebraic tests which involve inspecting the ranks of the **E**, **A** and **B** matrices. In the discussion of impulse modes (section 4.4) it was noted that an impulse does not always occur in the model: it depends on the type of discontinuity and commutation.

Recall that impulse modes occur when a storage element is in dynamic causality i.e. it switches between integral and derivative causality with commutation. In a well-constructed model there would not normally be any elements in static derivative causality.

Property 11: Impulse [Infinite] Modes of a Hybrid Bond Graph

The maximum number of impulse modes is given by the number of storage elements in dynamic causality: $dim\left[\tilde{\boldsymbol{X}}_d\right]$.

This is an extension of the property for switched bond graphs (using switched sources). The number of impulse modes in any single mode of operation is given by the number of storage elements in derivative causality. It therefore follows that the maximum possible number of impulse modes is given when all possible storage elements are in derivative causality, and this is in turn given by the storage elements in dynamic causality. Note that this is the maximum for the overall model: when some modes are mutually exclusive, there may not be a single mode of operation where all impulse modes occur.

Since the impulsive modes only exist when the respective storage element is in derivative causality, impulse controllability could be established by a causal path (and algebraic relation) between the element and a source (either directly or via another element which is controlled) in that mode of operation. Looking at the hybrid bond graph, since impulse modes relate to storage elements in dynamic causality, this manifests as a causal path (at least part of which will be dashed, i.e. dynamic) between a storage element in derivative [dynamic] causality and a

source element. Hence, Rahmani et al's criterion for impulse controllability [113] is adapted and reused here.

Property 12: Structural Impulse Controllability of a Hybrid Bond Graph

The model is impulse controllable iff there exists a causal path between an input source and a controlled junction passing through a storage element in derivative causality.

An uncontrolled impulse mode would indicate an element which has been severed from the sources in the system and switched to derivative causality, such as an accumulator or capacitor discharging when the pump/battery is disconnected.

4.6.2 Observability

Observability is assessed in much the same way as controllability, as it is the dual property. The difference is that the observability matrix is a function of the **C** matrix relating the outputs to the model states (as opposed to the **B** matrix relating the inputs to the model states). A standard output equation including a **C** matrix is derived for the hybrid bond graph in section 4.3.2.

Impulsive terms can occur when storage elements take derivative causality with commutation. Impulse observability is assumed to be the dual property of impulse controllability. Consequently R-observability for finite modes also exists and is assumed to be the dual of R-controllability. The following properties are therefore presented without proof.

Property 13: Structural R-Observability of a Hybrid Bond Graph

A Hybrid Bond Graph is structurally R-Observable iff:

1. There is a causal path between each storage element in integral causality and a detector element in all modes of operation i.e.:
    a. the causal path does not cross a controlled junction or,
    b. there is another path between it and a detector element crossing a controlled junction which operates in a mutually exclusive manner with the first, or,
    c. the causal path crosses a controlled junction which forces the storage element into derivative causality when it is OFF.

2. In the reference mode, the rank of the observability matrix is equal to the model order: i.e. the number of storage elements in integral casuality when preferred integral causality is applied is equal to the number of storage elements in derivative causality when preferred derivative causality is applied (allowing dualisation of detector elements).

Property 14: Structural Impulse Observability of a Hybrid Bond Graph

The model is impulse observable iff there exists a causal path between an detector and a controlled junction passing through a storage element in derivative causality.

4.6.3 Asymptotic Stability

Asymptotic stability is typically established by finding the solutions of the characteristic polynomial. The roots for all possible modes of operation can be obtained and plotted: roots with positive real parts indicate unstable behaviour. This is a numeric approach rather than a structural one, and outside the scope of structural analysis.

Where asymptotic stability does not exist, it indicates the presence of 'zero modes' (eigenvectors with vanishing eigenvalues). Recall that 'structurally null modes' (i.e. eigenvalues which are zero, or the poles at the origin) are given by the storage elements which are in integral causality when preferred derivative causality is assigned [111].

For the Hybrid Bond Graph this philosophy can be extended to the number of I and C elements which have to stay in [static] integral causality plus the number of I and C elements in dynamic causality when a preferred derivative causality is assigned to the bond graph model.

Property 15: Structurally Null Modes of a Hybrid Bond Graph

The maximum possible number of structurally null modes is given by the number of storage elements which can take integral causality when preferred derivative causality is assigned to the bond graph.

This is the number of storage elements in [static] integral causality, plus the number of storage elements in dynamic causality in the BGD.

$$D_0 = \left(dim\left[\hat{\boldsymbol{X}}_i\right] + dim\left[\tilde{\boldsymbol{X}}_i\right] \right)_{BGD} \quad \textbf{(53)}$$

This property is a logical extension of the procedure for finding structurally null modes in a static bond graph. Recall that placing the bond graph in preferred derivative causality yields a mathematical model in an alternative form including the inverse of the system matrices (as described in section 2.5.6). When storage elements remain in integral causality, it means that **A** is singular and there are no unique solutions to the system of equations. In particular, inspection of the characteristic equation reveals that there are *k* structurally null modes relating to the rows of **A** in which the causal constraints (in the BGD) exist, and these in turn relate to the storage elements that remain in integral causality in the BGD. The characteristic polynomial for the hybrid system is shown in (54):

$$P(s) = \left| s\mathbf{E}(\Lambda) - \mathbf{A}(\Lambda) \right| = s^k \left(s^q + a_{q-1} s^{q-1} + \ldots + a_1 s + a_0 \right) \quad \textbf{(54)}$$

The *k* structurally null modes may not be obvious from the Hybrid Bond Graph in integral causality. Consider a simple example of two rotating bodies connected by a shaft with a clutch fitted. The Hybrid Bond Graph in preferred derivative causality is shown in Figure 23.

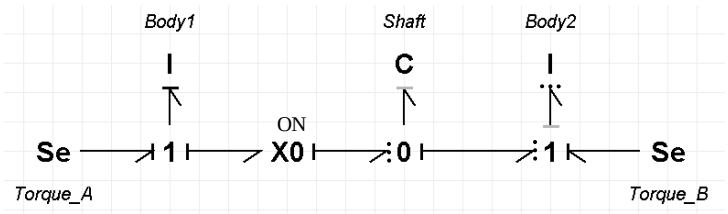

Figure 23: Example System in Preferred Derivative Causality, with Ideal Clutch.

In preferred derivative causality, the reference mode (the mode with most elements in derivative causality) occurs with the clutch engaged (ON), in which case body 1 is still in integral causality. When the clutch is OFF, body 2 is also sent to integral causality. Hence there are two possible structurally null modes, with one of them dependent on commutation of the clutch.

4.7 Summary

The structural switching and dynamic causality in this proposed hybrid bond graph naturally affects structural analysis and exploitation of causal assignment. This chapter revisits some of the most common results from these fields with respect to the hybrid bond graph.

The dynamic causality assignment has been investigated, and it can be shown that there are two types of discontinuities (type 1 and type 2), reflecting the algebraic constraints which occur with commutation.

The presence of structural discontinuities can give mixed-Boolean transfer function and output equations. These are used in control engineering to determine dynamic and control properties so it becomes clear that system dynamics (poles and zeros, stability) and controllability / observability can vary with commutation. Since matrix-rank criteria can be reflected in the bond graph itself, some revised criteria for commonly used control properties are proposed.

Mathematical impulses occur where storage elements are in dynamic causality, but these only have magnitude in the case of type-1 discontinuities. In type-2 discontinuities, there is no step change in the value of a state variable as the storage element switches from integral to derivative causality.

Variable structure systems and impulse modes are discussed. An important observation is that this hybrid bond graph dictates that discontinuities are abstracted to sliding modes. This is an important result because it dispenses with the need to reinitialise state variables after commutation or allow for unknown impulsive losses.

Chapter 5: Case Studies

5.1 Preliminaries

This chapter presents a number of case studies to demonstrate the proposed hybrid bond graph method.

The power boost converter is used as a widely-used example in the literature, and therefore enables comparison with other methods. The implicit state equation is derived for this purpose. This case study was used to illustrate structural switching in a journal paper on the subject [124], available on http://online.sagepub.com. The final, definitive version of this paper has been published in the Proceedings of the IMechE Part I: Journal of Systems and Control Engineering, Vol. 227 Issue 3, March 2013 by SAGE Publications Ltd., All rights reserved. © IMechE 2013.

The drop test case study is presented as a model with several types of discontinuity, which can be problematic to compute efficiently. Using controlled junctions and elements, a model can be constructed in the commercial software package 20Sim and simulated. A version of this model and results form a paper which was presented at IASTED MIC 2013 [127]. The final, definitive version of this paper has been published in Proceedings of the IASTED Multiconferences: Modelling, Identification, and Control (MIC 2013), Vol. 794, February 2013 by ACTA Press.

A study of contact between bodies is presented in order to investigate impulse models and their associated losses on commutation. The hybrid bond graph produces a switching model which considers the ‘in contact’ phase of a collision and conservation of momentum holds true. Newton’s collision law can be obtained from this model, including the systematic derivation of a coefficient of restitution from the bond graph elements.

5.2 Power Converter

5.2.1 Overview

A boost converter is shown in Figure 24, as an example incorporating both electrical switches and a mechanical clutch. Buisson et al [98] use this example to demonstrate the use of switching sources, as do Edström et al [37] on a simplified version. Here, controlled junctions will be used.

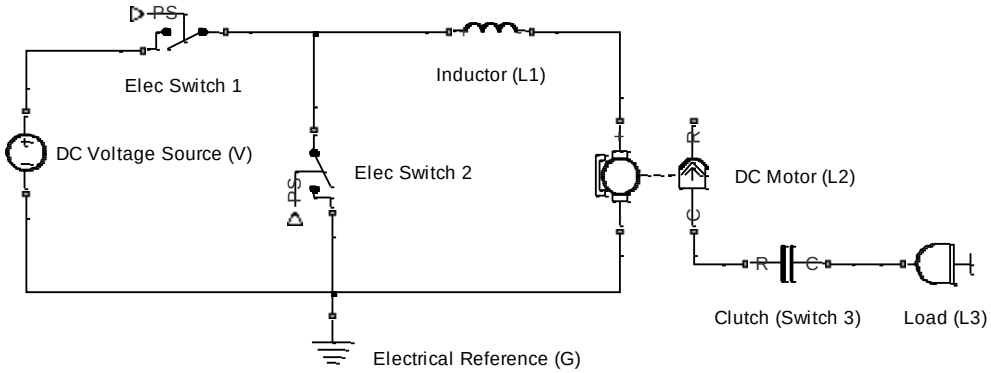

Figure 24: Schematic Diagram of a Boost Converter Supplying a D.C. Motor with Load

5.2.2 Hybrid Bond Graph

The bond graph of the power converter is shown in Figure 25. Note that some resistance elements have been added (R_1 and R_2) to model losses in the circuit and friction in the moving parts. The full bond graph, incorporating the ground, is shown for completeness, and then systematically simplified by removing bonds to the ground (which is 0V) where appropriate. The ground still needs to be represented and attached to switch 2; it is worth noting that this source and controlled junction arrangement is remarkably similar to the switching source in principle.

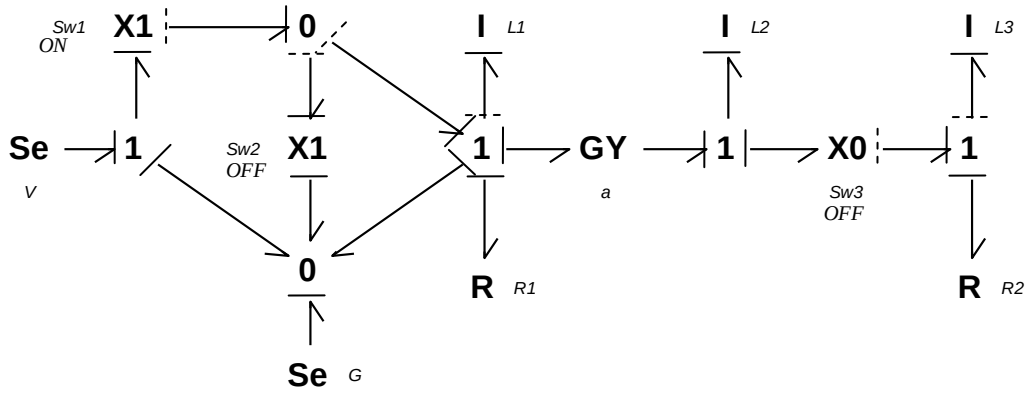

(a) Complete Model

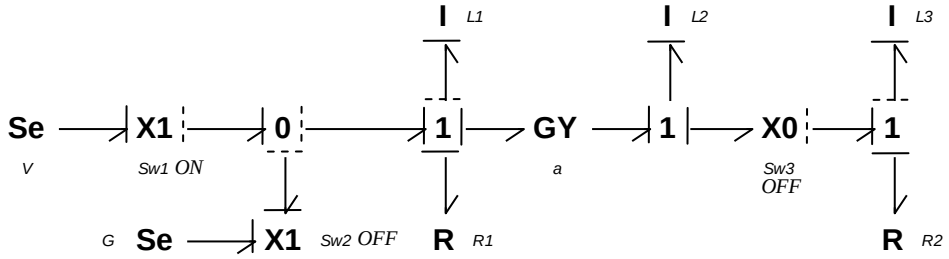

(b) Simplified Model

Figure 25: Hybrid Bond Graph Model of the Boost Converter.

The solid causal strokes in Figure 25 show the reference configuration, which is the configuration in which the most storage elements are in integral causality. This is given by switch 1 being ON and switches 2 and 3 being OFF. Note that it would also be given if switch 1 was OFF and switch 2 was ON; in this case a reference mode can be selected arbitrarily.

5.2.3 Deriving the Junction Structure and Implicit State Equations

In order to construct the Junction Structure Matrix, the modes of operation and any consequential dynamic causality must be identified. This gives the functions of λ used in the JSM and state equations. These are in turn used to construct a matrix $\mathbf{\Lambda}$, which multiplies the equation by zeros and ones to ensure that state variables disappear from the model when they are not part of a mode of operation.

Dashed causal lines show the alternative causality assignment where causality is dynamic (i.e. it changes with mode of operation). Controlled junctions become a source of zero flow/effort when they are 'OFF,' which means that they do not take any other flow/effort inputs in that mode of operation. 'Paths' of dynamic causality can be traced, showing the effect of switches on other elements (noted in Table 10). It can be seen that switches 1 and 2 both affect the causal assignment of L_1, while switch 3 solely governs the assignment of L_3. In order to derive a switching rule for inclusion in the junction structure matrix (and, subsequently, the state space matrices), a truth table can be used. Looking at Table 11 it can be seen that L_3 is in integral causality when switch 3 is OFF. The state variable must therefore be 'active' when switch 3 is OFF: this can be achieved by multiplying the relevant row of the junction structure matrix by a Boolean $\overline{\lambda}_3$ (equal to 1 when switch 3 is not on, and otherwise equal to 0). The pseudo-state variable is likewise activated when the switch is on by multiplying the relevant row of the junction structure matrix by the Boolean λ_3 (equal to 1 when switch 3 is on).

Table 10: Effects of Switches on Causality of 1-Port Elements

Switch	Dynamic Causal Path to Storage Element?	Dynamic Causal Path to Resistor Element?
Sw1	L1	-
Sw2	L1	-
Sw3	L3	-

Table 11: Truth Table of the effect of switches on dynamic causal elements

Sw1	Sw2	Sw3	Causality on L1	Causality on L3
0	0	-	Derivative	-
0	1	-	Integral	-
1	0	-	Integral	-
1	1	-	Causal Conflict	-
-	-	0	-	Integral
-	-	1	-	Derivative

Looking at Table 11 a slightly more complex Boolean expression must be defined. L_1 is in integral causality when switch 1 *or* switch 2 is on. The element is in derivative causality when both switches are OFF. The case where both are on is a forbidden mode since the voltage source is short circuited, and this is

reflected by a causal conflict. The state variable can therefore be activated using a Boolean factor of $\lambda_1 \oplus \lambda_2$ where the symbol '$\oplus$' denotes an 'exclusive or' (XOR) operation. The pseudo-state variable is activated when this is not true, i.e. $\overline{\lambda_1 \oplus \lambda_2}$.

The junction structure matrix (given below) is constructed as for a regular system, but includes further Booleans where an input/output depends on the state of a switch. The subscript '*d*' denotes derivative causality.

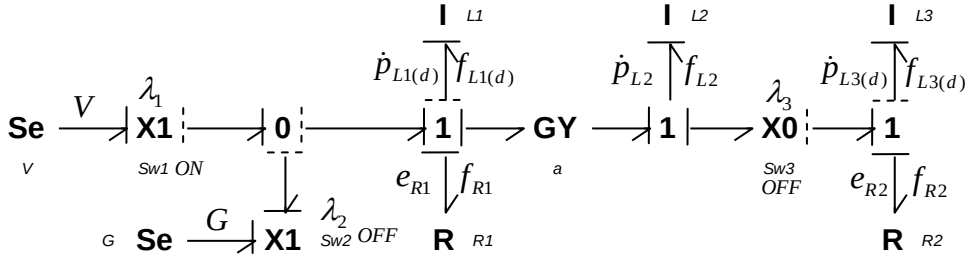

Figure 26: Hybrid Bond Graph Model of the Boost Converter with Notation

$$\Lambda \begin{bmatrix} \dot{p}_{L1} \\ \dot{p}_{L2} \\ \dot{p}_{L3} \\ \hline f_{L1d} \\ f_{L3d} \\ \hline f_{R1} \\ f_{R2} \end{bmatrix} = \left[\begin{array}{ccc:cc:cc:cc} 0 & -a(\lambda_1 \oplus \lambda_2) & 0 & 0 & 0 & -(\lambda_1 \oplus \lambda_2) & 0 & \lambda_1 & \lambda_2 \\ a(\lambda_1 \oplus \lambda_2) & 0 & 0 & 0 & -\lambda_3 & 0 & -\lambda_3 & 0 & 0 \\ 0 & 0 & 0 & 0 & 0 & 0 & -\overline{\lambda}_3 & 0 & 0 \\ \hdashline 0 & 0 & 0 & 0 & 0 & 0 & 0 & 0 & 0 \\ 0 & \lambda_3 & 0 & 0 & 0 & 0 & 0 & 0 & 0 \\ \hdashline (\lambda_1 \oplus \lambda_2) & 0 & 0 & 0 & 0 & 0 & 0 & 0 & 0 \\ 0 & \lambda_3 & \overline{\lambda}_3 & 0 & 0 & 0 & 0 & 0 & 0 \end{array}\right] \begin{bmatrix} f_{L1} \\ f_{L2} \\ f_{L3} \\ \hline \dot{p}_{L1d} \\ \dot{p}_{L3d} \\ \hline e_{R1} \\ e_{R2} \\ \hline V \\ G \end{bmatrix} \qquad \textbf{(55)}$$

Where:

$$\mathbf{\Lambda} = diag\left[(\lambda_1 \oplus \lambda_2) \quad 1 \quad \overline{\lambda}_3 \quad (\overline{\lambda_1 \oplus \lambda_2}) \quad \lambda_3 \quad 1 \quad 1\right] \qquad \textbf{(56)}$$

Remember that switches are thought of as null sources when they are 'OFF.' The input flows and efforts representing the switches in the OFF position could be explicitly shown as inputs, but since these are inherently zero, it is sufficient to imply them by sending terms in the JSM to zero.

The state space matrices for this system seem a little complicated, since there is a causal path between L_2 and L_3 (in derivative causality) when the clutch is engaged. This can be seen from the coefficient in submatrices $\mathbf{S_{21}}$ and $\mathbf{S_{12}}$ of the junction structure matrix. If the classical state equations were to be found, there

may be a motivation here for adding a parasitic element to break the causal path. Instead, the use of pseudo-states for those elements in derivative causality handles the loop.

The constitutive law of the R-field is:

$$D_{in} = \mathbf{L} D_{out}$$
$$\begin{bmatrix} f_{R1} \\ f_{R2} \end{bmatrix} = \begin{bmatrix} R_1^{-1} & 0 \\ 0 & R_2^{-1} \end{bmatrix} \begin{bmatrix} e_{R1} \\ e_{R2} \end{bmatrix} \qquad \textbf{(57)}$$

The constitutive law for the storage elements:

$$\begin{bmatrix} Z_{int} \\ Z_{der} \end{bmatrix} = \begin{bmatrix} \mathbf{F}_i & \mathbf{F} \\ \mathbf{F}^T & \mathbf{F}_d \end{bmatrix} \begin{bmatrix} X_{int} \\ X_{der} \end{bmatrix} \qquad \textbf{(58)}$$

Where: $\mathbf{F}_i = \begin{bmatrix} L_1^{-1} & 0 & 0 \\ 0 & L_2^{-1} & 0 \\ 0 & 0 & L_3^{-1} \end{bmatrix}$, $\mathbf{F}_d = \begin{bmatrix} L_1^{-1} & 0 \\ 0 & L_3^{-1} \end{bmatrix}$, $\mathbf{F} = \begin{bmatrix} 0 & 0 \\ 0 & 0 \\ 0 & 0 \end{bmatrix}$

The implicit equation for the power converter example is therefore:

$$\begin{bmatrix} (\lambda_1 \oplus \lambda_2) & 0 & 0 & 0 & 0 \\ 0 & 1 & 0 & 0 & \lambda_3 \\ 0 & 0 & \bar{\lambda}_3 & 0 & 0 \\ 0 & 0 & 0 & 0 & 0 \\ 0 & 0 & 0 & 0 & 0 \end{bmatrix} \begin{bmatrix} \dot{p}_{L1} \\ \dot{p}_{L2} \\ \dot{p}_{L3} \\ \dot{p}_{L1d} \\ \dot{p}_{L3d} \end{bmatrix} = \begin{bmatrix} \frac{-(\lambda_1 \oplus \lambda_2)}{L_1 R_1} & \frac{-a(\lambda_1 \oplus \lambda_2)}{L_2} & 0 & 0 & 0 \\ \frac{a(\lambda_1 \oplus \lambda_2)}{L_1} & \frac{-\lambda_3}{L_2 R_2} & 0 & 0 & 0 \\ 0 & 0 & \frac{-\bar{\lambda}_3}{L_3 R_2} & 0 & 0 \\ 0 & 0 & 0 & \frac{(\bar{\lambda}_1 \oplus \bar{\lambda}_2)}{L_1} & 0 \\ 0 & \frac{\lambda_3}{L_2} & 0 & 0 & -\frac{\lambda_3}{L_3} \end{bmatrix} \begin{bmatrix} p_{L1} \\ p_{L2} \\ p_{L3} \\ p_{L1d} \\ p_{L3d} \end{bmatrix} + \begin{bmatrix} \lambda_1 & \lambda_2 \\ 0 & 0 \\ 0 & 0 \\ 0 & 0 \\ 0 & 0 \end{bmatrix} \begin{bmatrix} V \\ G \end{bmatrix} \qquad \textbf{(59)}$$

For the reference configuration ($\lambda_1 = 1$, $\lambda_2 = 0$, $\lambda_3 = 0$), this gives:

$$\begin{bmatrix} 1 & 0 & 0 & 0 & 0 \\ 0 & 1 & 0 & 0 & 0 \\ 0 & 0 & 1 & 0 & 0 \\ 0 & 0 & 0 & 0 & 0 \\ 0 & 0 & 0 & 0 & 0 \end{bmatrix} \begin{bmatrix} \dot{p}_{L1} \\ \dot{p}_{L2} \\ \dot{p}_{L3} \\ \dot{p}_{L1d} \\ \dot{p}_{L3d} \end{bmatrix} = \begin{bmatrix} \frac{-1}{L_1 R_1} & \frac{-a}{L_2} & 0 & 0 & 0 \\ \frac{a}{L_1} & 0 & 0 & 0 & 0 \\ 0 & 0 & \frac{-1}{L_3 R_2} & 0 & 0 \\ 0 & 0 & 0 & 0 & 0 \\ 0 & 0 & 0 & 0 & 0 \end{bmatrix} \begin{bmatrix} p_{L1} \\ p_{L2} \\ p_{L3} \\ p_{L1d} \\ p_{L3d} \end{bmatrix} + \begin{bmatrix} 1 & 0 \\ 0 & 0 \\ 0 & 0 \\ 0 & 0 \\ 0 & 0 \end{bmatrix} \begin{bmatrix} V \\ G \end{bmatrix} \qquad \textbf{(60)}$$

Giving an explicit state space model with the equations:

$$\begin{aligned}
\dot{p}_{L1} &= \frac{-1}{L_1 R_1} p_{L1} - \frac{a}{L_2} p_{L2} + V \\
\dot{p}_{L2} &= \frac{a}{L_1} p_{L1} \\
\dot{p}_{L3} &= \frac{-1}{L_3 R_2} p_{L3}
\end{aligned} \qquad \textbf{(61)}$$

There are state equations for each of the three storage elements in integral causality, as expected. With the clutch disengaged, the load L_3 is clearly disconnected from the rest of the system.

For the case where most elements are in derivative causality (i.e. $\lambda_1 = 0$, $\lambda_2 = 0$, $\lambda_3 = 1$):

$$\begin{bmatrix} 0 & 0 & 0 & 0 & 0 \\ 0 & 1 & 0 & 0 & 1 \\ 0 & 0 & 0 & 0 & 0 \\ 0 & 0 & 0 & 0 & 0 \\ 0 & 0 & 0 & 0 & 0 \end{bmatrix} \begin{bmatrix} \dot{p}_{L1} \\ \dot{p}_{L2} \\ \dot{p}_{L3} \\ \dot{p}_{L1d} \\ \dot{p}_{L3d} \end{bmatrix} = \begin{bmatrix} 0 & 0 & 0 & 0 & 0 \\ 0 & \frac{-1}{L_2 R_2} & 0 & 0 & 0 \\ 0 & 0 & 0 & 0 & 0 \\ 0 & 0 & 0 & L_1^{-1} & 0 \\ 0 & L_2^{-1} & 0 & 0 & -L_3^{-1} \end{bmatrix} \begin{bmatrix} p_{L1} \\ p_{L2} \\ p_{L3} \\ p_{L1d} \\ p_{L3d} \end{bmatrix} + \begin{bmatrix} 0 & 0 \\ 0 & 0 \\ 0 & 0 \\ 0 & 0 \\ 0 & 0 \end{bmatrix} \begin{bmatrix} V \\ G \end{bmatrix} \qquad \textbf{(62)}$$

Giving an implicit model with the equations:

$$\begin{aligned}
\dot{p}_{L2} + \dot{p}_{L3d} &= \frac{-1}{L_2 R_2} p_{L2} \\
0 &= \frac{1}{L_1} p_{L1d} \\
0 &= \frac{1}{L_2} p_{L2} - \frac{1}{L_3} p_{L3d}
\end{aligned} \qquad \textbf{(63)}$$

With both electrical switches off and the clutch engaged, the inertia of the DC Motor exerts no torque on the system and the load is not free to rotate. This is consistent with what would be expected.

An interesting case occurs in the mode where both switches 1 and 2 are ON. This is a ‘forbidden’ mode, which short-circuits the voltage source and sets up a causal conflict in the bond graph. The implicit state equations are (assuming clutch is disengaged).

$$\begin{bmatrix} 0 & 0 & 0 & 0 & 0 \\ 0 & 1 & 0 & 0 & 0 \\ 0 & 0 & 1 & 0 & 0 \\ 0 & 0 & 0 & 0 & 0 \\ 0 & 0 & 0 & 0 & 0 \end{bmatrix} \begin{bmatrix} \dot{p}_{L1} \\ \dot{p}_{L2} \\ \dot{p}_{L3} \\ \dot{p}_{L1d} \\ \dot{p}_{L3d} \end{bmatrix} = \begin{bmatrix} 0 & 0 & 0 & 0 & 0 \\ 0 & 0 & 0 & 0 & 0 \\ 0 & 0 & \frac{-1}{L_3 R_2} & 0 & 0 \\ 0 & 0 & 0 & L_1^{-1} & 0 \\ 0 & 0 & 0 & 0 & 0 \end{bmatrix} \begin{bmatrix} p_{L1} \\ p_{L2} \\ p_{L3} \\ p_{L1d} \\ p_{L3d} \end{bmatrix} + \begin{bmatrix} 1 & 1 \\ 0 & 0 \\ 0 & 0 \\ 0 & 0 \\ 0 & 0 \end{bmatrix} \begin{bmatrix} V \\ G \end{bmatrix} \qquad \textbf{(64)}$$

The first line gives $V = -G$ i.e. the input voltage is equal to 0V (Ground voltage). This clearly reflects the short circuit. The forces on the inertia components transpire to be zero.

5.2.4 Discontinuities on Variables at Commutation

Consider the case where the system is in the reference mode, and then the clutch (Switch 3) engages. Recalling the reference configuration:

$$\begin{bmatrix} 1 & 0 & 0 & 0 & 0 \\ 0 & 1 & 0 & 0 & 0 \\ 0 & 0 & 1 & 0 & 0 \\ 0 & 0 & 0 & 0 & 0 \\ 0 & 0 & 0 & 0 & 0 \end{bmatrix} \begin{bmatrix} \dot{p}_{L1} \\ \dot{p}_{L2} \\ \dot{p}_{L3} \\ \dot{p}_{L1d} \\ \dot{p}_{L3d} \end{bmatrix} = \begin{bmatrix} \frac{-1}{L_1 R_1} & -\frac{a}{L_2} & 0 & 0 & 0 \\ \frac{a}{L_1} & 0 & 0 & 0 & 0 \\ 0 & 0 & \frac{-1}{L_3 R_2} & 0 & 0 \\ 0 & 0 & 0 & 0 & 0 \\ 0 & 0 & 0 & 0 & 0 \end{bmatrix} \begin{bmatrix} p_{L1} \\ p_{L2} \\ p_{L3} \\ p_{L1d} \\ p_{L3d} \end{bmatrix} + \begin{bmatrix} 1 & 0 \\ 0 & 0 \\ 0 & 0 \\ 0 & 0 \\ 0 & 0 \end{bmatrix} \begin{bmatrix} V \\ G \end{bmatrix} \quad \textbf{(65)}$$

After the clutch connects:

$$\begin{bmatrix} 1 & 0 & 0 & 0 & 0 \\ 0 & 1 & 0 & 0 & 1 \\ 0 & 0 & 0 & 0 & 0 \\ 0 & 0 & 0 & 0 & 0 \\ 0 & 0 & 0 & 0 & 0 \end{bmatrix} \begin{bmatrix} \dot{p}_{L1} \\ \dot{p}_{L2} \\ \dot{p}_{L3} \\ \dot{p}_{L1d} \\ \dot{p}_{L3d} \end{bmatrix} = \begin{bmatrix} \frac{-1}{L_1 R_1} & \frac{-a}{L_2} & 0 & 0 & 0 \\ \frac{a}{L_1} & \frac{-1}{L_2 R_2} & 0 & 0 & 0 \\ 0 & 0 & 0 & 0 & 0 \\ 0 & 0 & 0 & 0 & 0 \\ 0 & L_2^{-1} & 0 & 0 & -L_3^{-1} \end{bmatrix} \begin{bmatrix} p_{L1} \\ p_{L2} \\ p_{L3} \\ p_{L1d} \\ p_{L3d} \end{bmatrix} + \begin{bmatrix} 1 & 0 \\ 0 & 0 \\ 0 & 0 \\ 0 & 0 \\ 0 & 0 \end{bmatrix} \begin{bmatrix} V \\ G \end{bmatrix} \quad \textbf{(66)}$$

The equations are:

Reference Configuration

$$\begin{aligned} \dot{p}_{L1} &= \frac{-1}{L_1 R_1} p_{L1} - \frac{a}{L_2} p_{L2} + V \\ \dot{p}_{L2} &= -\frac{a}{L_1} p_{L1} \\ \dot{p}_{L3} &= \frac{-1}{L_3 R_2} p_{L3} \end{aligned} \quad \textbf{(67)}$$

Clutch engaged

$$\begin{aligned}
\dot{p}_{L1} &= \frac{-1}{L_1 R_1} p_{L1} - \frac{a}{L_2} p_{L2} + V \\
\dot{p}_{L2} + \dot{p}_{L3d} &= -\frac{a}{L_1} p_{L1} - \frac{1}{L_2 R_2} p_{L2} \\
0 &= \frac{1}{L_2} p_{L2} - \frac{1}{L_3} p_{L3d}
\end{aligned} \qquad \textbf{(68)}$$

The system changes from having three differential state equations, to having two differential equations and an associated algebraic relationship. The equation for $\dot{p}_{L1}$ remains unchanged with commutation. The equation for $\dot{p}_{L2}$ becomes a function of p_{L2} and pseudo-state $\dot{p}_{L3d}$ in addition to p_{L1}, and the algebraic relation can be rearranged to give p_{L3d} in terms of p_{L2}. If the clutch commutes back from engaged to disengaged, the state of L_3 just after commutation is equal to the state just before i.e. $p_{L3d} = p_{L3}$ and $\dot{p}_{L3d} = \dot{p}_{L3}$, and there is no need to reinitialise the state.

In this model, any slippage occurring between fully engaged and fully disengaged would be modelled by resistance element R_2. Some authors would define slippage as an extra mode of operation. Here the controlled junction purely represents whether contact has been made or not. Any additional non-linear dissipation can be modelled using a resistance element, which could itself be abstracted to discrete modes of operation (i.e. parametric switching) and captured in a controlled element.

5.2.5 Structural Analysis of the Power Converter

The *order* of the model varies, since two of the storage elements are in dynamic causality. The reference mode gives the highest order, which in this case is 3. It is possible to achieve a mode of operation where the order is only 1.

The *rank* of the model is 2 or 3, again depending on the mode of operation: this is clearly seen if a causally dynamic hybrid bond graph with preferred derivative causality is constructed (Figure 27). Alternatively, the maximum number of linearly independent columns in $(\mathbf{S}_{11}\ \mathbf{S}_{13})$ can be seen to vary between 2 and 3. This is because the second column of $\mathbf{S}_{13}$ is linearly independent when switch 3 is OFF but not when it is ON.

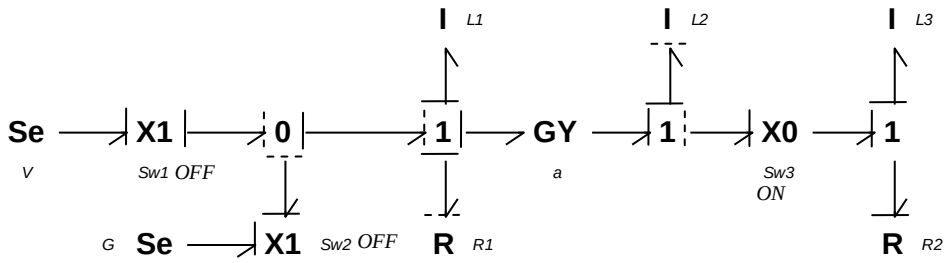

Figure 27: Hybrid Bond Graph Model of the Boost Converter in Preferred Derivative Causality

Asymptotic stability is also established from the bond graph with preferred derivative causality assigned (Figure 27). There are no storage elements in integral causality and hence no structurally null modes in the [preferred derivative causality] reference mode. This means that the model is asymptotically stable in this mode of operation. However, L2 is in dynamic causality and can take integral causality if the switches commutate, yielding a possible structurally null mode. Hence the model is unstable when the clutch (Sw3) is OFF.

Structural controllability is assessed by revisiting the bond graph in preferred integral causality. When switch 3 is OFF the subsystem formed by L_3 and R_2 is not controllable: there is no causal path between L_3 and either of the sources, shown in Figure 28. This may or may not be important depending on whether that subsystem needs to be controlled or can be ignored when OFF. In addition, if both switches 1 and 2 are OFF, there are no causal paths between any of the elements and the sources. Note that null sources (applied by controlled junctions when OFF) are not considered as sources for the purposes of controllability, since they literally add nothing to the system. There is a case for ignoring sinks and grounds (when they are zero – note that they are sometimes non-zero) for the same reason: a user would not normally change the value of a ground source in order to manipulate desired results.

This assessment of structural R-controllability is fairly intuitive. If the L_3-R_2 subsystem needs to be controlled when it is disconnected from the rest of the system, an additional source element can be added.

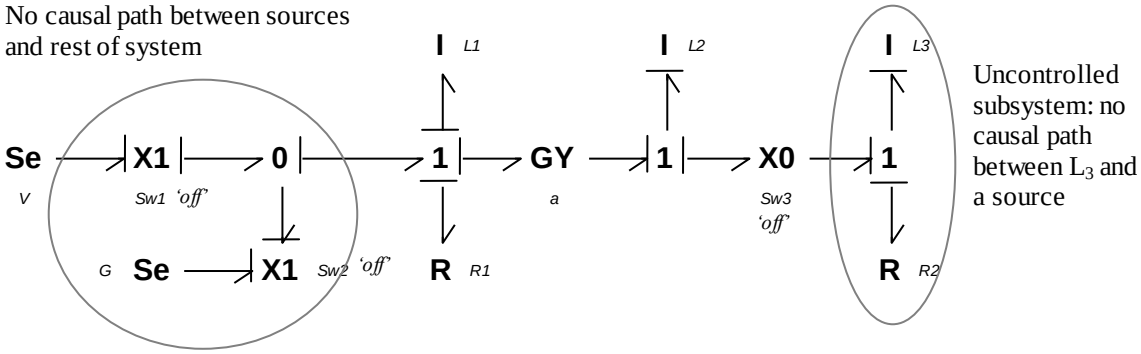

Figure 28: Static Bond Graph of the Boost Converter showing a mode with least structural R-Controllability

Impulse controllability is assessed by looking at whether there are causal paths between input sources and controlled junctions, passing through storage elements in dynamic causality in their derivative causality cases. Revisiting Figure 25, it can be seen that causal paths can be traced throughout the model when all switches are ON and L_3 is in derivative causality, indicating controllability of the impulse mode associated with L_3 provided switches 1 or 2 are ON. However, L_1 is only in derivative causality when both switch 1 AND switch 2 are OFF, which means there is never a causal path between a source element and L_1 in derivative causality: hence this impulse mode is uncontrollable. This is intuitive: when the sources are disconnected, the inductance represented by L_1 discharges uncontrollably.

In order for the model to be *observable*, detectors must be placed so as to satisfy the criteria for structural R-observability and impulse observability. The logical way to achieve structural R-observability is to add detector-elements to the system close to the storage elements so that the causal paths do not cross any controlled junctions. Rank and order of the obervability matrix should then be checked. Impulse observability is likewise ensured by positioning detector elements so that the path between them and a controlled junction passes through a storage element in derivative causality.

The four detectors added in Figure 29 ensure both R-observability and impulse observability.

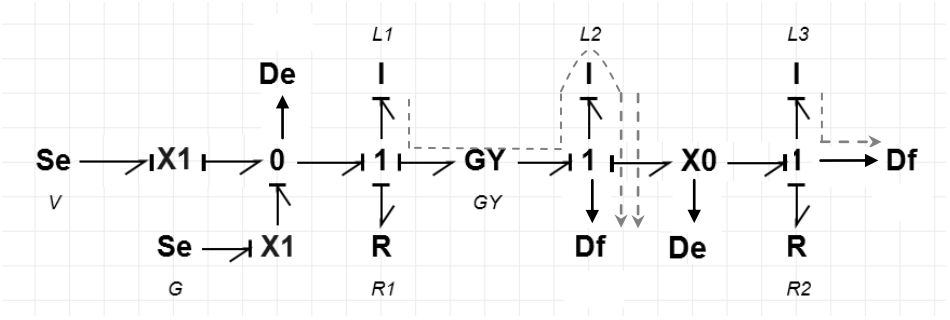

a) Reference Mode for R-Observability

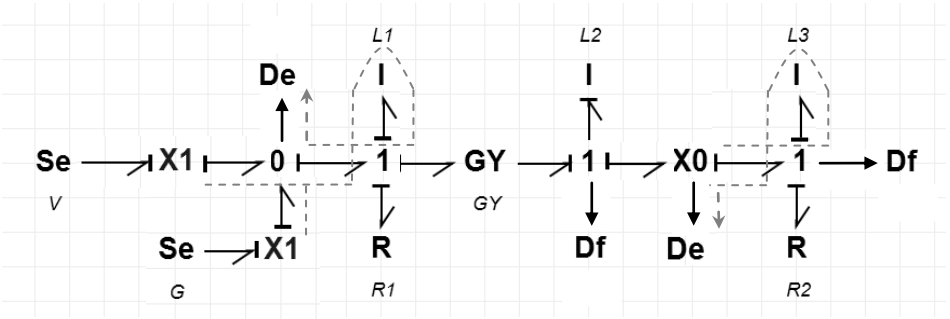

b) L_1 & L_3 in Derivative Causality for Impulse Observability

Figure 29: Adding Detector Elements to the Model in Preferred Integral Causality, with Causal Paths marked

In order to verify the properties of the model, the output equation can be found for the system. The junction structure matrix can be revised to include the detector elements:

$$\Lambda \begin{bmatrix} \dot{p}_{L1} \\ \dot{p}_{L2} \\ \dot{p}_{L3} \\ f_{L1d} \\ f_{L3d} \\ f_{R1} \\ f_{R2} \\ e_{D1} \\ f_{D2} \\ e_{D3} \\ f_{D4} \end{bmatrix} = \begin{bmatrix} 0 & -a(\lambda_1 \oplus \lambda_2) & 0 & 0 & 0 & -(\lambda_1 \oplus \lambda_2) & 0 & \lambda_1 & \lambda_2 \\ a(\lambda_1 \oplus \lambda_2) & 0 & 0 & 0 & -\lambda_3 & 0 & -\lambda_3 & 0 & 0 \\ 0 & 0 & 0 & 0 & 0 & 0 & -\bar{\lambda}_3 & 0 & 0 \\ 0 & 0 & 0 & 0 & 0 & 0 & 0 & 0 & 0 \\ 0 & \lambda_3 & 0 & 0 & 0 & 0 & 0 & 0 & 0 \\ (\lambda_1 \oplus \lambda_2) & 0 & 0 & 0 & 0 & 0 & 0 & 0 & 0 \\ 0 & \lambda_3 & \bar{\lambda}_3 & 0 & 0 & 0 & 0 & 0 & 0 \\ 0 & a(\overline{\lambda_1 \oplus \lambda_2}) & 0 & (\overline{\lambda_1 \oplus \lambda_2}) & 0 & (\overline{\lambda_1 \oplus \lambda_2}) & 0 & \lambda_1 & \lambda_2 \\ 0 & 1 & 0 & 0 & 0 & 0 & 0 & 0 & 0 \\ 0 & 0 & 0 & 0 & \lambda_3 & 0 & \lambda_3 & 0 & 0 \\ 0 & \lambda_3 & \bar{\lambda}_3 & 0 & 0 & 0 & 0 & 0 & 0 \end{bmatrix} \begin{bmatrix} f_{L1} \\ f_{L2} \\ f_{L3} \\ \dot{p}_{L1d} \\ \dot{p}_{L3d} \\ e_{R1} \\ e_{R2} \\ V \\ G \end{bmatrix} \quad \textbf{(69)}$$

$$\begin{bmatrix} 1 & 0 & 0 & 0 & -(\bar{\lambda}_1+\bar{\lambda}_2) & 0 \\ 0 & 1 & 0 & 0 & 0 & 0 \\ 0 & 0 & 1 & 0 & 0 & -\lambda_3 \\ 0 & 0 & 0 & 1 & 0 & 0 \end{bmatrix} \begin{bmatrix} y_1 \\ y_2 \\ y_3 \\ y_4 \\ \dot{p}_{L1d} \\ \dot{p}_{L3d} \end{bmatrix} = \begin{bmatrix} -\frac{(\bar{\lambda}_1+\bar{\lambda}_2)(\lambda_1 \oplus \lambda_2)}{L_1 R_1} & \frac{a(\bar{\lambda}_1+\bar{\lambda}_2)}{L_2} & 0 & 0 & 0 \\ 0 & \frac{1}{L_2} & 0 & 0 & 0 \\ 0 & -\frac{\lambda_3}{L_2 R_2} & 0 & 0 & 0 \\ 0 & \frac{\lambda_3}{R_2} & \frac{\bar{\lambda}_3}{L_3} & 0 & 0 \end{bmatrix} \begin{bmatrix} p_{L1} \\ p_{L2} \\ p_{L3} \\ p_{L1d} \\ p_{L3d} \end{bmatrix} + \begin{bmatrix} \lambda_1 & \lambda_2 \\ 0 & 0 \\ 0 & 0 \\ 0 & 0 \end{bmatrix} \begin{bmatrix} V \\ G \end{bmatrix} \quad \textbf{(70)}$$

The Transfer function can now be found. Take, as an example, the transfer function between the voltage source and a detector measuring the angular velocity of L_2. There are four possible causal paths, and hence four possible flat loops, shown in Figure 30. Two are 'touching,' because they share junctions and 1-port elements in the same mode.

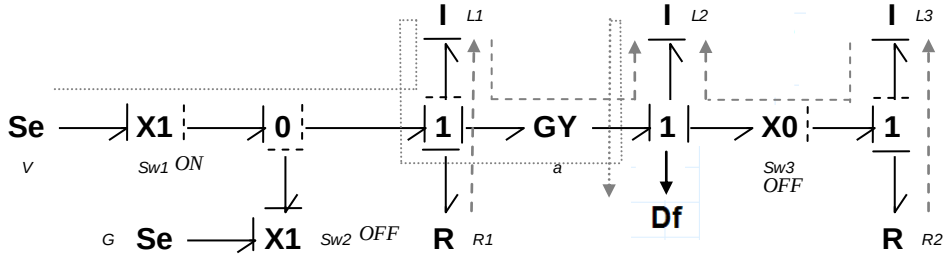

Figure 30: Hybrid Bond Graph in Preferred Integral Causality, Causal Paths representing Flat Loops Marked.

The gains of these flat loops are:

1. between R1 and L1 in integral causality, marked in blue $-(\lambda_1 \oplus \lambda_2)R_1 / sI_{L1}$
2. disjoint path across the gyrator, between L1 and L2 in integral causality, marked in red $-(\lambda_1 \oplus \lambda_2)a^2 / s^2 I_{L1} I_{L2}$
3. between L3 in derivative causality and L2 in integral causality, marked in green $-\lambda_3 / s^2 I_{L2} I_{L3}$
4. between R2 and L3 in integral causality, marked in blue $-\bar{\lambda}_3 R_2 / sI_{L3}$

This gives a graph determinant Δ of:

$$\Delta = 1 + \left[\frac{(\lambda_1 \oplus \lambda_2)R_1}{sI_{L1}} + \frac{(\lambda_1 \oplus \lambda_2)a^2}{s^2 I_{L1} I_{L2}} + \frac{\lambda_3}{s^2 I_{L2} I_{L3}} + \frac{\bar{\lambda}_3 R_2}{sI_{L3}} \right] + \left[\frac{\lambda_3(\lambda_1 \oplus \lambda_2)R_1}{s^3 I_{L1} I_{L2} I_{L3}} + \frac{(\lambda_1 \oplus \lambda_2)\bar{\lambda}_3 R_2 a^2}{s^3 I_{L1} I_{L2} I_{L3}} + \frac{(\lambda_1 \oplus \lambda_2)\bar{\lambda}_3 R_2 R_1}{s^2 I_{L1} I_{L3}} \right] \quad \textbf{(71)}$$

Assume we want to find the transfer function between the applied voltage V and a flow sensor: the path, marked in orange on Figure 30, has a gain:

$$G_1 = {-\lambda_1 a^2}\Big/{s^2 I_{L1} I_{L2}} \qquad \textbf{(72)}$$

Note that this path only exists when switch 1 is ON. The first three loops (blue, red and green) touch this path, so a reduced graph determinant can be defined by eliminating them.

$$\Delta_1 = 1 + \frac{\bar{\lambda}_3 R_2}{s I_{L3}} \qquad \textbf{(73)}$$

By Shannon-Mason Loop rule:

$$\frac{\omega}{V} = \frac{G_1 \Delta_1}{\Delta} \qquad \textbf{(74)}$$

$$\frac{\omega}{V} = \frac{\dfrac{-\lambda_1 a^2}{s^2 I_{L1} I_{L2}}\left(1 + \dfrac{\bar{\lambda}_3 R_2}{s I_{L3}}\right)}{1 + \left[\dfrac{(\lambda_1 \oplus \lambda_2) R_1}{s I_{L1}} + \dfrac{(\lambda_1 \oplus \lambda_2) a^2}{s^2 I_{L1} I_{L2}} + \dfrac{\lambda_3}{s^2 I_{L2} I_{L3}} + \dfrac{\bar{\lambda}_3 R_2}{s I_{L3}}\right] + \left[\dfrac{\lambda_3 (\lambda_1 \oplus \lambda_2) R_1}{s^3 I_{L1} I_{L2} I_{L3}} + \dfrac{(\lambda_1 \oplus \lambda_2) \bar{\lambda}_3 R_2 a^2}{s^3 I_{L1} I_{L2} I_{L3}} + \dfrac{(\lambda_1 \oplus \lambda_2) \bar{\lambda}_3 R_2 R_1}{s^2 I_{L1} I_{L3}}\right]} \qquad \textbf{(75)}$$

The poles and zeros of the system can be seen to depend on commutation and a simplified transfer function can be obtained for any single mode of operation.

5.3 Landing Gear Drop Test

5.3.1 A High-Level Bond Graph of the Landing Gear

The landing gear on the ground compresses under load and cannot be modelled as a rigid body. A landing gear is similar in principle to the standard quarter car model used extensively in automotive engineering. They usually have an oleo-pneumatic strut in place of the mechanical suspension (spring and damper mounted in parallel) found on a typical car. A spring-mass-damper diagram is shown in Figure 31, and a high level model is presented in Figure 32.

A rigid body with mass and weight equal to the effective vertical load and inertia effects of the aircraft fuselage is attached to the upper end of the gear. The gear is assumed to act as a lumped mass with a centre of gravity coincident with that of the wheel. The oleo strut is attached via a [common effort] 0-junction, because it is known that there is common effort and a difference in velocities across the strut. The behaviour of the tyre and its contact with the ground, and of the oleo strut will be covered in sections 5.3.2 and 5.3.3. This model is implemented in the commercial software package 20Sim.

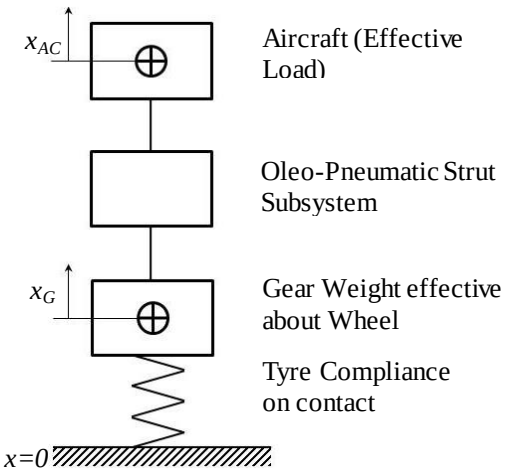

a) In-Situ on an Aircraft [128] **b) Spring-Mass-Damper Diagram**

Figure 31: A Typical Aircraft Landing Gear

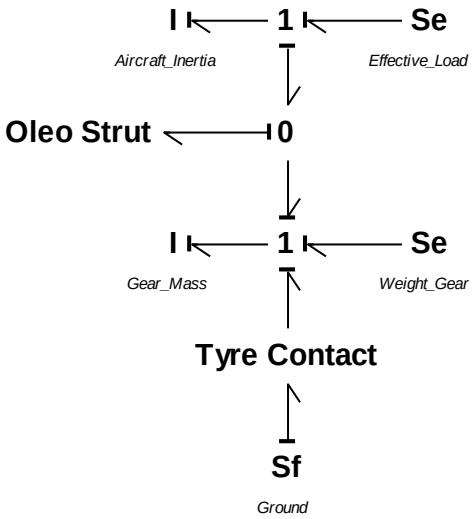

Figure 32: A High Level Bond Graph of a Landing Gear

5.3.2 Structural Discontinuities: Contact with the Ground

Contact is represented here using a controlled junction, in an identical way to the contact between bodies discussed in Chapter 4. Contact gives a variable topology system, which can lead to dynamic causal assignment and/or a change in the size of the underlying equations. It is implemented in this study via a bespoke coded element in 20Sim, where the displacement of the gear and ground are compared to establish whether contact occurs. The ideal causal assignment for the model changes with commutation. In this case, the tyre resistance prevents the dynamic causality from propagating throughout the model significantly, which means that the model can be simulated with a standard commercial software package. The model is shown in Figure 33.

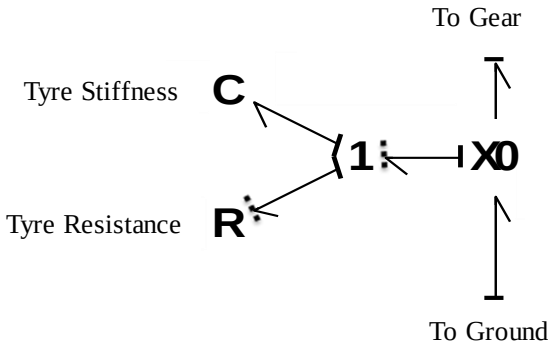

Figure 33: The Tyre & Contact Model, with Dynamic Causality Notation

In this model the tyre stiffness and resistance were given typical approximate linear values.

5.3.3 Parametric Discontinuities: The Oleo Strut

A typical oleo strut consists of a chamber filled with a fluid and gas mixture (which acts as a fluid spring), and an orifice plate which controls the rate at which the strut is compressed (adding damping). The use of '2-stage' oleo struts is commonplace (especially for the main landing gear of heavier aircraft) where there are two chambers of fluid and the second becomes active after a 'breakover' load is reached. A great many designs for oleo-pneumatic shock absorber exist [129] and Figure 34 details a typical configuration.

The constitutive equation for the fluid compliance varies depending on the volume of fluid displaced (i.e. the stroke of the oleo). When the aircraft is in the air, the oleo is fully extended and no load is applied: the piston rests on its end stops. When the aircraft first touches down, the oleo compliance is that of the fluid in the primary chamber. As load on the oleo increases, it reaches a breakout point and the second chamber starts to compress. There are therefore three modes of operation. The compliant modes are modelled by equation (76).

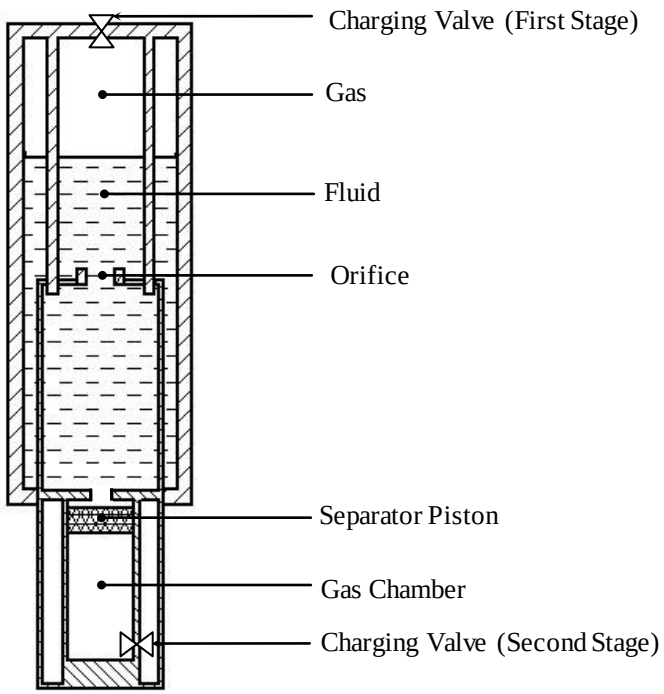

Figure 34: Detail of a Typical Two Stage Oleo-Pneumatic Strut

$$P_1 = \frac{P_0 V_0^{\gamma}}{(V_0 - \int Q dt)^{\gamma}} \qquad \textbf{(76)}$$

Each mode of operation could be described by a standard compliance element in bond graph notation, and activated by a controlled junction. In the 'rigid' mode the strut simply reacts the weight of the gear and could be represented as a modulated effort source. A 'tree' arrangement of controlled junctions is shown in Figure 35. The controlled 1-junctions – denoted X1 – become a source of zero flow when OFF. Switching coefficients λ_n are mutually exclusive.

Since the switching coefficients are mutually exclusive, and the causality on the bond connected to the rest of the system is static, the 'tree' could be concatenated into a single controlled element as proposed in Figure 36. The constitutive equation for this element is given by equation (77).

$$e = \lambda_1 \Phi_{C1}^{-1}\left(\int f \cdot dt\right) + \lambda_2 \Phi_{C2}^{-1}\left(\int f \cdot dt\right) + \lambda_3 \Phi_{C3}^{-1}\left(\int f \cdot dt\right) \qquad \textbf{(77)}$$

It is worth noting that the resistance provided by the orifice plate is also non-linear, in this case modelled using the standard equation for an orifice.

$$Q = C_f A_o \sqrt{\frac{2\Delta P}{\rho}} \qquad \textbf{(78)}$$

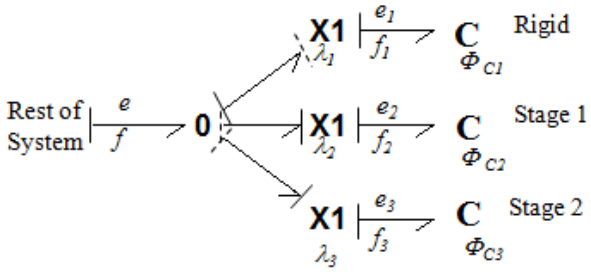

Figure 35: A 2-Stage Oleo represented by a 'Tree' of Bond Graph Elements.

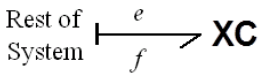

Figure 36: A 2-Stage Oleo represented by a Controlled Element

5.3.4 Determination of the State Equations

Some of the elements in this case study have nonlinear constitutive relations, rendering any Linear Time-Invariant (LTI) assumptions invalid. However, in this case the derivation can still be followed with nonlinear functions in place of linear coefficients.

The bond graph of the full model, including the detail of the contact and 2-stage oleo compliance, is given in Figure 37. A transformer (TF-element) with piston area as its modulation coefficient is inserted to formalise the transition between mechanical and hydraulic domains.

Inspection of this graph yields the junction structure equation (79) which relates all inputs and outputs, and this is turn can be used to derive the implicit state equations (80).

It can be seen that the switching term for the contact manifests in the equations, clearly disconnecting the ground velocity from the gear. The tyre resistance and

compliance also cease to have any effect on the gear when it is not in contact with the ground, which is consistent with expectation. The switching terms inside the controlled element representing the oleo fluid compliance do not manifest in the equations: they are contained inside the compliance function.

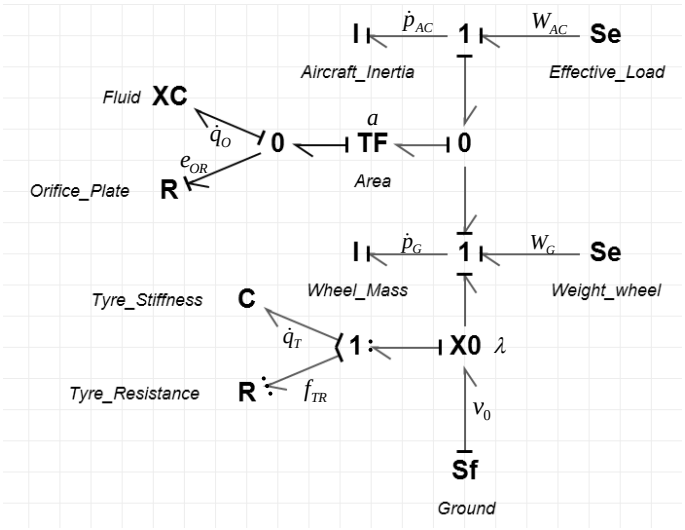

Figure 37: Complete Model of the Gear, Control Signals omitted for clarity

Deriving the state equations yields a mathematical model which can be transported to other modelling environments for simulation purposes. This would be necessary if the model is to be used as part of a larger programme or on a Model-in-the-loop apparatus which uses a specific code.

In Matlab, for example, a descriptor state-space model object can be defined from the explicit or implicit state and output equations (provided all elements have linear relationships). Some code would be required to establish the mode of operation at each time-step and hence values of the Boolean switching parameters λ_n. The nonlinear nature of this model means that nonlinear techniques must be used rather than relying on the LTI functionality in most common software packages.

$$\boldsymbol{\Lambda}\begin{bmatrix}\dot{p}_{AC}\\ \dot{q}_O\\ \dot{p}_G\\ \dot{q}_T\\ e_{OR}\\ f_{TR}\\ e_{TR}\end{bmatrix}=\begin{bmatrix}0 & a & 0 & 0 & 0 & 0 & 0 & 1 & 0 & 0\\ -a^{-1} & 0 & -a^{-1} & 0 & -1 & 0 & 0 & 0 & 0 & 0\\ 0 & a & 0 & \lambda & 0 & \lambda & 0 & 0 & 1 & 0\\ 0 & 0 & -\lambda & 0 & 0 & 0 & -\overline{\lambda} & 0 & 0 & \lambda\\ 0 & 1 & 0 & 0 & 0 & 0 & 0 & 0 & 0 & 0\\ 0 & 0 & -\lambda & 0 & 0 & 0 & 0 & 0 & 0 & \lambda\\ 0 & 0 & 0 & \overline{\lambda} & 0 & 0 & 0 & 0 & 0 & 0\end{bmatrix}\begin{bmatrix}f_{AC}\\ e_O\\ f_G\\ e_T\\ f_{OR}\\ e_{TR}\\ f_{TR}\\ W_{AC}\\ W_G\\ v_0\end{bmatrix} \quad \textbf{(79)}$$

$$\boldsymbol{\Lambda} = diag\begin{bmatrix}1 & 1 & 1 & 1 & 1 & \lambda & \overline{\lambda}\end{bmatrix}$$

$$\begin{aligned}
\dot{p}_{AC} &= a\Phi_{C_O}^{-1}(q_O)+W_{AC}\\
\dot{q}_O &= -\frac{1}{aM_{AC}}p_{AC}-\frac{1}{R_O\Phi_{C_O}(q_O)}-\frac{1}{aM_W}p_G\\
\dot{p}_G &= a\Phi_{C_O}^{-1}(q_O)-\frac{\lambda R_T}{M_W}p_G+\frac{\lambda}{C_T}q_T+W_G+\lambda R_T v_0\\
\dot{q}_T &= -\frac{\lambda}{M_W}p_G-\frac{\overline{\lambda}}{C_T R_T}q_T+\lambda v_0
\end{aligned} \quad \textbf{(80)}$$

5.3.5 Results & Discussion

The model was populated with approximate data for a typical aircraft and a simulation was run in 20Sim. The oleo was sized for the applied load. Since the model does not relate to any production aircraft, the results are assessed against subjective engineering experience.

Initially the model did not run due to the highly nonlinear constitutive relationship of the orifice plate. Linearising this element relieved this problem. The model could be improved by implementing a more representative piecewise-continuous relationship, which could be formalised by a XR-element (in the same way that the piecewise-continuous fluid compliance was formalised using a XC-element).

The results are presented in Figure 38 - Figure 41. The system is in free-fall for the initial fraction of a second (shown by the not-in-contact portion of Figure 41).

On contact, the system exhibits a ring-down response as expected. Discontinuous behaviour is evident in the plot for oleo pressure (Figure 38) where the oleo reaches its 'breakover load' and the second stage becomes active.

The model was populated with parameters roughly typical of an airliner. Although the model could not be correlated to experimental data, it does exhibit a response consistent with expected behaviour. Figure 38 shows that the oleo compresses instantly on contact, and there are discontinuities evident where the oleo 'breaks out.' There is some 'chattering' at ~3.5s where the oleo is operating very close to the breakover point. Figure 40 indicates that the tyre absorbs the remainder of the force on contact. Contact itself is verified by Figure 41, and it is clear that the gear 'bounces' before coming to rest on the ground. The 'aircraft' effective load (Figure 39) exhibits a typical 'ring-down' response and comes to rest in 6s.

The state equations (80) could be used to inspect the system a little further. The parametric switching relationship used to describe the fluid compliance is contained in the nonlinear compliance function. Only the switching coefficient λ denoting contact with the ground affects the form of these equations by multiplying terms by 1 or 0.

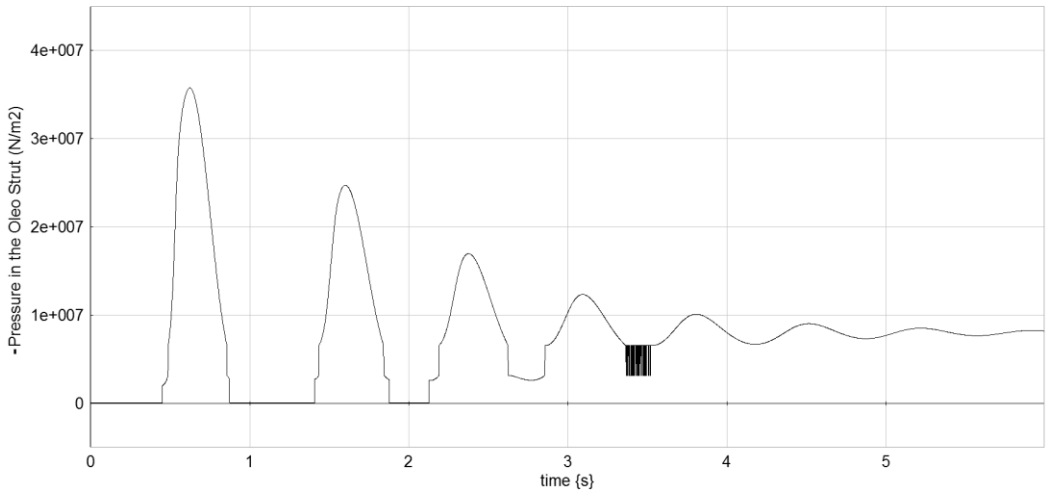

Figure 38: Simulation of the Drop Test, Pressure in Oleo Strut

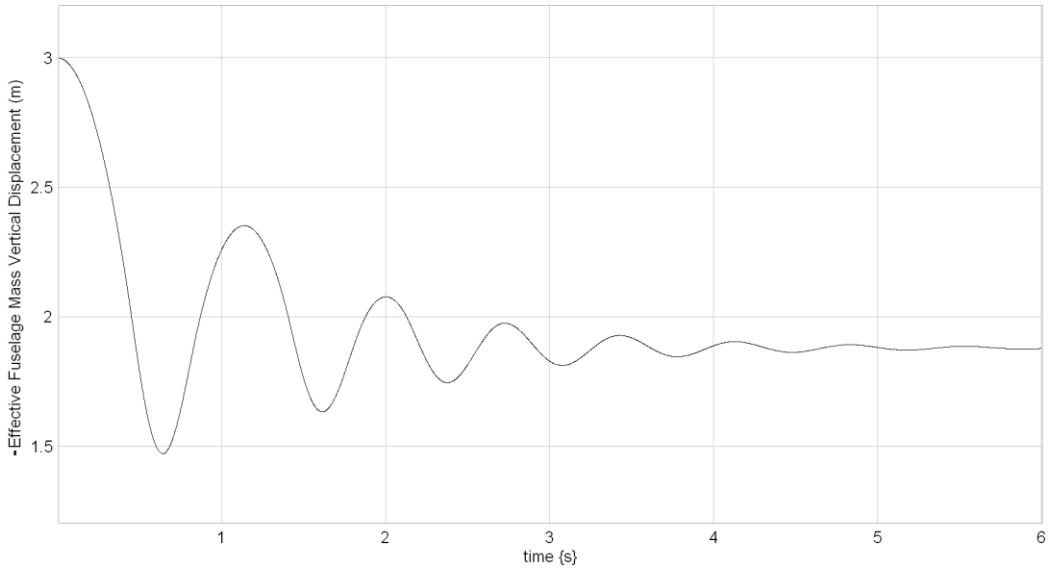

Figure 39: Simulation of the Drop Test, Fuselage Vertical Displacement x_{AC}

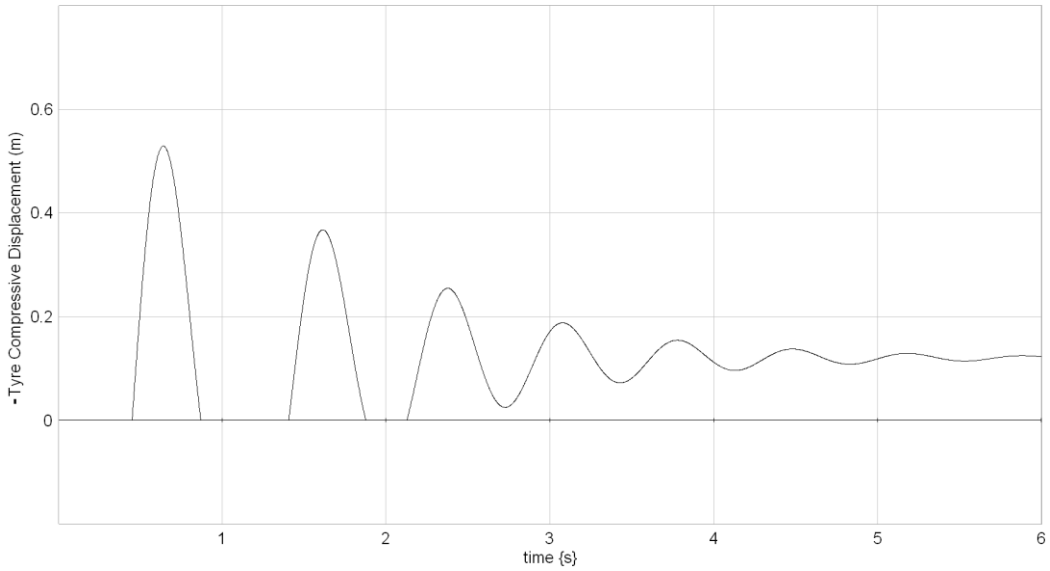

Figure 40: Simulation of the Drop Test, Vertical Compression of Tyre

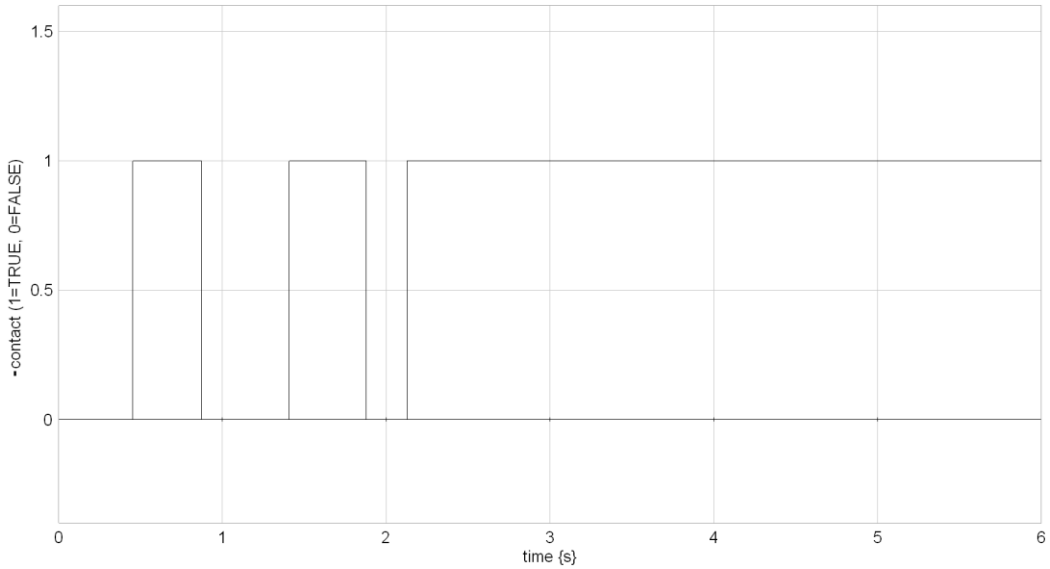

Figure 41: Simulation of the Drop Test, Contact

5.4 Variable Topology Systems

Variable topology systems have attracted specific attention over the years, forming the basis for developments such as HyBrSim [13] and the Impulse Bond Graph [14]. Cellier stated at the 2012 'International Conference on Bond Graph Modelling and Simulation' that developing a bond graph method to handle variable topology systems remained the next big challenge for bond graph modelling.

Variable topology systems are those where the size of the state equation matrices changes, such as contact. The classic case studies are the bouncing ball and Newton's Cradle, usually modelled using Newton's collision law with restitution. This model is an *impulse model* rather than a *switched model*, and impulse models require special attention to ensure that the impulse of energy released on impact is included.

Variable topology systems can be modelled using the hybrid bond graph developed here, and mechanical contact is an example of structural switching with a type 1 discontinuity. That is to say that the structure of the system changes with commutation, and when contact is made some constraints will typically be set up. In the mixed Boolean implicit model derived from the Hybrid Bond Graph described here, this change manifests as rows being set to zeros in some modes of operation and given nonzero values in others.

The main difference between the Hybrid Bond Graph presented here and the use of Newton's collision law is that the contact problem is abstracted to a switched model, rather than an impulsive one. The controlled junction dictates that the short 'in contact' phase is considered. The following case studies illustrate this and demonstrate that the switching model can be simplified to an impulsive one if required.

5.4.1 Collision of Rigid Bodies: Newton's Cradle

Consider the case of rigid bodies colliding, such as snooker balls or a Newton's cradle (Figure 42). For simplicity, consider the one-dimensional problem i.e. the snooker balls acting in-line on a flat table, or the portion of the Newton's cradle acting horizontally. This is shown in Figure 43.

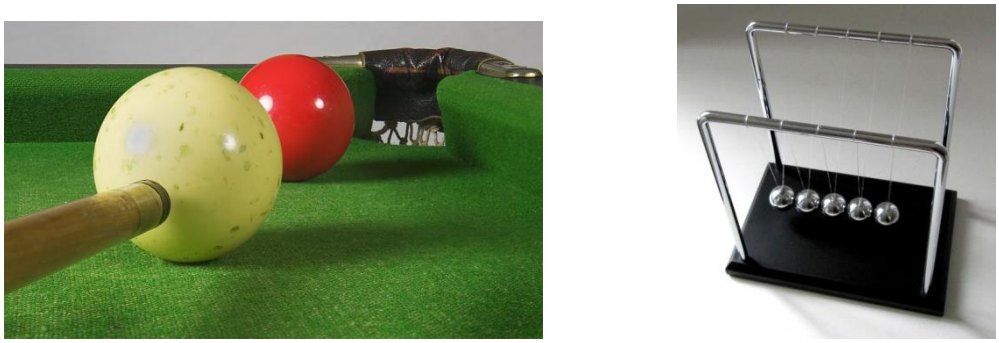

To Pot the Red by Michael Maggs / CC-BY-SA-3.0

Figure 42: Examples of Rigid Contact, Snooker Balls [130] (left) and Newton's Cradle [131] (right)

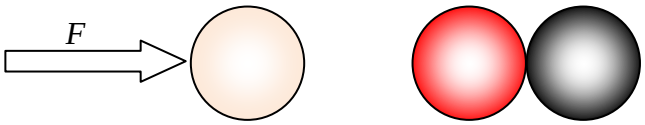

Figure 43: Schematic of Rigid Balls acting in one-dimension

Figure 43 shows the initial condition of the Newton's cradle, or a common situation in snooker. For clarity, snooker terms are used here. There are some balls in contact. The cue ball approaches under a force *F*, applied by the cue. If *F* is sufficiently large, the cue ball halts on contact with the middle ball, the middle ball remains stationary, and the black ball departs with an initial velocity equal to the final velocity of the cue ball. There is an audible dissipation of energy on contact. The Hybrid Bond Graph is given below in Figure 44.

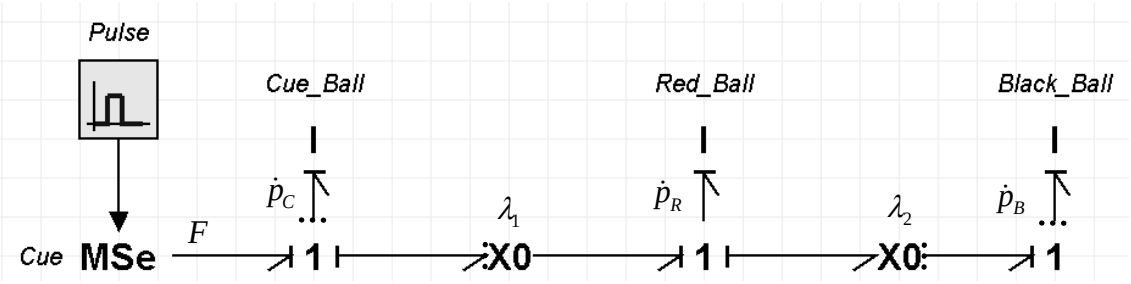

Figure 44: Hybrid Bond Graph of Rigid Balls acting in One Dimension

From this bond graph the following mathematical model can be derived:

$$diag\begin{bmatrix}\overline{\lambda}_1 & 1 & \overline{\lambda}_2 & \lambda_1 & \lambda_2\end{bmatrix}\begin{bmatrix}\dot{p}_C\\ \dot{p}_R\\ \dot{p}_B\\ f_{Cd}\\ f_{Bd}\end{bmatrix}=\begin{bmatrix}0 & 0 & 0 & 0 & 0 & \overline{\lambda}_1\\ 0 & 0 & 0 & \lambda_1 & \lambda_2 & \lambda_1\\ 0 & 0 & 0 & 0 & 0 & 0\\ 0 & -\lambda_1 & 0 & 0 & 0 & 0\\ 0 & -\lambda_2 & 0 & 0 & 0 & 0\end{bmatrix}\begin{bmatrix}f_C\\ f_R\\ f_B\\ \dot{p}_{Cd}\\ \dot{p}_{Bd}\\ F\end{bmatrix} \quad \textbf{(81)}$$

$$\begin{bmatrix}\overline{\lambda}_1 & 0 & 0 & 0 & 0\\ 0 & 1 & 0 & -\lambda_1 & -\lambda_2\\ 0 & 0 & \overline{\lambda}_2 & 0 & 0\\ 0 & 0 & 0 & 0 & 0\\ 0 & 0 & 0 & 0 & 0\end{bmatrix}\begin{bmatrix}\dot{p}_C\\ \dot{p}_R\\ \dot{p}_B\\ \dot{p}_{Cd}\\ \dot{p}_{Bd}\end{bmatrix}=\begin{bmatrix}0 & 0 & 0 & 0 & 0\\ 0 & 0 & 0 & 0 & 0\\ 0 & 0 & 0 & 0 & 0\\ 0 & -\lambda_1/m_R & 0 & -\lambda_1/m_C & 0\\ 0 & -\lambda_2/m_R & 0 & 0 & -\lambda_2/m_B\end{bmatrix}\begin{bmatrix}p_C\\ p_R\\ p_B\\ p_{Cd}\\ p_{Bd}\end{bmatrix}+\begin{bmatrix}\overline{\lambda}_1\\ \lambda_1\\ 0\\ 0\\ 0\end{bmatrix}[F] \quad \textbf{(82)}$$

A dynamic causality assignment has been chosen such that the red ball is in static causality. It is immediately apparent that the reference mode (all balls not touching) is different to the initial condition of the problem outlined in Figure 43. In order to look at the impulsive behaviour more closely, consider the regular bond graph and model for the single modes of operation before and after commutation (Table 12). At this point, *F*=0 and can be neglected because the cue ball has left the cue (another controlled 0-junction could be used to express contact with the cue). However, the cue ball is travelling with a velocity *v* as a result of having been pushed by the cue.

When the cue ball was hit by the cue, $\dot{p}_C$ was equal to *F*. The momentum p_C can be used to give the velocity of the cue ball, since $p_C = m_C v_C$. The velocity remains constant because there are no losses. The velocity of the red and black balls is known to be zero.

On collision, p_C instantaneously changes from v_c to zero, giving an impulsive term:

$$\dot{p}_C = \frac{m_C\left(v_C - v_{Cd}\right)}{dt} \text{ where } v_{Cd} = v_R = 0 \text{ and } dt \to 0 \qquad \textbf{(83)}$$

For a brief moment, all the balls are in contact and both the cue ball and black ball are constrained to the red.

$$\dot{p}_R = \dot{p}_{Cd} + \dot{p}_{Bd} \text{ where } \dot{p}_{Cd} = \dot{p}_C \qquad \textbf{(84)}$$

This means that incrementally after contact, the initial value of $\dot{p}_B$ is:

$$\dot{p}_B = \dot{p}_{Bd} = \dot{p}_R - \dot{p}_{Cd} = \dot{p}_R - \dot{p}_C \qquad \textbf{(85)}$$

And consequently:

$$p_B = p_R - p_C \qquad \textbf{(86)}$$

This is an important result as it establishes conservation of momentum. Assuming the balls have equal mass, the black ball departs after contact with an initial velocity equal to the final velocity of the cue ball prior to contact. This is consistent with Newton's Collision Law.

Table 12: Individual Modes of Operation for the Snooker Balls Study

Mode 1: Before Cue Ball makes Contact	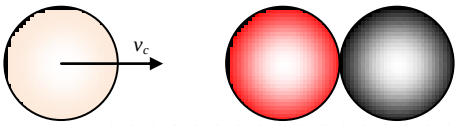 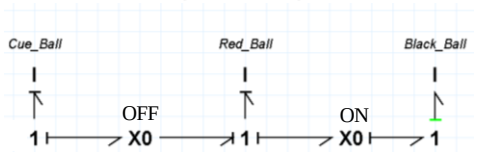 $\begin{bmatrix} 1 & 0 & 0 \\ 0 & 1 & -1 \\ 0 & 0 & 0 \end{bmatrix} \begin{bmatrix} \dot{p}_C \\ \dot{p}_R \\ \dot{p}_{Bd} \end{bmatrix} = \begin{bmatrix} 0 & 0 & 0 \\ 0 & 0 & 0 \\ 0 & -1/m_R & -1/m_B \end{bmatrix} \begin{bmatrix} p_C \\ p_R \\ p_{Bd} \end{bmatrix}$
Mode 2: All Balls briefly in Contact	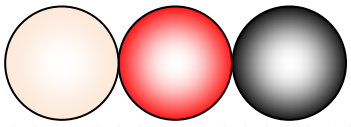 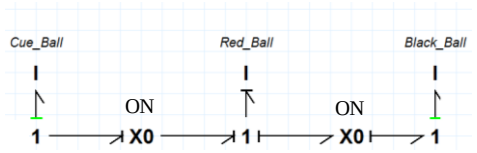 $\begin{bmatrix} 1 & -1 & -1 \\ 0 & 0 & 0 \\ 0 & 0 & 0 \end{bmatrix} \begin{bmatrix} \dot{p}_R \\ \dot{p}_{Cd} \\ \dot{p}_{Bd} \end{bmatrix} = \begin{bmatrix} 0 & 0 & 0 \\ -1/m_R & -1/m_C & 0 \\ -1/m_R & 0 & -1/m_B \end{bmatrix} \begin{bmatrix} p_R \\ p_{Cd} \\ p_{Bd} \end{bmatrix}$
Mode 3: Black Ball no longer in Contact	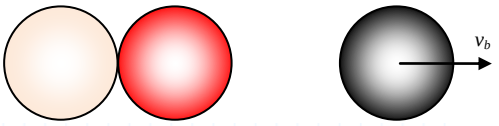 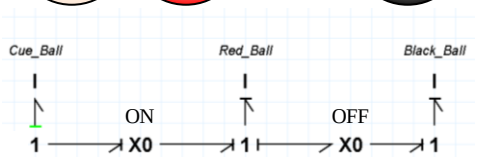 $\begin{bmatrix} 1 & 0 & -1 \\ 0 & 1 & 0 \\ 0 & 0 & 0 \end{bmatrix} \begin{bmatrix} \dot{p}_R \\ \dot{p}_B \\ \dot{p}_{Cd} \end{bmatrix} = \begin{bmatrix} 0 & 0 & 0 \\ 0 & 0 & 0 \\ 0 & -1/m_R & -1/m_C \end{bmatrix} \begin{bmatrix} p_R \\ p_B \\ p_{Cd} \end{bmatrix}$

5.4.2 Collision of Elastic Bodies

A problem which has received a lot of attention with hybrid bond graph modellers is the application of Newton's collision law to elastic bodies, such as a bouncing ball. There are two modes of operation - before and after collision – and a coefficient of restitution is used to give the difference in velocities.

$$\Delta v^{+} = -\varepsilon\left(\Delta v^{-}\right) \qquad \textbf{(87)}$$

The hybrid bond graph developed here abstracts the collision differently, into *contact = TRUE* and *contact = FALSE*. This gives three sliding modes of operation: before contact, during contact and after contact. The 'during contact' mode is so short as to be negligible. However, during this mode, energy storage and dissipation may occur, which is what causes the ball to bounce until it reaches rest. Restitution is used to give faster simulation times than would be achieved by forcing a computer to calculate behaviour during the contact phase. It has already been shown that this hybrid bond graph conserves momentum, so it now remains to use the hybrid bond graph to establish a coefficient of restitution.

The classic bouncing ball problem is described in Figure 45, with the associated bond graph in Figure 46.

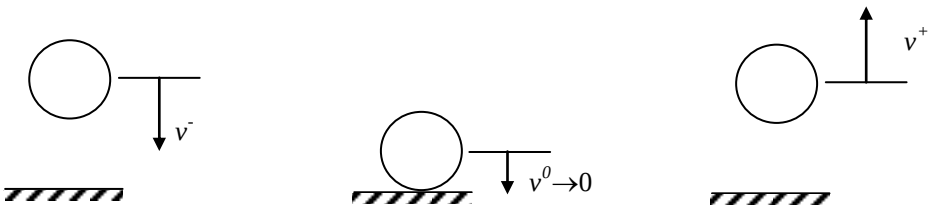

a) before Contact **b) in Contact with Ground** **c) after Contact i.e. rebound**

Figure 45: Motion of a Bouncing Ball

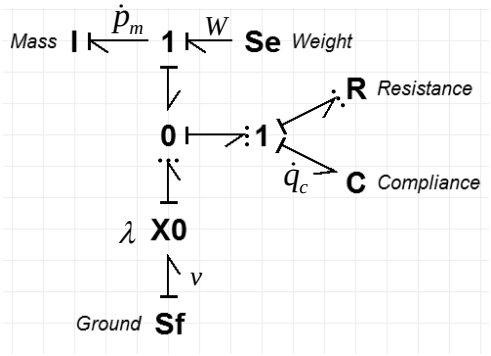

Figure 46: Hybrid Bond Graph of a Bouncing Ball

The equations for the bouncing ball can be obtained:

$$\begin{bmatrix} 1 & 0 & 0 & 0 \\ 0 & 1 & 0 & 0 \\ 0 & 0 & \lambda & 0 \\ 0 & 0 & 0 & \bar{\lambda} \end{bmatrix} \begin{bmatrix} \dot{p}_m \\ \dot{q}_c \\ f_r \\ e_r \end{bmatrix} = \begin{bmatrix} 0 & -\lambda & -\lambda & 0 & 1 & 0 \\ \lambda & 0 & 0 & -\bar{\lambda} & 0 & \lambda \\ \lambda & 0 & 0 & 0 & 0 & \lambda \\ 0 & -\bar{\lambda} & 0 & 0 & 0 & 0 \end{bmatrix} \begin{bmatrix} f_m \\ e_c \\ e_r \\ f_r \\ W \\ v \end{bmatrix} \qquad \textbf{(88)}$$

$$\begin{bmatrix} \dot{p}_m \\ \dot{q}_c \end{bmatrix} = \begin{bmatrix} -\lambda/mR & -\lambda/C \\ \lambda/m & -R\bar{\lambda}/C \end{bmatrix} \begin{bmatrix} p_m \\ q_c \end{bmatrix} + \begin{bmatrix} 1 & -\lambda/R \\ 0 & \lambda \end{bmatrix} \begin{bmatrix} W \\ v \end{bmatrix} \qquad \textbf{(89)}$$

Consider each mode of operation in isolation, as shown in Table 13. Before contact, the ball falls under its own weight. The velocity associated with the compliance (i.e. the velocity of deformation) $\dot{q}_c$ is zero because the ball has not yet been compressed, i.e. q_c (the deformation of the ball) is zero. Note that the velocity of the ball itself is not explicitly expressed by the state equation.

On contact, the force on the ball (row 1 of equation (89)) changes from simply the weight of the ball to become a function of deformation and inertia. The ball deforms with a velocity which is equal to the velocity of the ball (row 2). The initial momentum on contact is equal to the final momentum before, so the state does not need to be reinitialised.

Immediately after contact, the ball is travelling upwards as a result of the forces applied during the contact phase. The initial momentum of the ball is equal to the final momentum incrementally before losing contact.

Table 13: Static Bond Graphs and Equations for Each Mode of Operation

Mode 1: Before Contact	Mode 2: Contact	Mode 3: After Contact
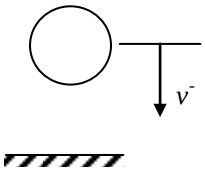	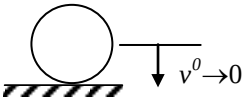	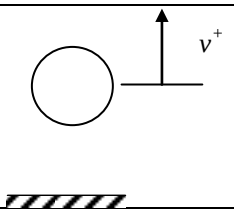
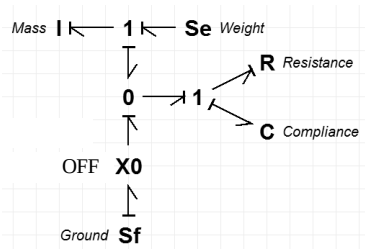	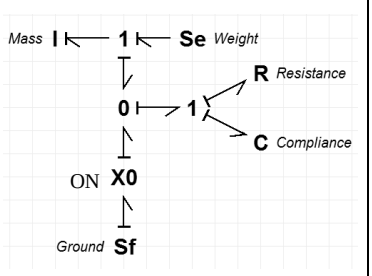	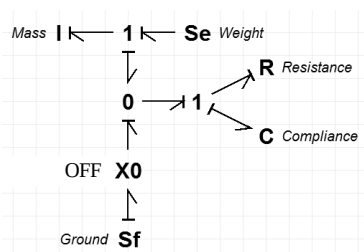
$\begin{bmatrix}\dot{p}_m \\ \dot{q}_c\end{bmatrix} = \begin{bmatrix}0 & 0 \\ 0 & -R/C\end{bmatrix}\begin{bmatrix}p_m \\ q_c\end{bmatrix} + \begin{bmatrix}1 & 0 \\ 0 & 0\end{bmatrix}\begin{bmatrix}W \\ v\end{bmatrix}$	$\begin{bmatrix}\dot{p}_m \\ \dot{q}_c\end{bmatrix} = \begin{bmatrix}-1/mR & -1/C \\ 1/m & 0\end{bmatrix}\begin{bmatrix}p_m \\ q_c\end{bmatrix} + \begin{bmatrix}1 & -1/R \\ 0 & 1\end{bmatrix}\begin{bmatrix}W \\ v\end{bmatrix}$	$\begin{bmatrix}\dot{p}_m \\ \dot{q}_c\end{bmatrix} = \begin{bmatrix}0 & 0 \\ 0 & -R/C\end{bmatrix}\begin{bmatrix}p_m \\ q_c\end{bmatrix} + \begin{bmatrix}1 & 0 \\ 0 & 0\end{bmatrix}\begin{bmatrix}W \\ v\end{bmatrix}$

Inspection of the contact phase in more detail could yield the coefficient of restitution which amends the velocity (and hence momentum) of the ball after contact.

Consider the local minima where velocity tends to zero and deformation is at its greatest. Assume that this occurs at point $t_{i.}$ I.e. The contact phase is assumed to be taking place over a time period (t_{i-1} to $t_{i+1.}$), during which the body compresses linearly between t_{i-1} and $t_{i,}$ and decompresses linearly between t_i and $t_{i+1.}$

At the point of maximum compression t_i, $p_m = mv_m$, ground velocity v is zero, and $v_m \rightarrow 0$ at the local mimina.

$$\dot{p}_m = -p_m/mR - q_c/C + W - v/R$$

$$(\dot{p}_m)_i = -(q_c)_i/C \qquad \textbf{(90)}$$

where $(q_c)_i$ is the maximum deformation of the ball.

Now consider the point incrementally before losing contact, at point t_{i+1}: the deformation $q_c \rightarrow 0$ but the ball is still just in contact. The momentum of the ball at this point is the initial value of $\dot{p}_m$ in the next mode of operation. Recall that $p_m = mv_m$, ground velocity v is zero, $q_c \rightarrow 0$ and $v_m \neq 0$.

$$(\dot{p}_m)_{i+1} = -(v_m)_{i+1} \Big/ R + W \qquad \textbf{(91)}$$

and

$$(\dot{q}_c)_{i+1} = (v_m)_{i+1} \qquad \textbf{(92)}$$

Since the duration of the contact phase is so small, assume:

$$(\dot{q}_c)_{i+1} = \frac{(q_c)_{i+1} - (q_c)_i}{t_{i+1} - t_i} \qquad \textbf{(93)}$$

Which gives:

$$(\dot{p}_m)_{i+1} = \frac{(q_c)_i}{\Delta t} R^{-1} + W \qquad \textbf{(94)}$$

The maximum deformation is given by rearranging equation (90):

$$(q_c)_i = -C(\dot{p}_m)_i$$

And this can be substituted into (94):

$$(\dot{p}_m)_{i+1} = \frac{-C(\dot{p}_m)_i}{\Delta t} R^{-1} + W \qquad \textbf{(95)}$$

Recall that $(\dot{p}_m)_i$ is the change in momentum between the initial state on contact at t_{i-1} and full contact at t_i.

$$(\dot{p}_m)_i = \frac{m(v_i - v_{i-1})}{t_i - t_{i-1}} \qquad \textbf{(96)}$$

Assuming the time steps are equal, substitute in eqn. (95) to give:

$$(\dot{p}_m)_{i+1} = \frac{Cmv_{i-1}}{(t_{i+1} - t_i)(t_{i+1} - t_i)} R^{-1} + W$$

$$\left(\dot{p}_m\right)_{i+1} = \frac{Cmv_{i-1}}{\left(\Delta t\right)^2} R^{-1} + W \qquad \textbf{(97)}$$

This result is important because it gives the final force on the body in terms of the initial velocity. Neglecting weight, which is assumed to be small compared to the other forces, and integrating to obtain the velocities:

$$v_{i+1} = \frac{C}{R^{-1}\Delta t} v_{i-1} \qquad \textbf{(98)}$$

Comparing this equation to Newton's collision law with restitution yields:

$$\varepsilon = \frac{C}{R^{-1}\Delta t} \qquad \textbf{(99)}$$

This could be used to simplify the mathematical model for simulation, with the benefit of having obtained the coefficient of restitution systematically from the model instead of using generic or estimated values.

Chapter 6: Discussion & Conclusions

6.1 Discussion

The goal of this research was to propose a Hybrid Bond Graph which could be used to gain engineering insight (through structural analysis and exploiting causal assignment) and be suitable for simulation activities. In doing so, it was important to retain the graphical advantages of bond graph modelling and the principles of idealised physical, acausal model construction. This has been achieved by classifying discontinuities so that they can be represented in the most intuitive way, developing a causally dynamic general Hybrid Bond Graph (with a new dynamic causality notation and novel application of pseudo-state variables), and deriving a unique mixed-Boolean implicit system equation which describes the model in all possible modes of operation.

The original objectives have been satisfied by proposing a new method for representing the Hybrid Bond Graph. The use of controlled junctions and elements is not novel, but the way they are applied here is new.

Classifying discontinuities as *structural* or *parametric* immediately shows whether the hybrid assumptions will affect the structural analysis of the model or not, and the use of controlled junctions and elements (respectively) is often intuitive.

The use of the controlled junction, with its inherent dynamic causal assignment, clearly shows how structural commutations (dis)connect submodels and form algebraic constraints. This is reflected in the junction structure matrix by the use of Boolean variables, which denote connections between elements dependent on the state of a controlled junction.

The Dynamic causality notation is designed to facilitate analysis of the model's structure, as well as aiding in equation generation (which describes all modes of operation). Elements in dynamic causality reverse inputs and outputs depending on the mode of operation (i.e. they have an effort input and flow output in some modes, and a flow input and effort output in others). Hence elements in dynamic causality are assigned two inputs and two outputs during equation generation. During any single mode of operation, one input/output pair is active and the other is redundant.

If a storage element is in dynamic causality, it only yields a state output in some modes of operation (when it is in integral causality). In other modes it is in

derivative causality, in which case it can be assigned a ‘pseudo-state’ variable which generates an algebraic equation.

A model describing all possible modes of operation is generated. The dynamic causality offers engineering insight, for example when two rigid bodies contact and a kinematic constraint exists indicating that they behave as a single rigid body. This can be preferable to constraining causality through the addition of parasitic elements, which not only overcomplicates the model but can even mask an issue or give incorrect behaviour.

The dynamic causality notation offers a unique new way of visualising variable causality and variable topology problems: the latter is no longer strictly variable topology because all system elements are described; they are just not necessarily connected. Dynamic causality can be exploited in the same way as static causality notation, showing how system properties vary with commutation and enabling graph-based structural analysis.

Variable topology problems – notably impact – have received much attention with regard to hybrid bond graphs, due to concerns over whether losses are treated correctly. Using the hybrid bond graph developed here, conservation of momentum holds true because the impact is abstracted to capture the short contact phase, and, in addition, the parameters for Newton’s Collision Law can be derived and the model simplified to a classical collision problem.

Likewise, state reinitialisation has received some attention in the context of hybrid bond graphs. The way that discontinuities are abstracted using this method allows the initial value of each state to be logically deduced.

The unique model describing all possible modes of operation is suitable for both equation-based structural analysis (which is well-established for implicit descriptor systems) and simulation. Simulation would require the use of solvers developed for implicit descriptor systems, or the use of some model simplification or symbolic manipulation to produce an explicit equation for each mode of operation: both are readily available in commercial packages such as Matlab but have not been fully explored here.

The derivations and analyses presented in this thesis largely assume a linear time-invariant model, in order to facilitate comparison with existing control literature. However, the same derivations can be followed with nonlinear functions in place of the linear coefficients during equation generation. This has been demonstrated in the case studies.

In conducting this research, it was important to preserve the ideals of idealised physical modelling and port-based, acausal model construction. The use of intuitive switching devices for structural and parametric switching, and the proposed dynamic causality notation, are central to this.

6.2 Conclusions

A General Hybrid Bond Graph and a method for constructing it have been defined. This Hybrid Bond Graph features:

- Controlled junctions and controlled elements describe structural and parametric discontinuities respectively.
- Commutation (i.e. the state of controlled junctions) is assigned a Boolean parameter. This manifests in the junction structure matrix and subsequent equations for structural discontinuities, and can be used to derive the constituent equations of controlled elements for parametric discontinuities.
- Dynamic causality is represented using a new proposed notation.
- System equations are generated acknowledging that elements in dynamic causality have two possible inputs and outputs, depending on the mode of operation. In a single mode of operation, one input/output pair will be active and the other redundant. A vector of Boolean parameters activates the outputs accordingly, and sets rows of the system equation to zeros when they are redundant.
- Storage elements in dynamic causality are assigned pseudo-states for the case where they are in derivative causality, and this yields an algebraic constraint.
- The model generates a unique mixed-Boolean system equation, which will be implicit if any storage elements are in dynamic causality. This equation easily yields the system equation for a single mode of operation by assigning 1's and 0's to the Boolean parameters (to denote whether they are ON or OFF). The models for each constituent mode may change size, but all are captured in the unique system model.

This model is not only a more intuitive and holistic way of representing a hybrid system, but is also suitable for both analysis and simulation purposes.

The model has been compared to existing hybrid bond graphs and it can be seen that the switching mechanisms are very similar, and the equation derived for a single mode essentially the same. The novelty here is that commutation manifests

as state switching (rather than a switching input, or a collection of linked models for each mode) and a unique system model is produced which requires no extra derivations to obtain the equation for a single mode of operation.

The dynamic causality notation can be exploited to show how system properties vary with commutation: notably the transfer function and hence the poles and zeros of the system. It is clear that structural discontinuities directly affect structural system properties, whereas parametric ones do not. Established matrix-rank criteria can be applied to the implicit system equation, and the rank is reflected in the graphical model.

Finally, a selection of case studies is presented to demonstrate the method. These consist of the boost converter (widely used in the literature), landing gear drop test (a highly nonlinear contact problem, known to be problematic to simulate) and an investigation of collisions (contact between rigid bodies, and a bouncing ball: both widely used case studies in the literature). The latter demonstrates the derivation of an impulse model from the switched model generated by the hybrid bond graph.

6.3 Further Work

There is tremendous scope to extend and develop this hybrid bond graph.

The Hybrid Bond Graph is suitable for non-linear models, as demonstrated by the case study of a landing gear drop test in section 5.3. The derivations in Chapters 3 and 4 assume a Linear Time Invariant model for ease of development and comparison with the literature. A full study of the nonlinear case and its properties is recommended.

It can be laborious to derive the truth tables and Boolean vector $\mathbf{\Lambda}$ in order to obtain the system equations. Incorporating this method into a software tool is therefore recommended. The dynamic causality notation shows that models can be segmented to derive truth tables for isolated areas of dynamic causality, and some similarities between types of discontinuity can be observed, dispensing with the need to consider a vast array of possible modes of operation for the entire model. The procedures for a dynamic sequential causality assignment procedure (DSCAP) and deriving the system equations have been written so as to facilitate their adoption as algorithms for a computer programmer.

An algorithm for the systematic derivation of an impulse model from the [switched] hybrid bond graph could also be developed for a software package, and would aid efficient simulation.

The control properties observed here are a basic set in line with those already documented for standard bond graphs and hybrid bond graphs utilising switching sources. Further properties such as closed-loop stability and the definition of observers could be developed. Since bond graphs lend themselves to behavioural modelling, control properties could also be established in terms of geometric properties.

The use of this hybrid bond graph in developing hierarchical and port-Hamiltonian systems should be investigated, as dynamic causality may necessitate causally dynamic ports.

References

[1] Willems, J. C., "The Behavioural Approach to Open and Interconnected Systems," *IEEE Control Syst. Mag.*, iss. Dec. 2007.

[2] Hogan, N. *2.141 Modelling and Simulation of Dynamic Systems Fall 2002*. (Massachusetts Institute of Technology: MIT OpenCourseWare) http://ocw.mit.edu [Accessed 8th February 2010]. License: Creative Commons BY-NC-SA

[3] Karnopp, D. C., *et al.*, *System Dynamics Modeling and Simulation of Mechatronic Systems*, Fourth ed. Hoboken, N.J.: John Wiley & Sons, Inc., 2006.

[4] Birkett, S. H. and Roe, P. H., "The Mathematical Foundations of Bond Graphs — I. Algebraic Theory," *J. Franklin Institute*, vol. 326, iss. 3 pp. 329-350, 1989.

[5] Birkett, S. H. and Roe, P. H., "The Mathematical Foundations of Bond Graphs — II. Duality," *J. Franklin Institute*, vol. 326, iss. 5 pp. 691-708, 1989.

[6] Birkett, S. H. and Roe, P. H., "The Mathematical Foundations of Bond Graphs — III. Matroid Theory," *J. Franklin Institute*, vol. 327, iss. 1 pp. 87-108, 1990.

[7] Birkett, S. H. and Roe, P. H., "The Mathematical Foundations of Bond Graphs — IV. Matrix Representations and Causality," *J. Franklin Institute*, vol. 327, iss. 1 pp. 109-128, 1990.

[8] Borutzky, W., "Bond Graphs and Object-Oriented Modelling - A Comparison," *Proc. IMechE Part I - J. Syst. and Control Eng.*, vol. 216, iss. 11 pp. 21-33, 2002.

[9] Mosterman, P. J., *et al.*, "An Ontology for Transitions in Physical Dynamic Systems," in *15th Nat. Conf. on Artificial Intelligence (AAAI 98)*, Madison, WI, 1998, pp. 219-224.

[10] Van Der Schaft, A. J. and Schumacher, J. M., *An Introduction to Hybrid Dynamical Systems* (Lecture Notes in Control and Information Sciences) vol. 251. London: Springer, 1999.

[11] Vu, L. and Liberzon, D., "Invertibility of switched linear systems," *Automatica*, vol. 44, iss. 4 pp. 949-958, 2008.

[12] Branicky, M. S., *et al.*, "A Unified Framework for Hybrid Control: Model and Optimal Control Theory," *Ieee Transactions on Automatic Control*, vol. 43, iss. 1 pp. 31-45, 1998.

[13] Mosterman, P. J., "HyBrSim - A Modelling and Simulation Environment for Hybrid Bond Graphs," *Proc. IMechE Part I - J. Syst. and Control Eng.*, vol. 216, iss. 11 pp. 35-46, 2002.

[14] Zimmer, D. and Cellier, F. E., "Impulse-Bond Graphs," in *Proc. 2007 Int. Conf. on Bond Graph Modeling (ICBGM 2007)*, San Diego, California. , 2007, pp. 3-11.

[15] Marghitu, D. and Irwin, J., *Mechanical Engineer's Handbook* (Materials & Mechanical): Elsevier Academic Press, 2001.

[16] Holderbaum, W., "Control strategy for Boolean input systems," in *Proc. 2002 American Control Conf.*, Anchorage, AK, 2002, pp. 1260-1265.
[17] Holderbaum, W., "Control of Binary Input Systems," *IOSR Journal of Engineering*, vol. 2, iss. 12 pp. 1-15, Dec. 2012.
[18] Cheng, D. and Liu, J. B., "Stabilization of Boolean control networks," in *Proc. 48th IEEE Conf. on Decision and Control* Shanghai, China, 2009, pp. 5269-5274.
[19] Qi, H. and Cheng, D., "Analysis and control of Boolean networks: A semi-tensor product approach," in *Proc. 7th Asian Control Conf., ASCC 2009*, Hong Kong, China, 2009, pp. 1352-1356.
[20] Kobayashi, K. and Imura, J. I., "Observability analysis of Boolean networks with biological applications," in *Proc. ICCAS-SICE 2009 - ICROS-SICE Int. Joint Conf. 2009*, Fukuoka, Japan, 2009, pp. 4393-4396.
[21] Chaves, M., *et al.*, "Methods of robustness analysis for Boolean models of gene control networks," *IEE Proc. Systems Biology*, vol. 153, iss. 4 pp. 154-167, Jul. 2006.
[22] Thoma, J. U., *Introduction to Bond Graphs and their Applications*, 1st ed. Oxford, UK: Pergamon Press, 1975.
[23] Dransfield, P., Ed., *Hydraulic Control Systems - Design and Analysis of Their Dynamics* (Lecture Notes in Control and Information Sciences 33). Berlin, Germany: Springer-Verlag, 1981.
[24] Castelain, A., *et al.*, "Modelling and analysis of power electronic networks by bondgraph," in *Proc. 3rd Int. Conf. Modelling and Simulation of Electrical Machines and Static Converters, IMACS-TCI 90* Nancy, France., 1990, pp. 405-416.
[25] Dauphin-Tanguy, G. and Rombaut, C., "Why a Unique Causality in the Elementary Commutation Cell Bond Graph Model of a Power Electronics Converter," in *Proc. Int. Conf. on Systems, Man and Cybernetics: Systems Engineering In the Service of Humans*, Le Touquet, France, 1993, pp. 257-263.
[26] Broenink, J. F. and Wijbrans, C. J., "Describing discontinuities in bond graphs," in *Proc. 1993 Western Simulation Multiconference - Int. Conf. on Bond Graph Modeling ICBGM'93*, La Jolla, CA, 1993, pp. 120-125.
[27] Asher, G. M., "The Robust Modelling of Variable Topology Circuits Using Bond Graphs," in *Proc. 1993 Western Simulation Multiconference - Int. Conf. on Bond Graph Modeling ICBGM'93*, La Jolla, CA, 1993, pp. 126-131.
[28] Buisson, J., "Analysis and Characterization of Hybrid Systems With Bond-Graphs," in *Proc. Int. Conf. on Systems, Man and Cybernetics: Systems Engineering In the Service of Humans*, Le Touquet, France, 1993, pp. 264-269.
[29] Soderman, U., *et al.*, "The Conceptual Side of Mode Switching," in *Proc. Int. Conf. on Systems, Man and Cybernetics: Systems Engineering In the Service of Humans*, Le Touquet, France, 1993, pp. 245-250.
[30] Stromberg, J. E., *et al.*, "Variable Causality in Bond Graphs Caused by Discrete Effects," in *Proc. 1993 Western Simulation Multiconference - Int. Conf. on Bond Graph Modeling ICBGM'93*, La Jolla, CA, 1993, pp. 115-119.

[31] Mosterman, P. J. and Biswas, G., "Modeling Discontinuous Behavior with Hybrid Bond Graphs," in *9th Int. Workshop on Qualitative Reasoning about Physical Systems*, Amsterdam, Netherlands, 1995, pp. 139-147.

[32] Gawthrop, P. J., "Hybrid Bond Graphs using Switched I and C Components," Centre for Systems and Control, University of Glasgow, Glasgow, UK. CSC Report 97005, 1997.

[33] Borutzky, W., "Discontinuities in a bond graph framework," *J. Franklin Institute - Eng. and Appl. Math.*, vol. 332B, iss. 2 pp. 141-154, Mar. 1995.

[34] Samantaray, A. K., "Modeling and analysis of preloaded liquid spring/damper shock absorbers," *Simulation Modelling Practice and Theory*, vol. 17, iss. 1 pp. 309-325, 2009. doi: 10.1016/j.simpat.2007.07.009

[35] Umarikar, A. C. and Umanand, L., "Modelling of switching systems in bond graphs using the concept of switched power junctions," *J. Franklin Institute*, vol. 342, iss. 2 pp. 131-147, Mar. 2005.

[36] Low, C. B., *et al.*, "Causality assignment and model approximation for hybrid bond graph: Fault diagnosis perspectives," *IEEE Trans. Automation Sci. and Eng.*, vol. 7, iss. 3 pp. 570-580, Jul. 2010.

[37] Edstrom, K., *et al.*, "Modelling and simulation of a switched power converter," *Simulation Series*, vol. 29, iss. 1 pp. 195-200, 1997.

[38] Edstrom, K., *et al.*, "Aspects on simulation of switched bond graphs," in *Proc. 35th IEEE Conf. Decision and Control*, Kobe, Japan, 1996, pp. 2642-2647.

[39] Mosterman, P. J., "An overview of hybrid simulation phenomena and their support by simulation packages," in *Proc. 2nd Int. Workshop on Hybrid Systems: Computation and Control, HSCC'99*, Berg en Dal, The Netherlands, 1999, pp. 165-177.

[40] Mosterman, P. J. and Biswas, G., "Formal specifications for hybrid dynamical systems," in *Proc. 15th Int. Joint Conf. Artificial Intelligence IJCAI-97*, Nagoya, Japan, 1997, pp. 568-573.

[41] Mosterman, P. J. and Biswas, G., "A Theory of Discontinuities in Physical System Models," *J. Franklin Institute*, vol. 335B, iss. 3 pp. 401-439, Aug. 1996.

[42] Mosterman, P. J. and Biswas, G., "A comprehensive methodology for building hybrid models of physical systems," *Artificial Intelligence*, vol. 121, iss. 1-2 pp. 171-209, Aug. 2000.

[43] Mosterman, P. J., *et al.*, "Model Semantics and Simulation of Time Scale Abstractions in Collision Models," in *3rd Intl. Congr. Federation of EUROpean SIMulation Societies*, Helsinki, Finland, 1998, pp. 230–237.

[44] Edstrom, K., "Switched Bond Graphs: Simulation and Analysis" (Linköping Studies in Science and Technology Thesis No. 586), PhD. Dissertation, Dept. Electrical Engineering, Linköpings Universitet, Linköping, Sweden, 1999.

[45] Mosterman, P. J., "Implicit Modeling and Simulation of Discontinuities in Physical System Models," in *The 4th Intl. Conf. Automation of Mixed Processes: Hybrid Dynamic Systems ADPM2000*, Dortmund, Germany, 2000, pp. 35-40.

[46] Kofman, E. and Junco, S., "Quantized Bond Graphs: An Approach for Discrete Event Simulation of Physical Systems," in *Proc. 2001 Int. Conf. on Bond Graph Modeling ICBGM'01*, Phoenix, AZ, 2001, pp. 369-374.

[47] Kofman, E., "Quantized-state systems: A DEVS approach for continuous system simulation," *Trans. Soc. for Comput. Simulation*, vol. 18, iss. 3 pp. 123-132, 2002.

[48] Kofman, E., "Discrete event simulation of hybrid systems," *SIAM J. Sci. Comput.*, vol. 25, iss. 5 pp. 1771-1797, 2004.

[49] Borutzky, W., "Bond-graph-based fault detection and isolation for hybrid system models," *Proc. IMechE. Part I, J. Syst. and Control Eng.*, vol. 226, iss. 6 pp. 742-760, July 2012.

[50] Cellier, F. E., *et al.*, "Bond Graph Modeling of Variable Structure Systems," *Simulation Series*, vol. 27, iss. 1 pp. 49-49, 1994.

[51] Bidard, C., *et al.*, "Bond graph and variable causality," in *Proc. Int. Conf. on Systems, Man and Cybernetics: Systems Engineering In the Service of Humans*, Le Touquet, France, 1993, pp. 270-275.

[52] Breedveld, P. C., "An alternative Model for Static and Dynamic Friction in Dynamic System Simulation," in *1st IFAC Conf. Mechatronic Systems*, Darmstadt, Germany, 2000, pp. 717-722.

[53] Breedveld, P. C., "Modelling & Simulation Of Bouncing Objects: Newton's Cradle Revisited," in *Mechatronics 2002*, Twente, The Netherlands, 2002.

[54] Van Kampen, D., "Paper path modeling case in 20-SIM" (Report 2003CE025), M.Sc., Individual Design Assignment, Department of Electrical Engineering, University of Twente, Enschede, The Netherlands, 2003.

[55] Podgursky, B., *et al.*, "Efficient Tracking of Behavior in Complex Hybrid Systems via Hybrid Bond Graphs," in *Annu. Conf. Prognostics and Health Management Society*, Portland, OR, 2010.

[56] Borutzky, W., *Bond Graph Methodology: Development and Analysis of Multi-disciplinary Dynamic System Models*, 1st ed. London, UK: Springer-Verlag London Ltd., 2010.

[57] Otter, M., *et al.*, "Hybrid Models of Physical Systems and Discrete Controllers," *AT - Automatisierungstechnik*, vol. 48, iss. 9 pp. 35-40, Sept. 2000.

[58] Shiva, A., "Modeling Switching Networks Using Bond Graph Technique", M.Sc. Dissertation, Dept. Aerospace and Mechanical Engineering, University of Arizona, Tucson, AZ, 2004.

[59] Beers, C. (2005, Accessed: Aug. 2010). *Efficient Simulation Model for Hybrid Bond Graph* [Poster]. Available: http://fountain.isis.vanderbilt.edu/publications/BondITRReviewPoster.ppt

[60] Beers, C. D., *et al.*, "Building Effiecient Simulations from Hybrid Bond Graph Models," in *2nd IFAC Conf. on Analysis and Design of Hybrid Systems*, Alghero, Italy, 2006, pp. 71-76.

[61] Calvo, J. A., *et al.*, "BONDSYM: Simulink based educational software for analysis of dynamic system," *Comput. Applicat. in Engin. Educ.*, vol. 18, iss. 2 pp. 238-251, Jun. 2010.

[62] Geitner, G. H., "Power flow diagrams using a bond graph library under SIMULINK," in *32nd Annu. Conf. on IEEE Industrial Electronics IECON 2006*, Paris, France, 2006, pp. 1359-1365.
[63] Tudoret, S., *et al.*, "Co-simulation of hybrid systems: Signal-Simulink," in *Proc. 6th Int. Symp. Formal Techniques in Real-Time and Fault-Tolerant Systems FTRTFT 2000*, Pune, India, 2000, pp. 134-151.
[64] Van Der Schaft, A. (2005, Accessed: May 2010). *Theory of Port-Hamiltonian Systems Chapter 1: Port-Hamiltonian formulation of network models; the lumped-parameter case* [Online: PhD-course for the Dutch Institute of Systems and Control (DISC)]. Available: http://www.math.rug.nl/~arjan/teaching.html
[65] Van Der Schaft, A., "Port-Hamiltonian systems: an introductory survey," in *Proc. Int. Congr. Mathematicians*, Madrid, Spain, 2006, pp. 1339-1365.
[66] Van Der Schaft, A. (2009, Accessed: May 2010). *Port-Hamiltonian Systems: from Geometric Network Modeling to Control* [Online: Lecture notes for the EECI Graduate Course, LSS-Supelec, Gif-sur-Yvette]. Available: http://www.math.rug.nl/~arjan/teaching.html
[67] Narasimhan, S., "Model-Based Diagnosis of Hybrid Systems", PhD. Dissertation, Dept. Computer Science, Vanderbilt University, Nashville, Tenessee, 2002.
[68] Daigle, M. J., *et al.*, "A Qualitative Event-Based Approach to Continuous Systems Diagnosis," *IEEE Trans. Control Syst. Technol.*, vol. 17, iss. 4 pp. 780-793, Jul. 2009.
[69] Lattmann, Z., "A Multi-Domain Functional Dependency Modeling Tool Based on Extended Hybrid Bond Graphs", M.Sc. Dissertation, Dept. Electrical Engineeirng, Vanderbilt University, Nashville, TN, 2010.
[70] Roychoudhury, I., *et al.*, "Efficient simulation of hybrid systems: A hybrid bond graph approach," *Simulation*, vol. 87, iss. 6 pp. 467-498, Jun. 2011.
[71] Cuijpers, P. J. L. and Reniers, M. A., "Hybrid process algebra," *J. Logic and Algebraic Programming*, vol. 62, iss. 2 pp. 191-245, Feb. 2005.
[72] Cuijpers, P. J. L., *et al.*, "Constitutive Hybrid Processes: a Process-Algebraic Semantics for Hybrid Bond Graphs," *Simulation: Trans. Soc. for Modeling and Simulation Int.*, vol. 84, iss. 7 pp. 339-358, Jul 2008.
[73] Kalman, R., "On the general theory of control systems," in *Proc. 1st IFAC Congress Automatic Control*, Moscow, 1960, pp. 481-492.
[74] Kalman, R. E. (1968, Accessed: Dec. 2012). *Lectures on Controllability and Observability* [Online: Reproduced by the Clearinghouse for Federal Scientific & Technical Information, Springfield Va. 22151]. Available: http://www.dtic.mil/cgi-bin/GetTRDoc?AD=AD0704617
[75] Sontag, E. D., *Mathematical Control Theory: Deterministic Finite Dimensional Systems* (Textbooks in Applied Mathematics, Number 6), 2nd ed. New York: Springer, 1998.
[76] Lewis, F. L., "Review of 2-D implicit systems," *Automatica*, vol. 28, iss. 2 pp. 345-354, Mar. 1992.
[77] Yip, E. L. and Sincovec, R. F., "Solvability, Controllability and Observability of Continuous Descriptor Systems," *Ieee Transactions on Automatic Control*, vol. 26, iss. 3 pp. 702-707, Jun. 1981.

[78] Verghese, G. C., *et al.*, "A Generalized State-Space for Singular Systems," *Ieee Transactions on Automatic Control*, vol. 26, iss. 4 pp. 811-831, Aug. 1981.
[79] Lewis, F. L., "Survey of Linear Singular Systems," *Circuits, Systems and Signal Processing*, vol. 5, iss. 1 pp. 3-36, 1986.
[80] Lewis, F. L., "A Tutorial on the Geometric Analysis of Linear Time-Invariant Implicit Systems," *Automatica*, vol. 28, iss. 1 pp. 119-137, Jan. 1992.
[81] Dai, L., "Impulsive modes and causality in singular systems," *Int. J. Control*, vol. 50, iss. 4 pp. 1267-1281, 1989.
[82] Polderman, J. W. and Willems, J. C., *Introduction to Mathematical Systems Theory: A Behavioral Approach* (Texts in Applied Mathematics 26), 1st ed. New York, NY: Springer Verlag, 1998.
[83] Willems, J. C., "Modeling Interconnected Systems," in *2008 3rd Int. Symp. on Communications, Control and Signal Processing ISCCSP2008*, St. Julians, Malta, 2008, pp. 421-424.
[84] Lewis, F. L. and Ozcaldiran, K., "Geometric structure and feedback in singular systems," *Ieee Transactions on Automatic Control*, vol. 34, iss. 4 pp. 450-455, 1989.
[85] Rahmani, A., *et al.*, "On the Infinite Structure of Systems Modelled by Bond Graph : Disturbance Rejection," in *Proceedings of the 4th European Control Conference ECC'97*, Brussels, Belgium, 1997.
[86] Luenberger, D. G., "Time-Invariant Descriptor Systems," *Automatica*, vol. 14, iss. pp. 473-480, 1978.
[87] Dauphin-Tanguy, G., *et al.*, "Bond graph aided design of controlled systems," *Simulation Practice and Theory*, vol. 7, iss. 5 pp. 493-513, Nov. 1999.
[88] Margolis, D. L., "Exploiting Causality for Structured Models Using Bond Graphs," in *1987 American Control Conf.* , Minneapolis, MN, 1987, pp. 1457-1461.
[89] Rosenberg, R. C., "Exploiting Bond Graph Causality in Physical System Models," *Trans. ASME J. Dynamic Syst., Measurement and Control*, vol. 109, iss. 4 pp. 378-383, 1987.
[90] Ort, J. R. and Martens, H. R., "Properties of Bond Graph Junction Structure Matrices," *Trans. ASME J. Dynamic Syst., Measurement and Control*, vol. 95, iss. 4 pp. 362-367, 1973.
[91] Perelson, A. S., "Bond Graph Junction Structures," *Trans. ASME J. Dynamic Syst., Measurement and Control*, vol. 97, iss. 2 pp. 189-195, 1975.
[92] Perelson, A. S., *et al.*, "Discussion: The Properties of Bond Graph Junction Structure Matrices," *Trans. ASME J. Dynamic Syst., Measurement and Control*, vol. 98, iss. 2 pp. 209-211, 1976.
[93] Rosenberg, R. C. and Andry Jr, A. N., "Solvability of Bond Graph Junction Structures with Loops," *IEEE Trans. Circuits Syst.*, vol. CAS-26, iss. 2 pp. 130-137, 1979.
[94] Rosenberg, R. C., "State-Space Formulation for Bond Graph Models of Multiport Systems," *Trans. ASME J. Dynamic Syst., Measurement and Control*, vol. 93, iss. 1 pp. 35-40, Mar. 1971.

[95] Brown, F. T., "Direct Application of the Loop Rule to Bond Graphs," *Trans. ASME J. Dynamic Syst., Measurement and Control*, vol. 94, iss. 3 pp. 253-261, Sept. 1972.
[96] Karnopp, D., "Lagranges Equations for Complex Bond Graph Systems," *Trans. ASME J. Dynamic Syst., Measurement and Control*, vol. 99, iss. 4 pp. 300-306, Dec. 1977.
[97] Sueur, C. and Dauphin-Tanguy, G., "Structural Controllability / Observability of Linear Systems Represented by Bond Graphs," *J. Franklin Institute*, vol. 326, iss. 6 pp. 869-883, 1989.
[98] Buisson, J., *et al.*, "Analysis of the bond graph model of hybrid physical systems with ideal switches," *Proc. IMechE Part I - J. Syst. and Control Eng.*, vol. 216, iss. 1 pp. 47-63, Feb. 2002.
[99] Sueur, C. and Dauphin-Tanguy, G., "Bond-Graph Approach for Structural Analysis of MIMO Linear Systems," *J. Franklin Institute*, vol. 328, iss. 1 pp. 55-70, 1991.
[100] Sueur, C. and Dauphin-Tanguy, G., "Bond Graph Approach to Multi-time Scale Systems Analysis," *J. Franklin Institute*, vol. 328, iss. 5-6 pp. 1005-1026, 1991.
[101] Sueur, C. and Dauphin Tanguy, G., "Bond graph determination of controllability subspaces for pole assignment," in *Proc. Int. Conf. on Systems, Man and Cybernetics: Systems Engineering In the Service of Humans*, Le Touquet, France, 1993, pp. 14-19.
[102] Bertrand, J. M., *et al.*, "On the finite and infinite structures of bond-graph models," in *Proc. 1997 Int. Conf. on Systems, Man and Cybernetics: Systems Engineering In the Service of Humans*, Orlando, FL, 1997, pp. 2472-2477.
[103] Bertrand, J. M., *et al.*, "Bond-Graph for Modeling and Control: Structural Analysis Tools for the Design of Input-Output Decoupling State Feedbacks," *Simulation Series*, vol. 29, iss. 1 pp. 103-103, 1997.
[104] Rahmani, A., *et al.*, "On the Infinite Structure of Systems Modelled by Bond Graph: Feedback Decoupling," in *Proc. 1996 IEEE Int. Conf. on Systems, Man and Cybernetics*, Beijing, China, 1996, pp. 1617-1622.
[105] Golo, G., *et al.* (2000, Accessed: Dec. 2010). *Geometric formulation of generalized bond graph models Part I: Generalized junction structures* [Memorandum No. 1555]. Available: http://www.math.utwente.nl/publications/2000/1555.pdf
[106] Abadie, V. and Dauphin-Tanguy, G., "Control of switching continuous systems," in *Proc. Int. Conf. on Systems, Man and Cybernetics: Systems Engineering In the Service of Humans*, Le Touquet, France, 1993, pp. 595-600.
[107] Buisson, J. and Cormerais, H., "Modeling hybrid linear systems with Bond-Graph using an implicit formulation," *The Bond Graph Digest*, vol. 1, iss. 1.1 Jul. 1997.
[108] Buisson, J. and Cormerais, H., "Descriptor Systems for the Knowledge Modelling and Simulation of Hybrid Physical Systems," *J. Européen des Systèmes Automatisés APII-JESA*, vol. 32, iss. 9-10 pp. 1047-1072, Dec. 1998.

[109] Yang, X., *et al.*, "Controllability Analysis Based on Bond Graph," in *1st Int. Conf. Innovative Computing, Information and Control, 2006 (ICICIC '06)*, Beijing, China, 2006, pp. 356-359.
[110] Galindo, R., *et al.*, "Structural controllability and observability in closed loop for LTI stable systems," in *Joint 2006 IEEE Conf. Control Applications (CCA), Computer-Aided Control Systems Design Symp. (CACSD) and Int. Symp. Intelligent Control (ISIC)*, Munich, Germany, 2007, pp. 2623-2628.
[111] Dauphin-Tanguy, G. and Sueur, C. (2002, Accessed: Dec. 2010). *Bond Graph for Modelling, Analysis, Control Design, Fault Diagnosis* [Presentation Slides]. Available: www.fceia.unr.edu.ar/~kofman/seminario/Argentine-nov02.ppt
[112] Djeziri, M. A., *et al.*, "Fault detection of backlash phenomenon in mechatronic system with parameter uncertainties using bond graph approach," in *Proc. 2006 IEEE Int. Conf. Mechatronics and Automation (IEEE ICMA 2006)*, Luoyang, China, 2006, pp. 600-605.
[113] Rahmani, A. and Dauphin-Tanguy, G., "Structural analysis of switching systems modelled by bond graph," *Math. and Comput. Modelling of Dynamical Syst.*, vol. 12, iss. 2-3 pp. 235-247, Apr.-Jun. 2006.
[114] Djeziri, M. A., *et al.*, "Robust fault diagnosis by using bond graph approach," *IEEE/ASME Trans. Mechatron.*, vol. 12, iss. 6 pp. 599-611, Dec. 2007.
[115] Richard, P. Y., *et al.*, "Bond graph modelling of hard nonlinearities in mechanics: A hybrid approach," *Nonlinear Analysis: Hybrid Systems*, vol. 2, iss. 3 pp. 922-951, Aug. 2008.
[116] Low, C. B., *et al.*, "Monitoring ability analysis and qualitative fault diagnosis using hybrid bond graph," in *Proc. 17th IFAC World Congress* COEX, S. Korea, 2008, pp. 10516-10521.
[117] Low, C. B., *et al.*, "Fault Parameter Estimation for Hybrid Systems using Hybrid Bond Graph," in *2009 IEEE Control Applications (CCA) & Intelligent Control (ISIC)* Saint Petersburg, Russia, 2009, pp. 1338-1343
[118] Dauphin-Tanguy, G., *et al.*, "Symbolic Determination of the Steady State due to Gravity Effects on Mechanical Systems Modelled by Bond Graphs," in *Proc. 2005 Int. Conf. on Bond Graph Modeling (ICBGM 2005)*, New Orleans, LA, 2005, pp. 101-106.
[119] Weisstein, E. W. (Accessed: 15th March 2013). *Determinant* [MathWorld - A Wolfram Web Resource]. Available: http://mathworld.wolfram.com/Determinant.html
[120] Sueur, C., "Structural analysis and duality for bond graph models," in *2011 19th Mediterranean Conf. Control and Automation (MED 2011)*, Corfu, Greece, 2011, pp. 624-630.
[121] Buisson, J., *et al.*, "On the stabilisation of switching electrical power converters," in *8th Int. Workshop on Hybrid Systems: Computation and Control (HSCC 2005)*, Zurich, Switzerland, 2005, pp. 184-197.
[122] Van Der Schaft, A., "Port-controlled Hamiltonian Systems: Towards a Theory for Control and Design of Nonlinear Physical Systems," *J. Soc. Instrument and Control Engineers of Japan (SICE)*, vol. 39, iss. 2 pp. 91-98, 2000.

[123] Losse, P. and Mehrmann, V. (2007, Accessed: Aug. 2012). *Algebraic characterization of controllability and observability for second order descriptor systems* [Lecture Notes Preprint 2006/21]. Available: http://www3.math.tu-berlin.de/preprints/files/LosM06_ppt_updated.pdf

[124] Margetts, R., *et al.*, "Construction and Analysis of Causally Dynamic Hybrid Bond Graphs," *Proc. IMechE Part I - J. Syst. and Control Eng.*, vol. 227, iss. 3 pp. 329-346, Mar. 2013.

[125] Mosterman, P. J. and Biswas, G., "Hybrid automata for modeling discrete transitions in complex dynamic systems," in *7th IFAC Symp. Artificial Intelligence in Real-Time Control* Grand Canyon Natl. Pk., AR 1998, pp. 43-48.

[126] Strömberg, J. E., "A Mode Switching Philosophy" (Dissertation No. 353), PhD Thesis Linköping University, Linköping, Sweden, 1994.

[127] Margetts, R., *et al.*, "Modelling a Drop Test of a Landing Gear using a Hybrid Bond Graph," in *IASTED MIC 2013*, Innsbruck, Austria, 2013.

[128] Herzog, J., 2012, *Airbus A380 Nose Landing Gear*, (Own work) Wikimedia Commons. Available from: http://commons.wikimedia.org/wiki/File%3AAirbus_A380_Nose_Landing_Gear.jpg [Accessed 29 January 2013]. License: GFDL (http://www.gnu.org/copyleft/fdl.html) or CC-BY-SA-3.0-2.5-2.0-1.0 (http://creativecommons.org/licenses/by-sa/3.0), © Julian Herzog / Wikimedia Commons / CC-BY-SA-3.0 / GFDL

[129] Currey, N. S., *Aircraft Landing Gear Design - Principles and Practices* (AIAA education series). Washington D.C.: American Institute of Aeronautics and Astronautics, 1988.

[130] Maggs, M., 2008, *To Pot the Red*, (Own Work) Wikimedia Commons. Available from: http://commons.wikimedia.org/wiki/File%3ATo_pot_the_red.jpg [Accessed 27 February 2013]. License: CC-BY-SA-3.0

[131] Alsterdrache, 2011, *Kugelstoszpendel*, (Own Work) Wikimedia Commons. Available from: http://commons.wikimedia.org/wiki/File%3AKugelstoszpendel.jpg [Accessed 27th February 2013]. License: CC0